Encl. to ltr. dat 4/20/87, rec'd 4-23-87
To: Coleman
From: Harlan

SWIFT II Verification and Validation: A Survey of Previous Tests and Recommendations for Future Work

FIN A1158, Task IV - Code Validation & Verification

C. David Updegraff
Science Applications International Corporation
Under Contract 04-8899 to
Sandia National Laboratories
Albuquerque, New Mexico 87185

Contract Monitor: Charlene Harlan

April 1987

ABSTRACT

This letter report describes existing verification and validation tests for the Sandia Waste-Isolation Flow and Transport Model for Fractured Media (SWIFT II, Release 4.84). The adequacy and completeness of previous existing tests are discussed and recommendations are made for areas requiring additional development.

In general it was found that many aspects of the SWIFT II code have been adequately verified. These aspects include both local and global equations, pressure, mass transport and heat transport solutions, various boundary conditions, aquifer influence functions and some submodels. Aspects that have not been tested include local and global brine equations, parts of the repository submodel and the wellbore submodel. Recommendations are made for testing the local and global brine equations and parts of the repository submodel. The wellbore submodel is too complicated to verify against an analytical solution.

A review of several problems comparing SWIFT II results against field data reveals that the comparisons are parameter fitting problems. The SWIFT II runs were made to find parameters that make the SWIFT II results fit field data. This process does not test the validity of the models implemented in SWIFT II. Because of the complexity of SWIFT II, it is recommended that the SWIFT II code not be used to validate its physically based models where simpler codes or analytical solutions can be used for that purpose. Models unique to SWIFT II, such as transport by convection in the porous matrix of a dual porosity media, are the only physically based models that should be validated with the SWIFT II computer code.

CONTENTS

Page

1. INTRODUCTION 1

2. EXISTING VERIFICATION TESTS 4
   2.1 VERIFICATION OF FLOW 4
      2.1.1 Fully Penetrating Well with Constant Discharge 4
      2.1.2 Fully Penetrating Well with Constant Drawdown 5
      2.1.3 Fully Penetrating Well in a Horizontal Anisotropic Aquifer 8
      2.1.4 Fully Penetrating Well in a Leaky Aquifer, Small Values of Time 14
      2.1.5 Drawdown in a Fully Penetrating Well in a Leaky Aquifer 18
      2.1.6 The Dupuit-Forcheimer Steady-State Problem 21
      2.1.7 The Boussinesq Transient-State Problem 24
   2.2 VERIFICATION OF MASS TRANSPORT 27
      2.2.1 One-Dimensional Transport with Chain Decay and Equal Retardation Parameters 27
      2.2.2 One-Dimensional Transport with Chain Decay and Unequal Retardation Parameters 30
      2.2.3 Transport of a Decaying Radionuclide in a Fractured Porous Medium (prismatic representation of matrix) 32
      2.2.4 Transport of a Decaying Radionuclide in a Fractured Porous Medium (spherical representation of matrix) 40

Page

2.3 VERIFICATION OF HEAT TRANSPORT 45
2.3.1 One-Dimensional Convective-Dispersive Heat Transport 45
2.3.2 Linear Heat Transport During Injection 48
2.3.3 Radial Heat Transport During Injection 52
2.3.4 Radial Heat Transport with Loss to Confining Beds 53

3. EXISTING VALIDATION TESTS 58
3.1 VALIDATION OF FLOW 58
3.1.1 Analysis of Well Test-Data for a Dolomite Formation 58
3.1.2 Hydraulic Testing for Thermal-Energy Storage in an Aquifer 62
3.2 VALIDATION OF MASS TRANSPORT - Contaminant Migration from a Landfill 70
3.3 VALIDATION OF HEAT TRANSPORT - Thermal Energy Storage in an Aquifer 74

4. SUMMARY AND RECOMMENDATIONS 90
4.1 VERIFICATION RECOMMENDATIONS 90
4.2 VALIDATION RECOMMENDATIONS 92
4.3 PROBLEMS WITH VALIDATION 94
4.4 SUMMARY 96

5. REFERENCES 97

FIGURES

		Page
Figure 2-1	Drawdown as a Function of Time for a Constant-Discharge Well. [Ward et al., 1984a]	6
Figure 2-2	Drawdown as a Function of Distance for a Constant-Discharge Well. [Ward et al., 1984a]	7
Figure 2-3	Pumping Rate as a Function of Time for a Constant-Drawdown Well. [Ward et al., 1984a]	9
Figure 2-4	Drawdown as a Function of Time for a Constant-Drawdown Well. [Ward et al., 1984a]	10
Figure 2-5	Drawdown as a Function of Time for a Constant-Discharge Well in an Anisotropic Aquifer. [Ward et al., 1984a]	12
Figure 2-6	Drawdown as a Function of Distance for a Constant-Discharge Well in an Anisotropic Aquifer. [Ward et al., 1984a]	13
Figure 2-7	Drawdown as a Function of Time for a Leaky Aquifer. [Ward et al., 1984a]	16
Figure 2-8	Drawdown as a Function of Distance for a Leaky Aquifer. [Ward et al., 1984a]	17
Figure 2-9	Results from SWIFT II and the Analytical Solutions of Hantush (1960) for a Radial Distance of 117.4 m. [Reeves et al., 1986c]	20
Figure 2-10	Steady-State Free-Water Surface for the Dupuit-Forcheimer Problem. [Reeves et al., 1986c]	23
Figure 2-11	Time-dependent Free-Water Surface Elevation for the Boussinesq Problem. [Reeves et al., 1986c]	26
Figure 2-12	Radionuclide Discharge Concentration as a Function of Time. [Ward et al., 1984a]	29
Figure 2-13	Radionuclide Discharge Concentration as a Function of Time - Chain 1, Run 1. [Ward et al., 1984a]	33
Figure 2-14	Radionuclide Discharge Concentration as a Function of Time - Chain 1, Run 2. [Ward et al., 1984a]	34

		Page
Figure 2-15	Radionuclide Discharge Concentration as a Function of Time - Chain 2, Run 1. [Ward et al., 1984a]	35
Figure 2-16	Radionuclide Discharge Concentration as a Function of Time - Chain 2, Run 2. [Ward et al., 1984a]	36
Figure 2-17	Radionuclide Concentrations Within the Fracture for a Prismatic Characterization of the Rock Matrix. [Reeves et al., 1986c]	38
Figure 2-18	Radionuclide Concentrations Within the Rock Matrix for a Prismatic Characterization of the Rock Matrix. [Reeves et al., 1986c]	39
Figure 2-19	Radionuclide Concentrations Within the Fracture for a Spherical Characterization of the Rock Matrix. [Reeves et al., 1986c]	43
Figure 2-20	Radionuclide Concentrations Within the Rock Matrix for a Spherical Characterization of the Rock Matrix. [Reeves et al., 1986c]	44
Figure 2-21	Dimensionless Temperature Profiles at Two Values of Time. [Ward et al., 1984a]	47
Figure 2-22	Temperature as a Function of Time at a Fixed Distance for a Linear Aquifer System. [Ward et al., 1984a]	50
Figure 2-23	Temperature as a Function of Distance at a Fixed Time for a Linear Aquifer System. [Ward et al., 1984a]	51
Figure 2-24	Temperature as a Function of Time in a Radial Aquifer System. [Ward et al., 1984a]	54
Figure 2-25	Temperature as a Function of Distance in a Radial Aquifer System. [Ward et al., 1984a]	55
Figure 2-26	Temperature Breakthrough Within the Aquifer at 37.5 m from the Injection Well. [Reeves et al, 1986c]	57
Figure 3-1	Flow Rate During H2A Slug Test. [Reeves et al., 1986c]	61
Figure 3-2	Aquifer Drawdown as a Function of Time at Three Observation Wells for the Anisotropy Test. [Ward et al., 1984a]	65

Page

Figure 3-3	Aquifer Drawdown as a Function of Time for the Standard Pumping Test. [Ward et al., 1984a]	68
Figure 3-4	Aquifer Drawdown at a Fully Penetrating Observation Well as a Function of Time for the Standard Pumping Test. [Ward et al., 1984a]	69
Figure 3-5	Observed (September, 1976) and Simulated Chloride Concentrations (observed data from Cleary [1978]). Tic marks denote the numerical gridding. [Ward et al., 1984a]	73
Figure 3-6	East-West Ground-water Temperature Distributions at Selected Times. The vertical sections run between Wells 12 and 6. [Ward et al., 1984a]	80
Figure 3-7	North-South Ground-water Temperature Distributions at Selected Times. The vertical sections run between Wells 9 and 3. [Ward et al., 1984a]	81
Figure 3-8	Simulated Ground-Water Temperature Distributions at Selected Times. [Ward et al., 1984a]	82
Figure 3-9	Observed and Simulated Temperature as a Function of Time at a Radial Distance of 15 m in the Upper (Probe B), Middle (Probe D) and Lower (Probe E) Zones of the Aquifer. [Ward et al., 1984a]	83
Figure 3-10	Observed and Simulated Temperature as a Function of Distance at the End of the Injection Period in the Upper, Middle and Lower Layers of the Aquifer. Ward et al., 1984a]	85
Figure 3-11	Observed and Simulated Temperature as a Function of Distance at the End of the Storage Period in the Upper, Middle and Lower Layers of the Aquifer. [Ward et al., 1984a]	86
Figure 3-12	Observed and Simulated Temperature as a Function of Distance at the End of the Production Period in the Upper, Middle and Lower Layers of the Aquifer. [Ward et al., 1984a]	87
Figure 3-13	Observed and Simulated Production Temperature as a Function of Time (after Molz et al. [1983]). [Ward et al., 1984a]	88

TABLES

		Page
Table 3-1	Hydraulic and Heat-Transport Parameters Adopted for Aquifer Thermal Energy Storage Problem	77
Table 3-2	Values of Hydraulic Conductivity for the Three-layer Aquifer (from Buscheck et al. [1983]	78

1. INTRODUCTION

The SWIFT II code has been developed as part of the basalt methodology development performed by Sandia National Laboratories for the Nuclear Regulatory Commission (NRC). The code has descended from the code, SWIFT. SWIFT II differs from its predecessor by the inclusion of several new features not found in SWIFT. These new features include the ability to simulate confined aquifer with dual porosity systems, an aquifer with conductive confining layers, and an aquifer with a free water surface. The first two features constitute SWIFT II's ability to handle fractured media. The fractured media capability is implemented into the flow, brine, heat and radionuclide transport equations. SWIFT II is documented in Reeves et al. (1986a, 1986b) and illustrative problems are provided in Reeves et al. (1986c).

As part of the quality assurance performed on any computer code developed by SNL for the NRC's High-Level Waste Management Program, a code must be verified (Wilkinson and Runkle, 1986). Verification is a process which demonstrates that the software correctly performs its stated capabilities (Wilkinson and Runkle). Verification is usually performed by comparing the results of the numerical code being verified with an analytical solution. This process assures that the numerical code correctly solves the equations representing the physical processes implemented in it. This process does not assure that the equations in the code represent the true physics of any phenomena.

The process of testing whether the equations, or submodels, implemented in a code represent the real world is called validation. Notice that while verification tests whether the governing equations are being solved correctly, validation tests whether the equations represent the physics of the situation. Although useful in determining whether or not a computer code is adequate for modeling physical phenomena, validation is not required according to the existing NRC software QA guidelines (Wilkinson and Runkle, 1986).

The purpose of this report is to determine whether the computer code, SWIFT II, has been adequately verified and the models implemented in it validated. There is not a wealth of published information regarding problems solved by the SWIFT II computer code. A computer literature search of the NTIS, Georef, EI Engineering Meetings, and the DOE Energy databases provided no sources. The only published report containing potential verification and validation problems for SWIFT II is Reeves et al. (1986c). Geotrans, Inc. provided SWIFT II data input and output files for all the problems in Ward et al. (1984a). These are useful verification and validation exercises for SWIFT II. The Ward et al. report originally dealt with the SWIFT computer code but the problems have been rerun with the SWIFT II computer code. There is probably no doubt the SWIFT II computer code has been used to solve other problems, but these have not been published yet.

Although the Ward et al. (1984a) report intended to present verification problems for the SWIFT computer program, it did not intend to validate the models in the program because of difficulty in defining and performing validation work. As a result, Ward et al. present several calibration problems for SWIFT. Calibration (which Ward et al. define as the weak form of validation) is a process in which the model parameters are adjusted to fit experimental laboratory or field data. Similar comments apply to the self-teaching problems provided in Reeves et al. (1986c). The problems shown in Chapter 3 of this report present some of the difficulties in trying to call a comparison of field data and computer results a true validation exercise.

This report contains several chapters. Chapter 1 provides an introduction to the verification and validation effort expended on the SWIFT II computer code. Chapter 2 reviews several verification problems solved by the SWIFT II computer code. The problems cover flow, mass transport, and heat transport in systems utilizing both the single porosity and double porosity equations in SWIFT II. Chapter 3 provides a review of what might be considered validation problems. However, this chapter shows that the reviewed problems constitute calibration rather than validation exercises. Chapter 4 provides a summary of the reviewed problems and recommendations for additional problems to complete the verification and validation effort for SWIFT II. References are provided in Chapter 5.

2. EXISTING VERIFICATION TESTS

2.1 VERIFICATION OF FLOW

2.1.1 Fully Penetrating Well with Constant Discharge

In this problem SWIFT II simulates the well-known Theis (1935) equation. The problem is described in Ross et al. (1982). A well, pumping at a constant rate, fully penetrates an infinitely large isotropic, homogeneous, horizontal aquifer of constant thickness. Both radial and Cartesian coordinates are used to simulate the problem. The problem is designed to test several capabilities of the SWIFT II code including the ability to simulate pressure solutions, a rate controlled well, aquifer influence functions, radial and Cartesian coordinates, and SI and English engineering units.

Details of the simulation including the gridding system and the hydrologic parameters are presented in Ward et al. (1984a). The flow system is based on a well, pumped at a rate of 3.0×10^{-3} m^3/s, in an infinitely large, homogeneous, isotropic aquifer. The hydrologic properties include a transmissivity of 10^{-3} m^2/s and a storage coefficient of 10^{-3}. For the radial coordinate system, the center of the first grid block is located at 0.4755 m from the center of the well. The centers of the remaining forty-nine grid blocks are located such that $\hat{r}_{i+1}/\hat{r}_i$ is approximately 1.21 where $\hat{r}_i$ is the distance from the center of the well to the center of the i^{th} grid block. The distance to the outer boundary is 6096 m and the well radius is 0.1143 m. For the Cartesian grid, a 1 m by 1 m grid block represented the well. Subsequent grid block widths along both the x and y axes were 1.5 m, 2.5 m, 3.5 m, 5.0 m, and 8.0 m. After 8.0 m, grid block widths were double the preceding values until a maximum grid block width of 4096 m was reached. This resulted in a 15 x 15 grid, which was used to model only one quadrant of the x-y plane. At the outer boundary of both the radial and Cartesian grids, a Carter-Tracy boundary condition was applied.

Ward et al. (1984a) describe the results of the simulations with respect to both time and space. The results in time of the simulation for radial and Cartesian coordinates are presented in Figure 2-1. Simulations with both the radial and Cartesian grids compare very well with the analytical solution. The radial grid produces a more accurate comparison with the analytical solution because the grid system is much finer for the radial grid than for the Cartesian grid. Perhaps if the Cartesian grid were not coarser than the radial grid the results would have been more comparable.

The results with respect to space are presented in Figure 2-2 for both radial and Cartesian coordinate systems. As in the time solution (Figure 2-1), the SWIFT II solution compares favorably with the analytical solution. Again, the radial coordinate solution compares more favorably than the Cartesian coordinate solution.

Figure 2-2 shows the relationship between the grid spacing of the two coordinate systems. Approximately three or four radial grid blocks exist for each Cartesian grid block. This accounts for the better comparison of the radial solution with the analytical solution than with the Cartesian solution.

2.1.2 Fully Penetrating Well with Constant Drawdown

In this problem SWIFT II is used to simulate the Jacob and Lohman (1952) solution to a well with a constant drawdown. The problem is briefly described in Ward et al. (1984a). In this problem a well fully penetrates an infinitely large homogeneous, isotropic aquifer. The drawdown in the well is held constant, which allows the flow rate in the well to vary continuously with time. This problem tests several capabilities

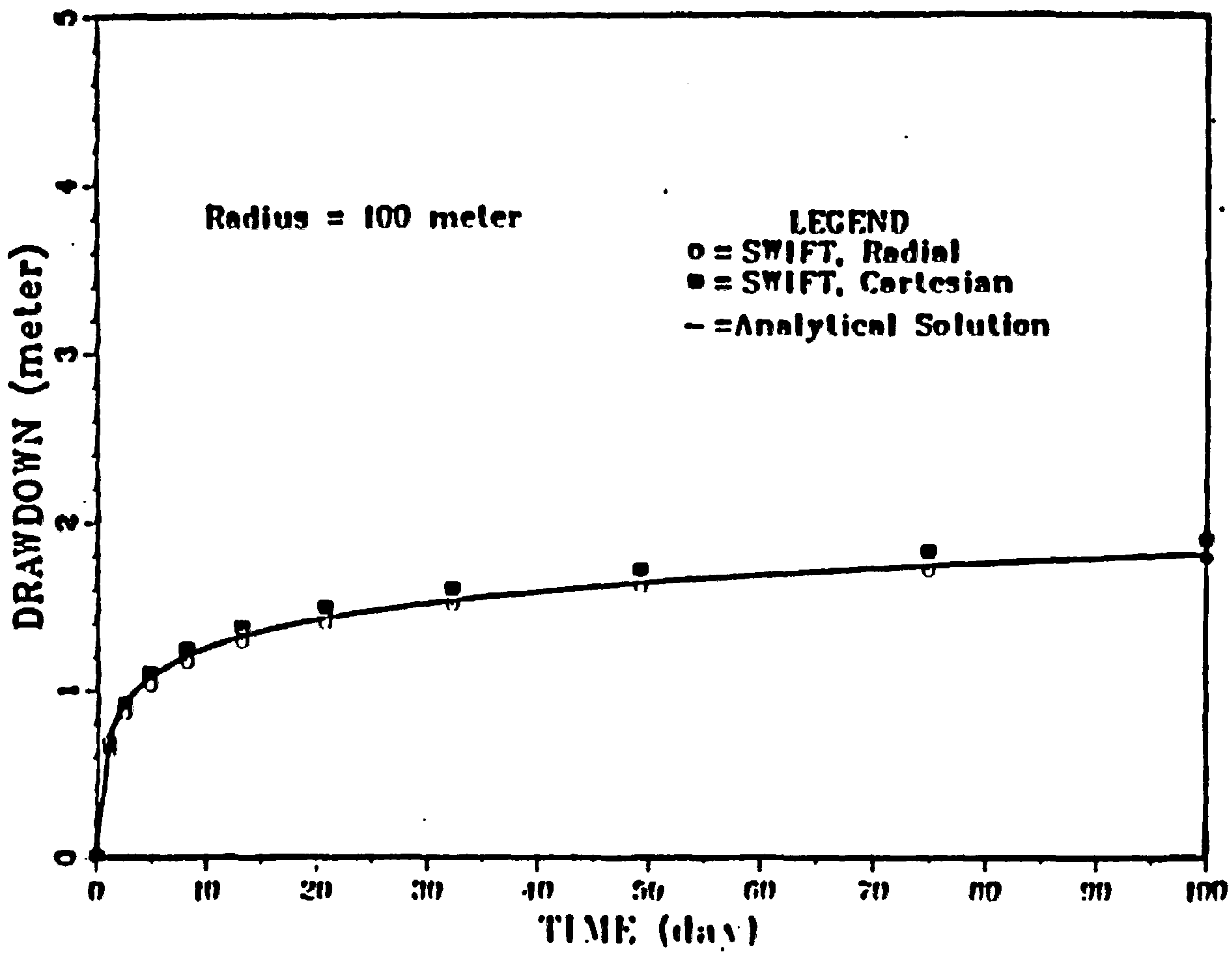

Figure 2-1 Drawdown as a Function of Time for a Constant-Discharge Well. [Ward et al., 1984a]

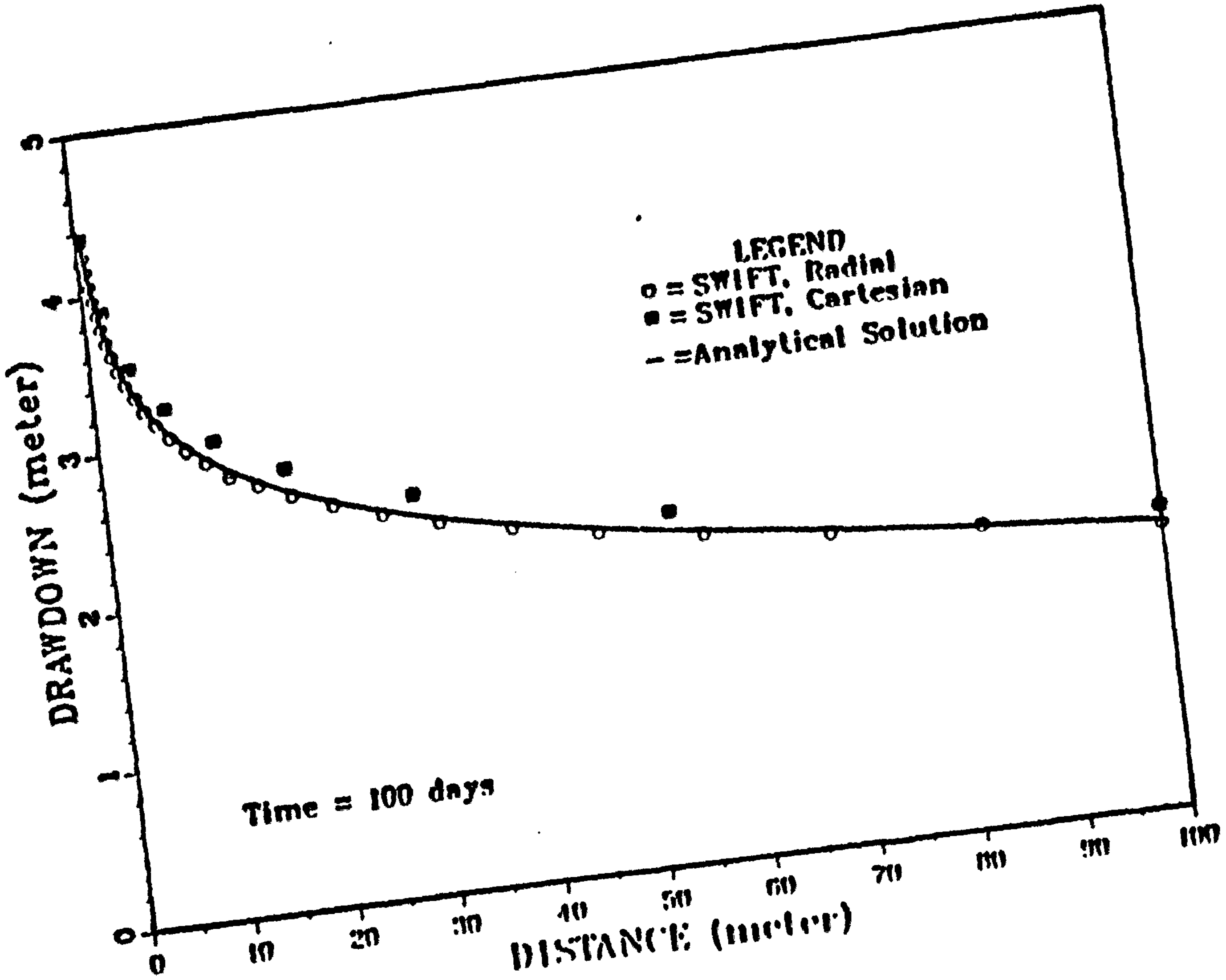

Figure 2-2 Drawdown as a Function of Distance for a Constant-Discharge Well. [Ward et al., 1984a]

of the SWIFT II code including pressure solutions, constant-pressure well aquifer-influence functions, radial coordinate systems, well index, and SI and English engineering units.

Details of the grid system and hydrologic parameters are the same as for the fully penetrating well with constant discharge problem presented in Section 2.1 (Ward et al., 1984a). However, instead of specifying a flow rate at the well, a constant drawdown of 3.999 m is used. This condition allows the flow rate in the well to vary with time. The boundary condition specified at the outer boundary is a Carter-Tracy boundary condition. In addition, the well index is set up such that the permeability of the well skin is equal to the permeability of the aquifer.

Results of the simulation are presented in Ward et al. (1984a) and are reproduced in Figures 2-3 and 2-4. Figure 2-3 compares the well flow rates generated by the analytical solution and the SWIFT II solution. The SWIFT II solution compares very well with the analytical solution. Figure 2-4 presents a comparison of drawdowns at 100 m from the center of the well. Again, there is a very good comparison between SWIFT II and the analytical solutions.

2.1.3 Fully Penetrating Well in a Horizontal Anisotropic Aquifer

In this problem, the SWIFT II code is used to simulate the Papadopulos (1965) solution to a pumping well in an anisotropic aquifer. The problem is described in Ross et al. (1982) as a fully penetrating well pumping at a constant rate from an infinitely large, homogeneous, anistropic aquifer. The effect of anisotropy accounts for the only difference between the Papadopulos solution and the Theis (1935) solution. The problem is designed to test several aspects of the SWIFT II

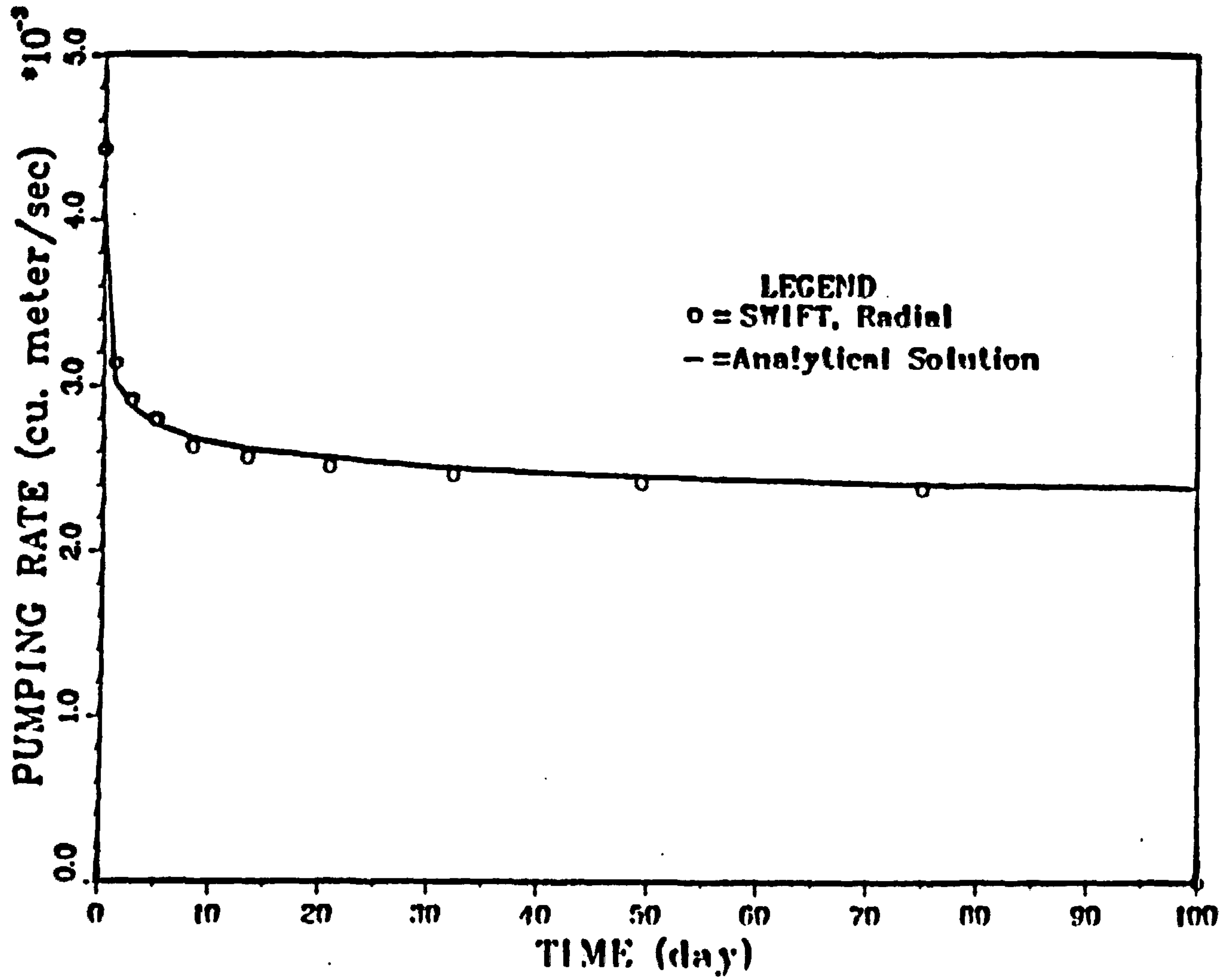

Figure 2-3 Pumping Rate as a Function of Time for a Constant-Drawdown Well. [Ward et al., 1984a]

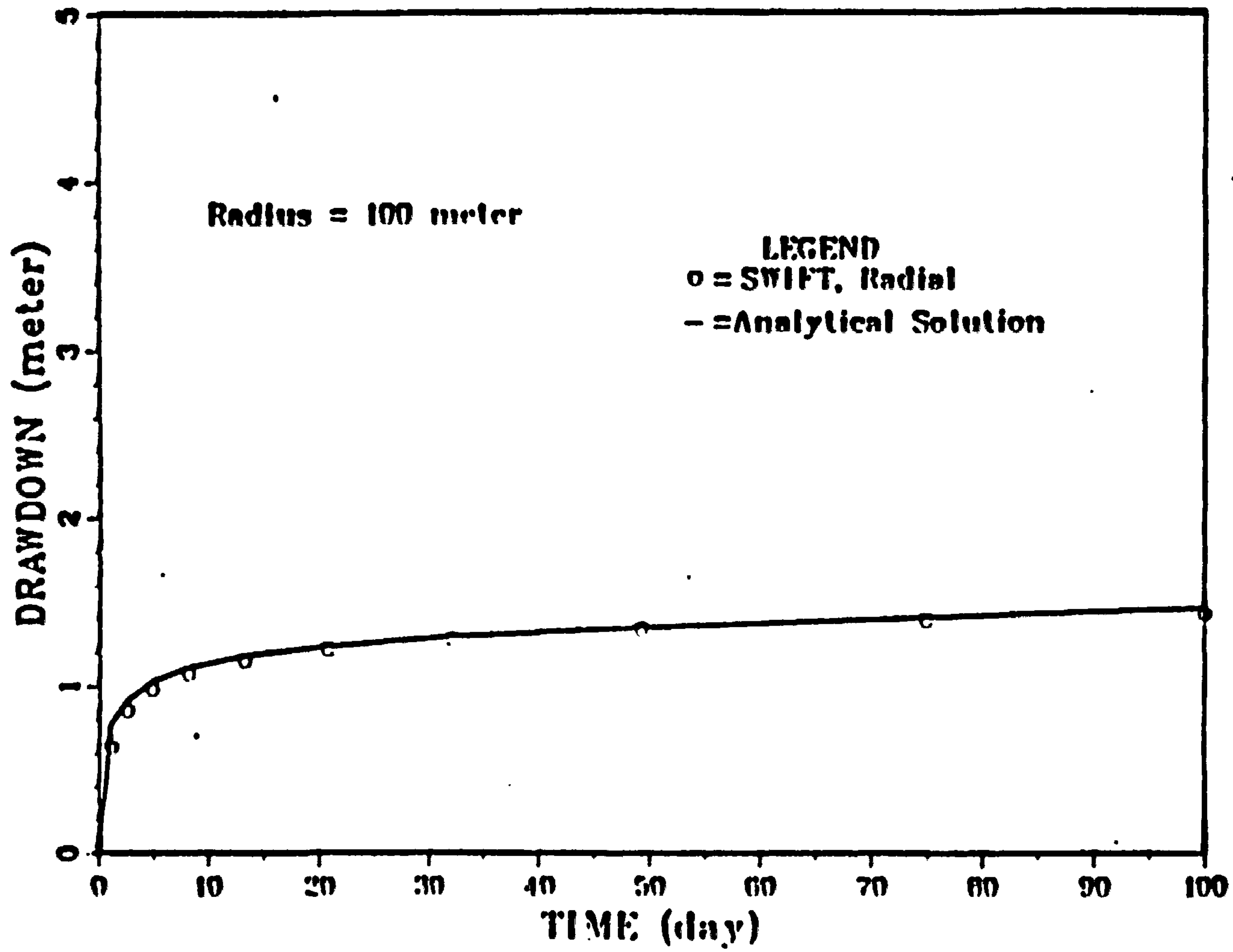

Figure 2-4 Drawdown as a Function of Time for a Constant-Drawdown Well. [Ward et al., 1984a]

code including pressure solutions, anisotropic permeability tensor, rate-controlled well condition, two-dimensional Cartesian geometry, SI and English engineering units.

Details of the grid and hydrologic parameters for this problem are presented in Ward at al. (1984a). Only one quadrant of the x-y plane needs to be modeled for this problem because of symmetry. The problem is gridded using a Cartesian geometry. Because the anisotropy of the porous media, this problem cannot be solved in radial coordinates. In addition the elliptical nature of the cone of depression caused by the anisotropy, requires the system length to be longer in the direction of the larger directional transmissivity, the x-direction in this case than in the direction of the smaller transmissivity. In the x-direction, the first five grid block widths as measured from the pumping well are 1 m, 1.5 m, 2.5 m, 3.5 m, 5.0 m, and 8.0 m. Subsequent, grid block widths are twice the width of the preceding grid block width. The maximum grid block width is 32786 m, which forms a total system length in the x-direction of 65541.5 m. In the y-direction, the grid block widths are the same as in the x-direction, except that the maximum grid block width is 4096 m for a total system length in the y-direction of 8197.5 m. Thus, an 18 x 15 grid is used to model the system.

The outer boundary condition is set to a zero flux condition because it is assumed that the cone of depression would not reach out to the boundary. The x-direction transmissivity is 10^{-3} m^2/s, the y-direction transmissivity is 10^{-4} m^2/s, and the storage coefficient is 10^{-3}. The pumping rate is 3×10^{-3} m^3/s.

Details of the modeling results for this problem are presented in Ward et al. (1984a) and are presented in Figures 2-5 and 2-6. Figure 2-5 presents drawdown with respect to time at points along both the x and y axes 100 m from the pumping

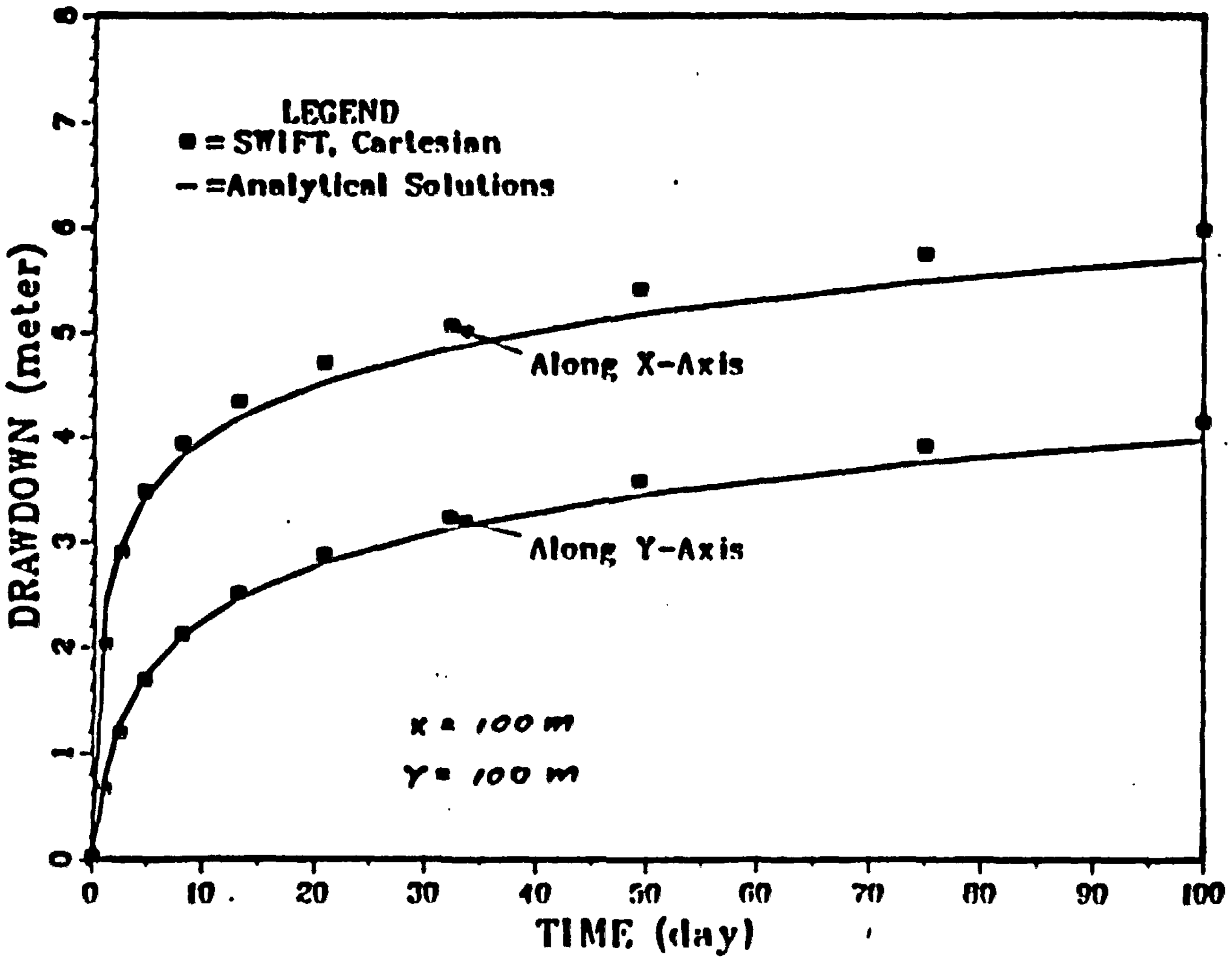

Figure 2-5 Drawdown as a Function of Time for a Constant-Discharge Well in an Anisotropic Aquifer. (Ward et al., 1984a)

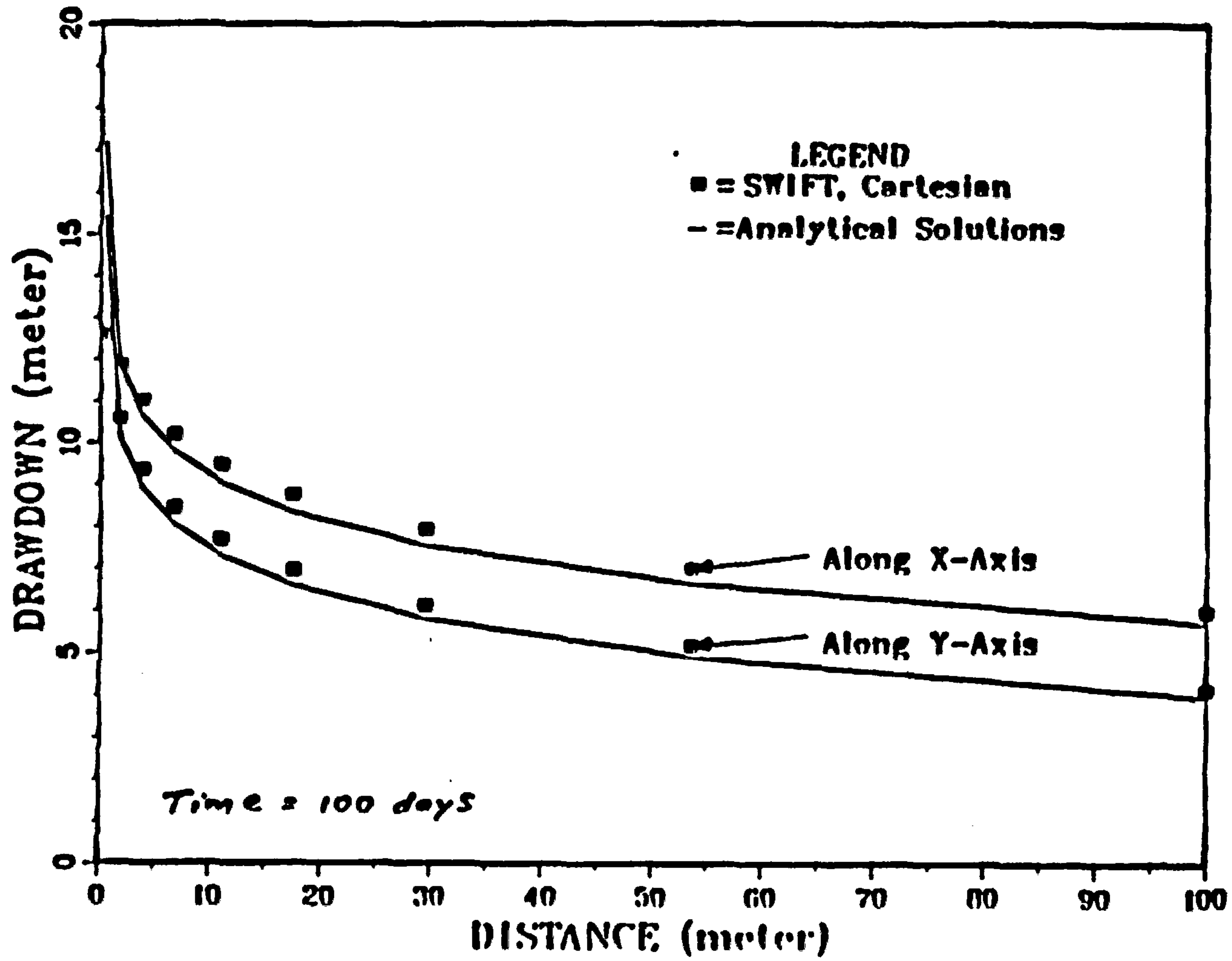

Figure 2-6 Drawdown as a Function of Distance for a Constant-Discharge Well in an Anisotropic Aquifer. [Ward et al., 1984a]

well. The SWIFT II code results seem to overpredict the results of the analytical solution by approximately three to four percent of the drawdown at any given time. However, the SWIFT II results seem to follow the same drawdown shape as that produced from the analytical solution. Results of drawdown along the x- and y- axes for various points and a time of 100 days are presented on Figure 2-6. The results on Figure 2-6 are similar to those found on Figure 2-5, namely that the SWIFT II results overpredict the analytical solution results by three to four percent and generally follow the same drawdown pattern as produced by the analytical solution.

The deviation of the SWIFT II solution from the analytical solution is cause for some minor concern. The use of smaller grid block widths in the SWIFT II modeling would probably produce a better comparison between the SWIFT II results and the analytical solution.

2.1.4 Fully Penetrating Well in a Leaky Aquifer, Small Values of Time

In this problem, SWIFT II is used to simulate the early time pumping response of a leaky aquifer (Hantush 1960). Ross et al. (1982) describe the problem. The modeled system consists of a highly permeable aquifer which is overlain by a low permeability fully saturated aquitard. Another highly permeable aquifer which is kept at a constant head overlies the aquitard. Radial flow in the aquifer and vertical flow in the aquitard are the primary assumptions made for this problem. When the lower aquifer is pumped, the resulting head drop coupled with the constant head in the upper aquifer forces water from the aquitard into the lower aquifer. Thus, the resulting head drop in the lower aquifer is not as great as if the aquitard had not been present. This problem is designed to test several aspects of the SWIFT II code including the pressure solution, the coupling of vertical flow in an aquitard with horizontal flow in an aquifer, a rate-controlled well solution, the aquifer-influence functions, radial geometry, and SI and English engineering units.

Ward et al. (1984a) present the details of the modeling effort for this problem. The axisymmetric grid system consists of two layers of 50 grid blocks each. The lower layer of grid blocks, 3.048 m high, represents the aquifer and the upper layer, 0.3 m high, represents the aquitard. In the radial direction, the distance to the center of the first grid block is 0.2957 m from the center of the well. Distances to the center of subsequent grid blocks are approximately 1.22 times the distance to the center of the preceding grid block. The distance to the outer boundary is 6096 m. The well radius is 0.1143 m. A Carter-Tracy boundary condition is applied at the outer boundary of the radial grid. The way in which the grid is set up implies a zero flux boundary condition at the bottom of the aquifer and the top of the aquitard. The upper aquifer is not modeled in this problem. Hence, results from modeling this problem are only valid for small times. The following hydrologic parameters were used to model the problem:

Aquifer storage coefficient	10^{-4}
Aquifer transmissivity	10^{-3} m^2/s
Aquitard specific storage	$3 \times 10^{-3}/m$
Aquitard hydraulic conductivity	3×10^{-10} m/s
Aquitard thickness	0.3 m
Pumping rate	0.014 m^3/s

This problem for both short and long times and different hydrologic parameters has been run using the dual porosity capability of SWIFT II and is presented in Section 2.1.5.

Results of the modeling effort are described in Ward et al. (1984a) and presented on Figures 2-7 and 2-8. Figure 2-7 presents drawdown with respect to time at 20 m from the pumping well. The SWIFT II solution tracks the analytical solution for the first six minutes and then begins to overpredict the

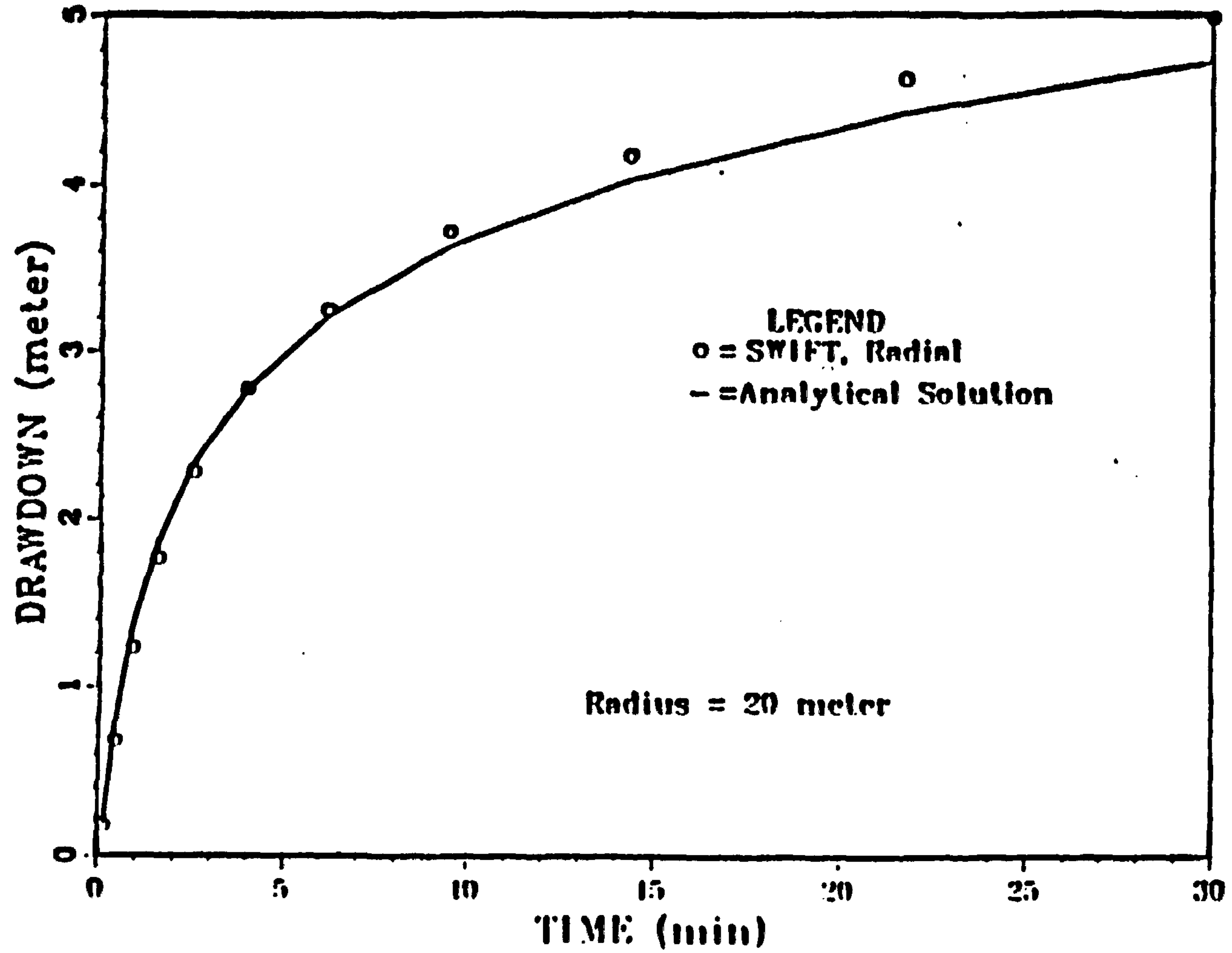

Figure 2-7 Drawdown as a Function of Time for a Leaky Aquifer. [Ward et al., 1984a]

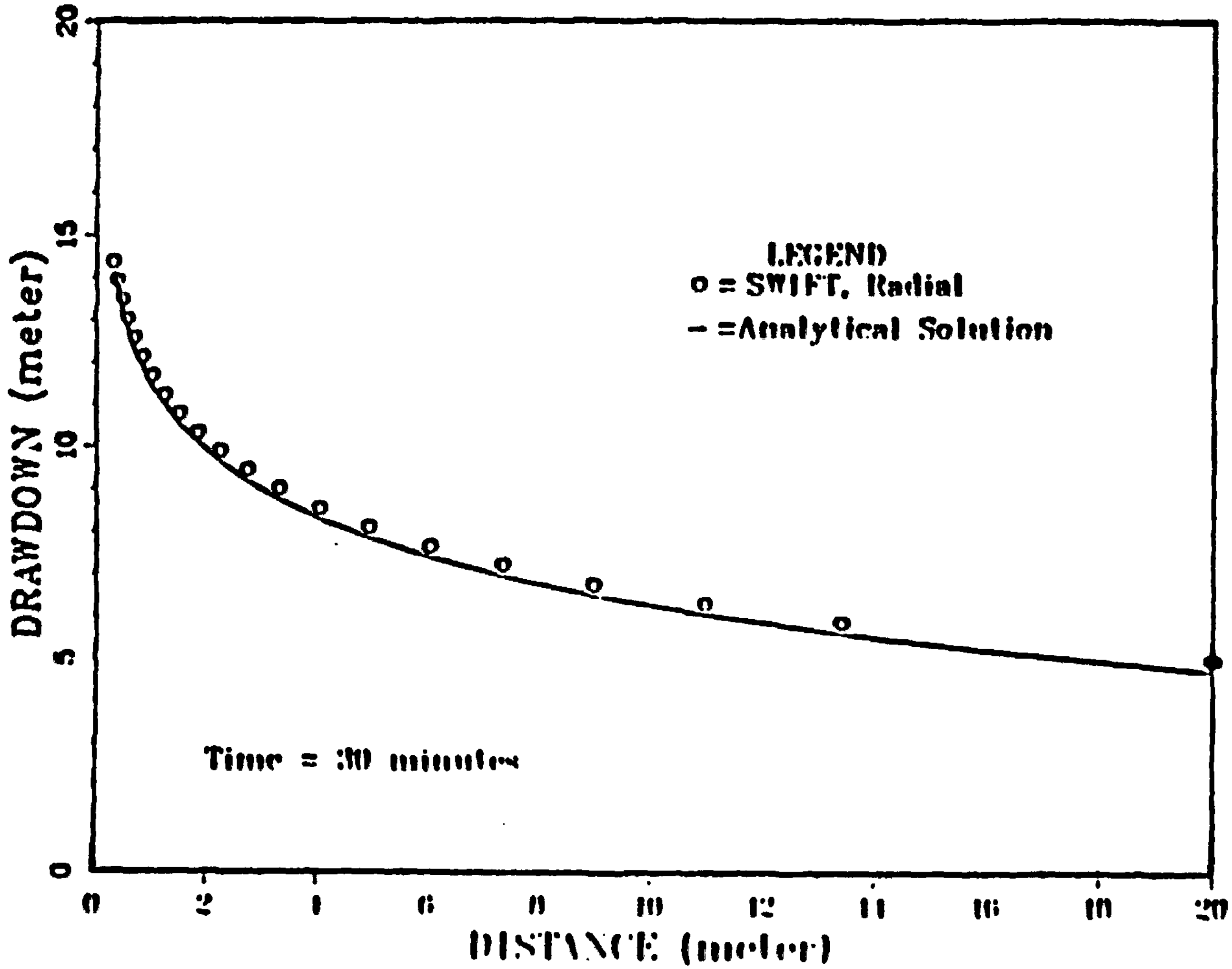

Figure 2-8 Drawdown as a Function of Distance for a Leaky Aquifer. [Ward et al., 1984a]

analytical solution. The deviation increases with time. Ward et al. attribute this increasing deviation to increasing time step size as time increases. However, it is possible that the deviation may be due to the zero flux boundary condition at the top of the aquitard. Because there is only one grid block in the aquitard, the solution senses the boundary almost immediately after pumping starts. If several layers of grid blocks were included in the aquitard, the zero flux boundary condition would not be sensed as quickly.

Figure 2-8 presents drawdown in the aquifer with respect to distance at a time of 30 minutes. At distances of less than two meters, the SWIFT II solution tracks the analytical solution fairly well. At distances greater than two meters, the SWIFT II solution begins to deviate from the analytical solution and the deviation increases with increasing distances. However, the deviations are fairly small. Possible reasons for the deviations are mentioned in the preceding paragraph.

2.1.5 Drawdown in a Fully Penetrating Well in a Leaky Aquifer

In this problem the SWIFT II code is used to simulate pumpage of a well in an infinitely large aquifer overlain by a leaky aquitard (Hantush, 1960). The aquitard is, in turn, overlain by a constant head source. This problem is similar in some respects to the leaky aquifer problem described in Section 2.1.4 except that in this problem both long and short term solutions are required and the hydrologic parameters are different (Ward et al. 1984b). This problem tests several aspects of the SWIFT II code including the pressure solution, radial coordinate system, the Carter-Tracy aquifer influence functions, well index, local grid blocks external to global grid blocks and prismatic representations of rock matrix.

Specifics of the problem are provided in Reeves et al. (1986c). In the radial direction there are fifty grid blocks. The distance from the center of the pumping well to the first grid block is 0.1263842 m. Distances from the well center to subsequent grid block centers are approximately 1.22 times the distance to the preceding grid block center. The well radius is 0.1143 m and the distance from the center of the well to the outer edge of the modeled system is 2646.7663 m. A pumping rate of 6.283 m^3/s is applied to the well and a Carter-Tracy influence function is applied to the outer boundary.

A local grid, used to simulate vertical flow in the aquitard, is connected to each of the radial direction grid blocks. The local grids consist of twenty nodes each. The distance between the first two nodes of the local grid is 0.5 m and the distance between subsequent pairs of nodes is approximately 1.15 times the distance between the preceding pair. The length of the local grid is 50 m. At the end the local grid, a constant head boundary condition, representing the constant head aquifer overlying the aquitard, is applied.

Other hydrologic data necessary for the simulation of the problem include:

Aquifer hydraulic conductivity	0.005 m/s
Aquifer thickness	10. m
Porosity	0.10203
Water density	1000. kg/m^3
Water compressibility	0./Pa
Rock compressibility	$5.\times10^{-7}$/Pa
Aquitard specific storativity	.0016/m
Aquitard hydraulic conductivity	$1.\times10^{-5}$ m/s
Aquitard thickness	50. m
Aquitard porosity	0.3265

Reeves et al. (1986c) present the results of the simulation which are depicted graphically on Figure 2-9 for a distance of 117.4 m from the pumping well. For times less than approximately 300 minutes, the SWIFT II solution slightly

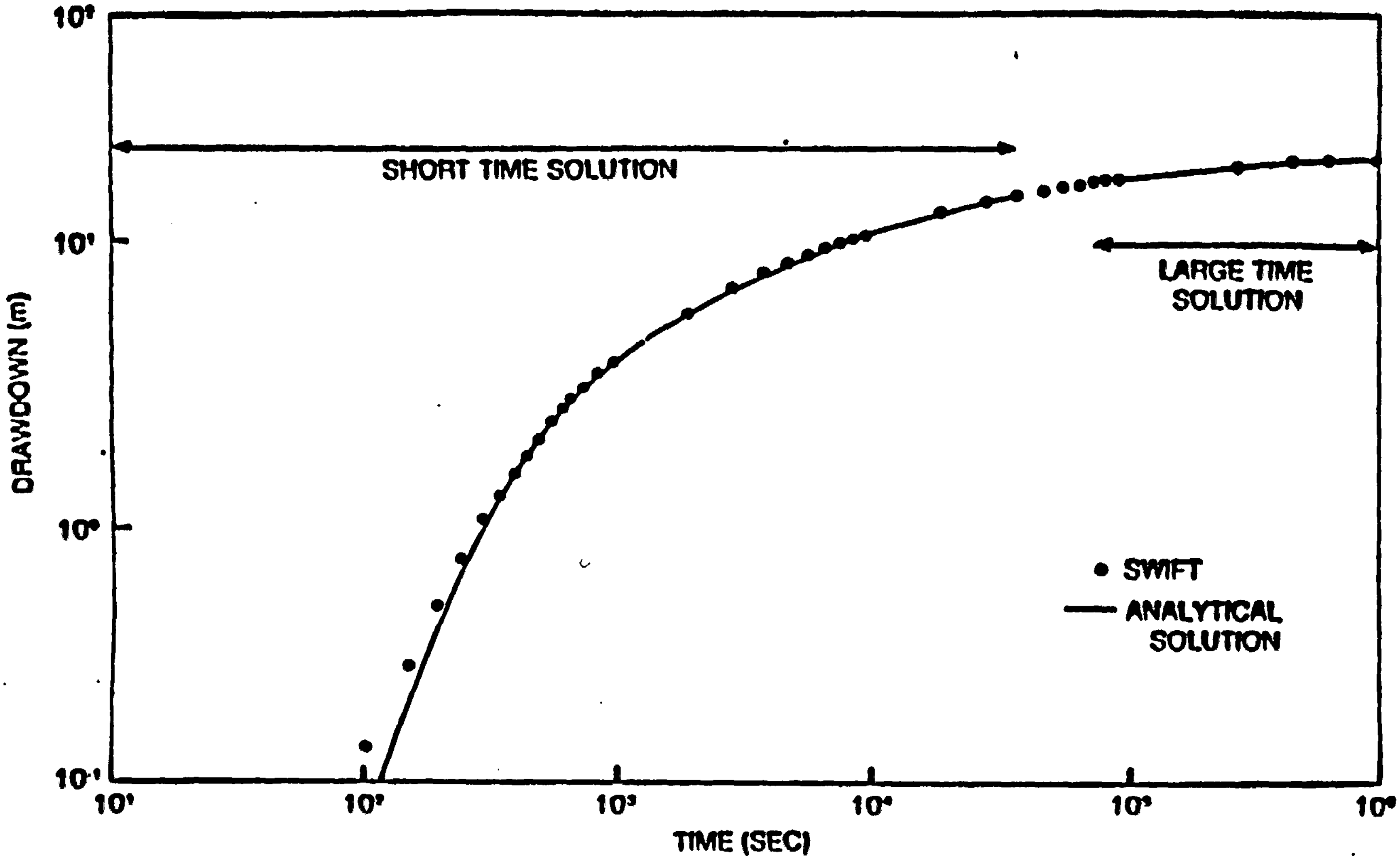

Figure 2-9 Results from SWIFT II and the Analytical Solutions of Hantush (1960) for a Radial Distance of 117.4 m. [Reeves et al., 1986c]

overpredicts the short time analytical solution. After 300 minutes the SWIFT II solution and the short time solution coincide. The SWIFT II solution agrees very well with the analytical solution for large times also. For the entire period of simulation, there is excellent agreement between the SWIFT II solution and the analytical solution.

The results of this SWIFT II simulation compare more favorably with the analytical solution than for the leaky aquifer simulation presented in Section 2.1.4. Because of the differences in the hydrologic parameters of the two problems, it is difficult to determine the reason one simulation produces better results than the other. One possible reason is the use of a local grid system with a constant head condition to represent leakage rather than an additional layer of global grid blocks with a zero flux condition applied to it.

2.1.6 The Dupuit-Forcheimer Steady-State Problem

In this problem the SWIFT II code is used to simulate the steady state flow in a homogeneous, isotropic, phreatic aquifer subject to a uniform recharge rate (Bear, 1972). A rectangular vertical plane block of soil, representing a phreatic aquifer, is subject to constant head boundary conditions of different elevations at each end. The lower boundary of the block is impermeable while recharge at a rate of 7.505×10^{-5} m/s enters the aquifer through the top of the block. This problem is designed to test several aspects of the SWIFT II code including a steady state solution, a pressure solution, vertical Cartesian geometry, a water table solution, pressure head boundary conditions, recharge rates, and SI units.

Reeves et al. (1986c) presented a description of the modeling of this problem. A vertical two-dimensional grid, 20 m wide and 1 m high, is used in the modeling. In the horizontal direction there were twenty columns of grid blocks, each 1 m long, and in the vertical direction there were twenty rows of grid blocks, each 0.05 m high. Altogether four hundred grid blocks were used to model the problem. A boundary condition was applied to three boundaries of the grid. On the left and right boundaries, constant head conditions of 0.75 m and 0.25 m were applied, respectively. A flux of 7.505 x 10^{-5} m/s was applied into the top boundary to represent aquifer recharge. No condition was applied to the lower boundary, which implies a zero flux or impermeable boundary condition.

The hydraulic conductivity used in the modeling was 0.03 m/s in both the horizontal and vertical directions which remained constant throughout the modeled region. Since this was a steady state problem, porosity and storage coefficients were not required for the simulation.

Results of the simulation are presented in Reeves et al. (1986c) and reproduced in Figure 2-10. Between the left boundary and ten meters, the SWIFT II solution and the analytical solution agree very well. Between ten meters and the right boundary, the SWIFT II solution overpredicts the analytical solution very slightly. Overall, the SWIFT II and analytical solutions agree very well.

On Figure 2-10, the region where the SWIFT II solution overpredicts the analytical solution is the area where the aquifer begins to thin drastically due to the water table decline. As a result, the aquifer transmissivity begins to decrease as one moves closer to the right boundary, resulting in steeper vertical and horizontal hydraulic gradients. Because the SWIFT II solution is a two-dimensional solution as opposed to the one-dimensional analytical solution, SWIFT II can simulate these vertical gradients while the analytical solution cannot. In essence, the analytical solution of the Dupuit-Forcheimer problem is an approximation to the way the

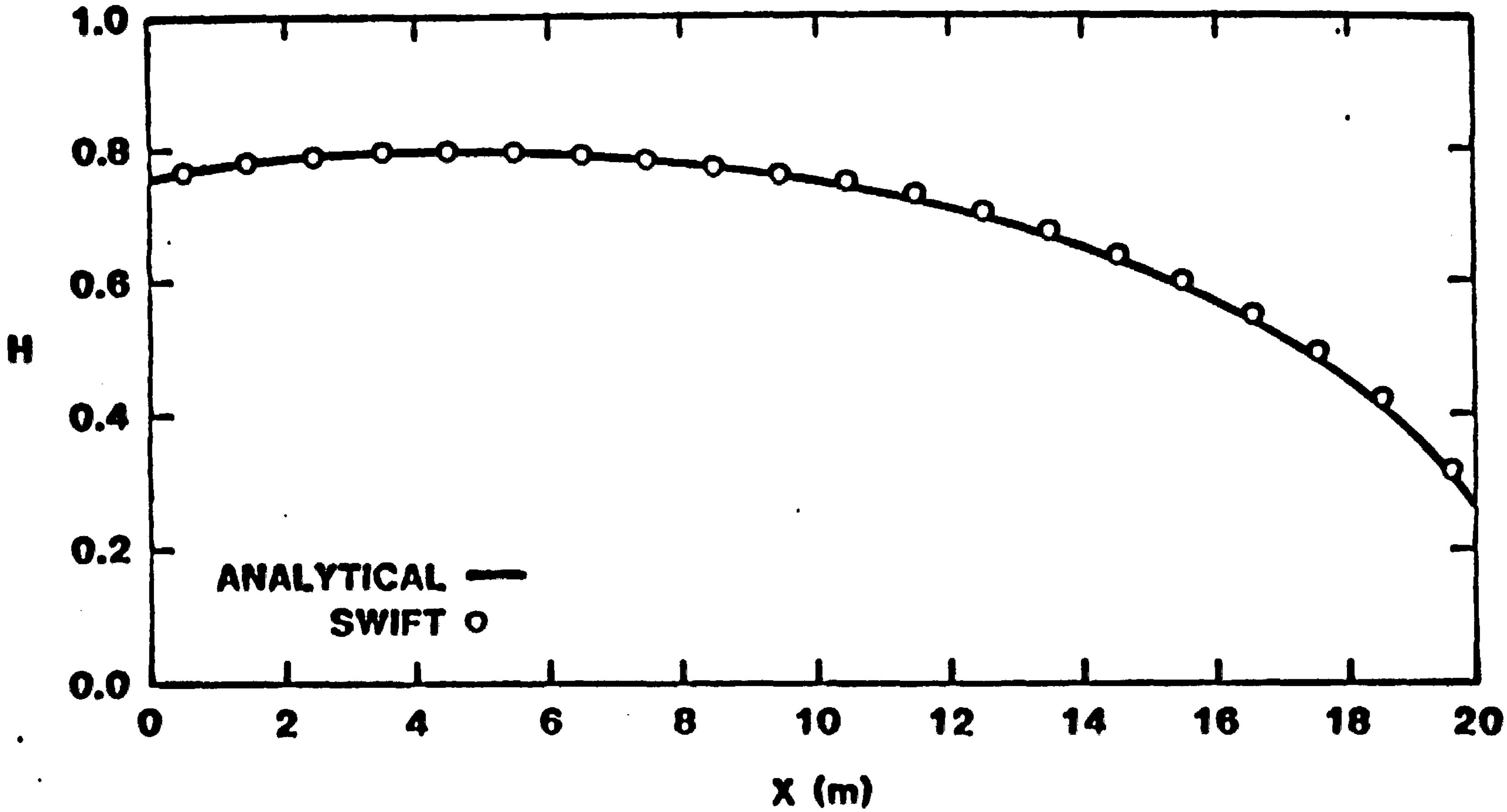

Figure 2-10 Steady-State Free-Water Surface for the Dupuit-Forcheimer Problem [Reeves et al., 1986c]

problem is formulated with the SWIFT II code. Therefore, the SWIFT II solution may be more accurate than the analytical solution for this problem.

2.1.7 The Boussinesq Transient-State Problem

In this problem the SWIFT II code is used to simulate transient flow in a homogeneous, isotropic phreatic aquifer (Bear, 1972). The water table in a rectangular, vertical phreatic aquifer is initially level. At some time the water level at one boundary is instantly lowered, causing the water table to decline with respect to time and space. This problem tests several aspects of the SWIFT II code including a transient solution, a pressure solution, a water table aquifer, vertical Cartesian geometry, pressure head boundary conditions, and SI units.

SWIFT II does not simulate the Boussinesq problem, but rather simulates two-dimensional flow in a plane, vertical aquifer. The Boussinesq problem is a one-dimensional horizontal flow approximation to the problem solved by SWIFT II. By choosing appropriate hydraulic parameters, SWIFT II can be forced to solve the Boussinesq problem.

The modeling of the problem is described in Reeves et al. (1986c). The grid consists of twenty blocks in both the horizontal and vertical directions. In the horizontal direction, the grid blocks are divided from left to right as follows: five blocks 0.01 m long, five blocks 0.05 m long, five blocks 0.10 m long, two blocks 0.50 m long, two blocks 1.0 m long, and one block 2.0 m long. The intent of the horizontal gridding keeps the distance of the right impermeable boundary far away from the observation points such that the modeled area is essentially infinitely long. In the vertical direction, each grid block is 0.05 m high, for a total of 1.00 m.

The top, right and bottom boundaries are zero flux boundaries. The left boundary is kept at a constant head equal to one-half the aquifer thickness. The initial head in the aquifer is based on a hydrostatic pressure distribution.

The hydraulic parameters include a horizontal hydraulic conductivity of 0.01 m/s, a vertical hydraulic conductivity of 100.0 m/s and a porosity of 0.50. The vertical hydraulic conductivity is relatively large compared to the horizontal conductivity in order to maintain an approximately horizontal flow in the porous media. This allows the SWIFT II code to approximate the Boussinesq problem more accurately.

The results of the simulation are presented in Reeves et al. (1986c) and summarized in Figure 2-11. Results for two distances, 0.025 m and 0.125 m, with respect to time are compared in dimensionless form to a solution presented in Bear (1972). The parameter, ζ is small for small distances and large times and large for large distances and small times. The figure uses small distances, as shown in the legend, and a range of times for the comparison. For small times the SWIFT II solution underpredicts the analytical solution, and for large times, the SWIFT II and analytical solutions compare very favorably. Reeves et al. attribute the discrepancy at small times to an initial rapid water table drop for the numerical solution. This may be caused by vertical gradients that form in the solution to the two-dimensional vertical plane flow problem. Except for early times, the comparison between the SWIFT II solution and the analytical solutions is very good. The differences at small time may be due to the fact that SWIFT II solves a two-dimensional vertical plane flow problem, while the analytical solution solves a one-dimensional horizontal flow approximation to the two-dimensional problem.

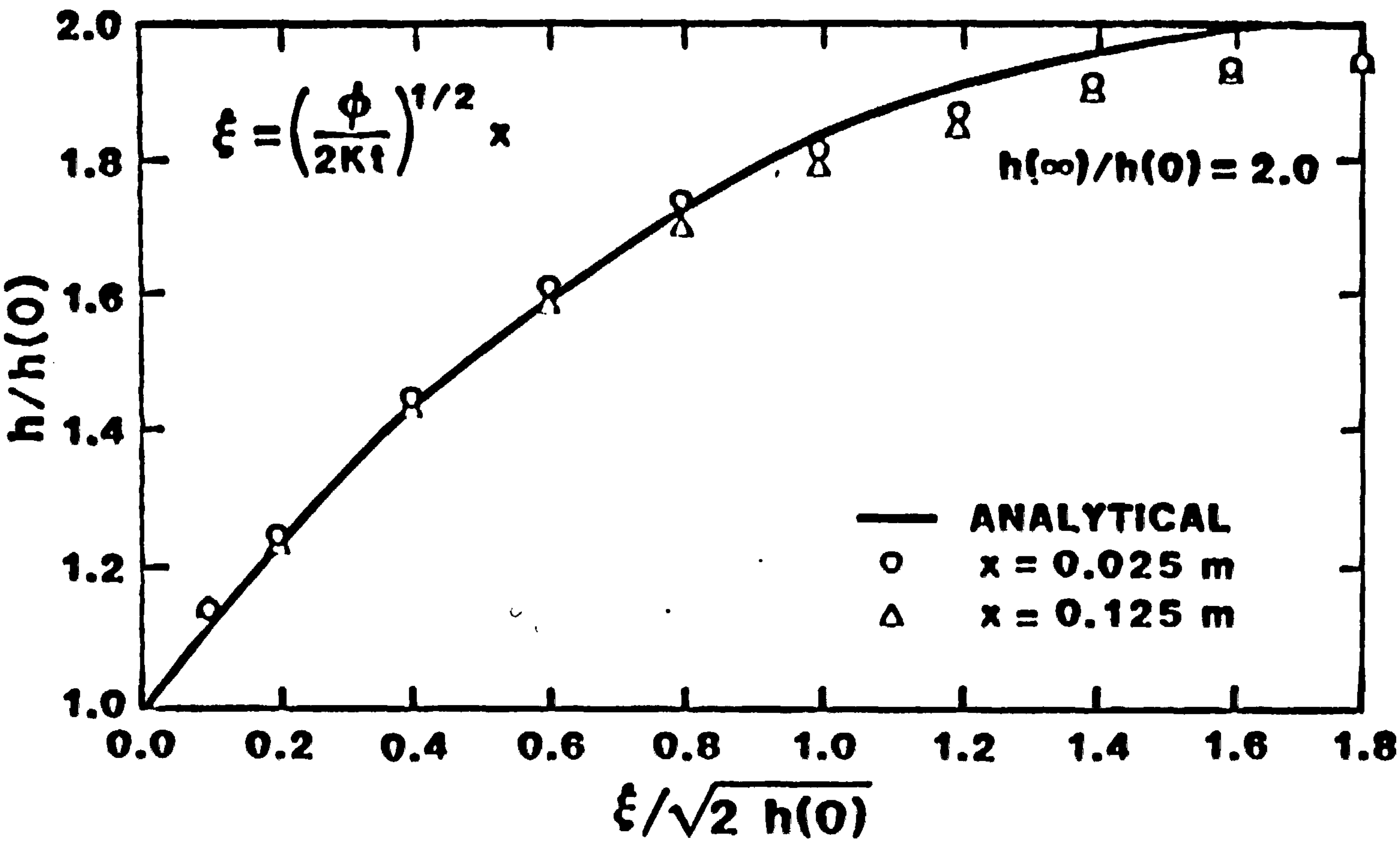

Figure 2-11 Time-dependent Free-Water Surface Elevation for the Boussinesq Problem [Reeves et al., 1986c]

2.2 VERIFICATION OF MASS TRANSPORT

2.2.1 One-Dimensional Transport with Chain Decay and Equal Retardation Parameters

In this problem SWIFT II is used to simulate the contaminant transport of a three-member radionuclide decay chain in a porous medium (Coats and Smith, 1964). Convection, dispersion and retardation are considered in modeling the one-dimensional problem, which is described in Ward et al. (1984a). An inventory of a chain of three radionuclides is released into a porous medium at one end of an infinitely long grid. As the radionuclides enter the porous media, they are subject to constant values of convection, dispersion and adsorption. The following aspects of the SWIFT II code are tested by this problem: contaminant transport including convection, dispersion, and retardation, radionuclide decay and generation of daughter components, waste-leach radionuclide-source model, Cartesian coordinates, English engineering units.

Ward et al. (1984a) present the modeling details of this problem. The grid is 254.2 ft long and is broken into three sections. The first section, whose end is located at the radionuclide source, consists of twenty 8.2 ft wide grid blocks. The second section consists of three 5.466667 ft wide grid blocks and the third of nine 8.2 ft wide blocks. The grid is designed to minimize numerical overshoot and is long enough such that the downstream boundary has no influence on the concentrations.

The flow rate was kept constant by application of constant pressure conditions at each end of the grid. The hydraulic gradient coupled with the hydraulic conductivity and porosity forces the ground-water velocity to remain constant at .656 ft/d.

The source of radionuclides is contained within a repository source block located in the first grid block. The source block contains an initial inventory of a parent radionuclide, but none of the daughter radionuclides. After the simulation begins, the concentration of the daughter radionuclides begins to increase within the repository. The radionuclides are moved into the system by flow of ground water through the repository, i.e. a type three boundary condition.

The hydrologic and mass transport properties used in the modeling are:

Darcy velocity	0.656 ft/d
Porosity	0.1
Dispersivity	8.5 ft
Retardation factor	9352

In addition the following data were known about the radionuclides:

Radionuclide	Half Life (yr)	Initial Concentration	Decay Fraction
1	433	1.	0.
2	15	0.	1.
3	6540	0.	1.

The equations were solved using the centered-in-space, centered-in-time approximations to the governing differential equation.

Ward et al. (1984a) present the comparison of the SWIFT II and analytical solutions which are reproduced in Figure 2-12. The SWIFT II breakthrough curves occur slightly faster in time than the analytical solution curves. For later times, generally greater than approximately five hundred years, the comparisons are excellent. Overall, the SWIFT II and analytical solution comparisons are very good.

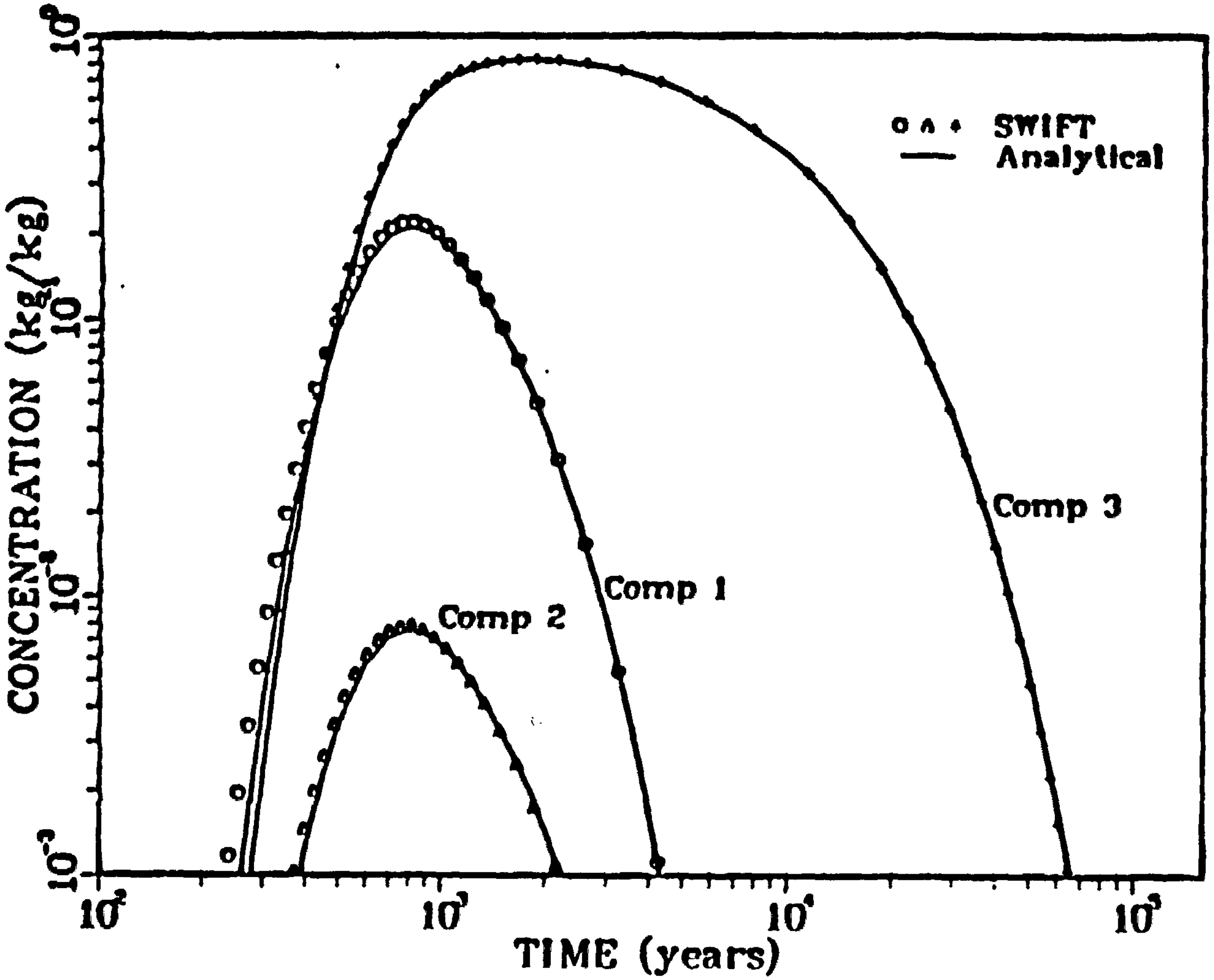

Figure 2-12 Radionuclide Discharge Concentration as a Function of Time. [Ward et al., 1984a]

2.2.2 One-Dimensional Transport with Chain Decay and Unequal Retardation Parameters

In this problem, the SWIFT II code is used to simulate the convective-dispersive transport of an initial inventory of a three-member radionuclide decay chain. The main difference between this problem and the previous one is that, in this problem, the retardation factor for each radionuclide is different. This problem corresponds to INTRACOIN problem one (INTRACOIN, 1984) and is described in INTRACOIN (1984), Ross et al. (1982), and Ward et al. (1984a).

This problem is similar to the previous one in many respects. An inventory of three radionuclides is leached into an infinitely long porous media, which is represented by a one-dimensional grid. As the radionuclides are transported, they are subject to convection, dispersion, retardation, and radioactive decay. However, the hydrologic and transport parameters are different for this problem than for the previous one. This problem is designed to test the following aspects of the SWIFT II code: contaminant transport of species with different retardation factors, radionuclide decay and generation of daughter components, waste-leach radionuclide-source model, Cartesian coordinates, and SI units.

A detailed description of the modeling of this problem is presented in Ward et al. (1984a). The grid is 800 m long and consists of 80 grid blocks, each 10 m wide with a cross-sectional area of 100 m^2. The downstream boundary is far enough away from the observation point that it has no effect on the concentration breakthrough curves. The grid block width and time step size were chosen to minimize numerical overshoot problems for the centered-in-time, centered-in-space approximation to the governing equations.

The flow rate was kept fixed by application of constant pressure conditions at each end of the grid. The hydraulic gradient coupled with the conductivity kept the Darcy velocity constant at 0.01 m/y.

The source of radionuclides is contained within a repository block located in the first grid block. The repository block contains an initial inventory of three radionuclides. As time progresses, the inventory of radionuclides changes because of radioactive decay, radioactive production, and leaching. The radionuclides are moved into the aquifer by flow of ground water through the repository, ie. a type three boundary condition. A zero mass flux boundary condition is imposed at the downstream boundary.

Four cases involving two decay chains and two sets of retardation factors were run for this problem. The radionuclide data is summarized below for the first radionuclide chain:

Radionuclide	Inventory (kg)	Half Life (yrs)	Retardation (Run 1)	Retardation (Run 2)
^{234}U	$1.58x10^{-1}$	$2.445x10^{5}$	$3.x10^{2}$	$6.x10^{1}$
^{230}Th	$4.9x10^{-4}$	$7.700x10^{4}$	$2.x10^{4}$	$5.x10^{2}$
^{226}Ra	$4.0x10^{-6}$	$1.600x10^{3}$	$1.x10^{4}$	$2.x10^{1}$

The data for the second radionuclide chain is:

Radionuclide	Inventory (kg)	Half Life (yrs)	Retardation (Run 1)	Retardation (Run 2)
^{245}Cm	$4.0x10^{-3}$	$8.5x10^{3}$	$5.x10^{3}$	$6.x10^{1}$
^{237}Np	$1.4x10^{0}$	$2.14x10^{6}$	$7.xx10^{2}$	$2.x10^{2}$
^{233}U	$4.1x10^{-4}$	$1.592x10^{5}$	$3.x10^{2}$	$6.x10^{1}$

Other hydrologic data needed to solve the problem are:

Leach time	$1.x10^{5}$ yr
Darcy velocity	$1.x10^{-2}$ m/yr
Porosity	$1.x10^{-2}$
Dispersivity	$5.x10^{1}$ m
Observation distance	$5.x10^{2}$ m

Ward et al. (1984a) describe the modeling results, which are presented on Figures 2-13 and through 2-16. In all cases, for all radionuclides, the SWIFT II results compare favorably with the analytical solution. On Figure 2-15, ^{245}Cm does not show because it has decayed away and its concentrations are negligible.

2.2.3 Transport of a Decaying Radionuclide in a Fractured Porous Medium (prismatic representation of matrix)

In this problem SWIFT II is used to estimate the concentration of a decaying radionuclide in a fracture connected to a porous medium (Tang et al., 1981). The problem is described in Reeves et al. (1986c). A radionuclide is convected at a constant velocity and dispersed along a single, infinitely long fracture. The radionuclide also diffuses from the fracture into an infinitely large porous medium. The concentration of the radionuclides is kept constant at the inlet to the fracture. The problem tests the following aspects of the SWIFT II code: contaminant transport in global coordinates, contaminant transport in local coordinates, radionuclide decay, Cartesian coordinates, and SI units.

Reeves et al. (1986c) provide a description of the modeling of this problem. Twenty one global grid blocks are used to model the problem. Global grid block lengths are variable, ranging from a minimum of 0.0005 m for the two grid blocks near the radionuclide source to a maximum of 1.024 m for nine grid blocks at the grid location opposite the radionuclide source. Grid blocks between the minimum and maximum grid block lengths are expanded such that a grid block length is twice the size of the one preceding it. The overall length of the grid is 10.24 m, which is long enough such that the boundary condition at the end of grid opposite the radionuclide source does not impact the concentrations. The global grid blocks are 1.0 m wide and 2.4 m high. Attached to each global grid block

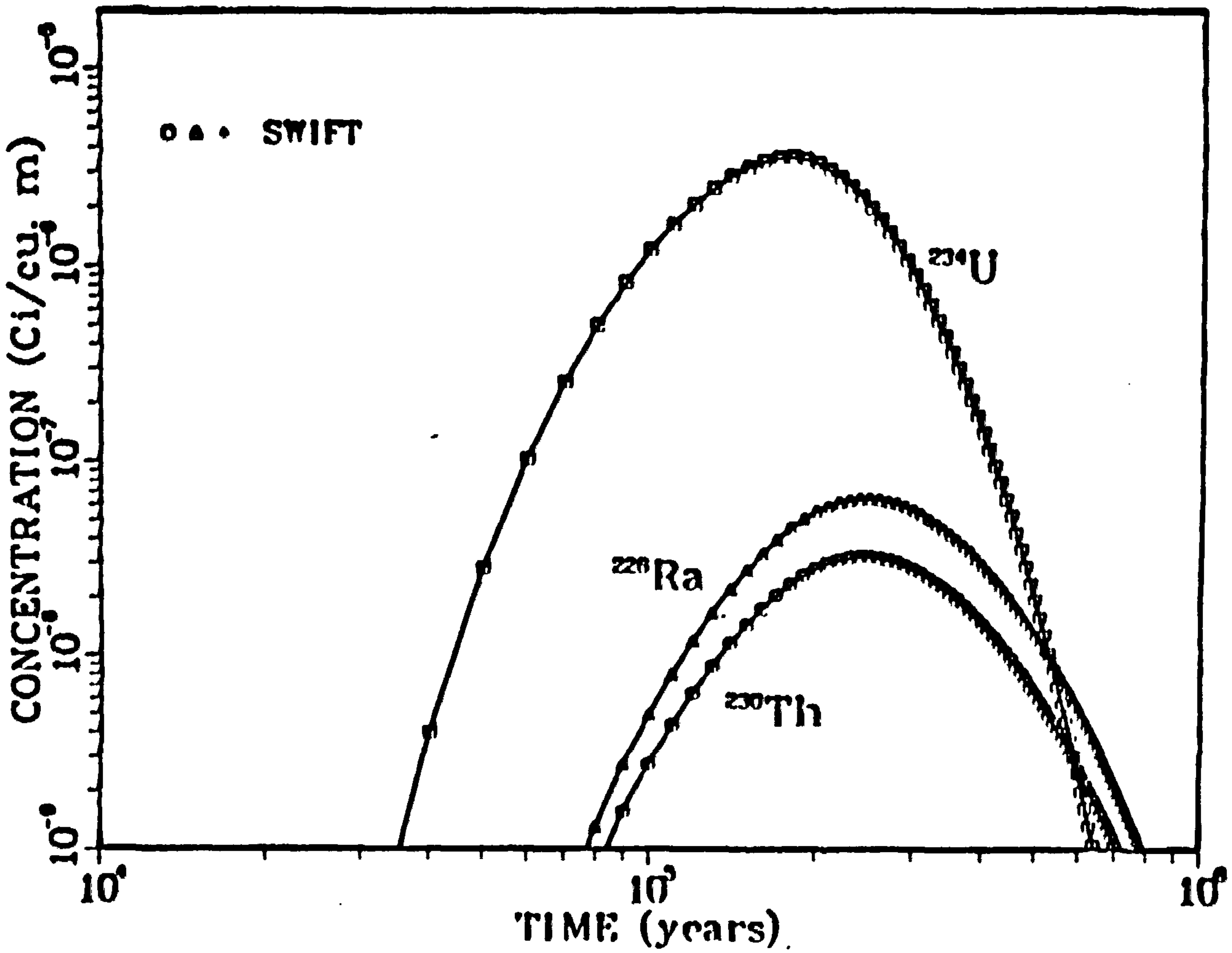

Figure 2-13 Radionuclide Discharge Concentration as a Function of Time - Chain 1, Run 1. [Ward et al., 1984a]

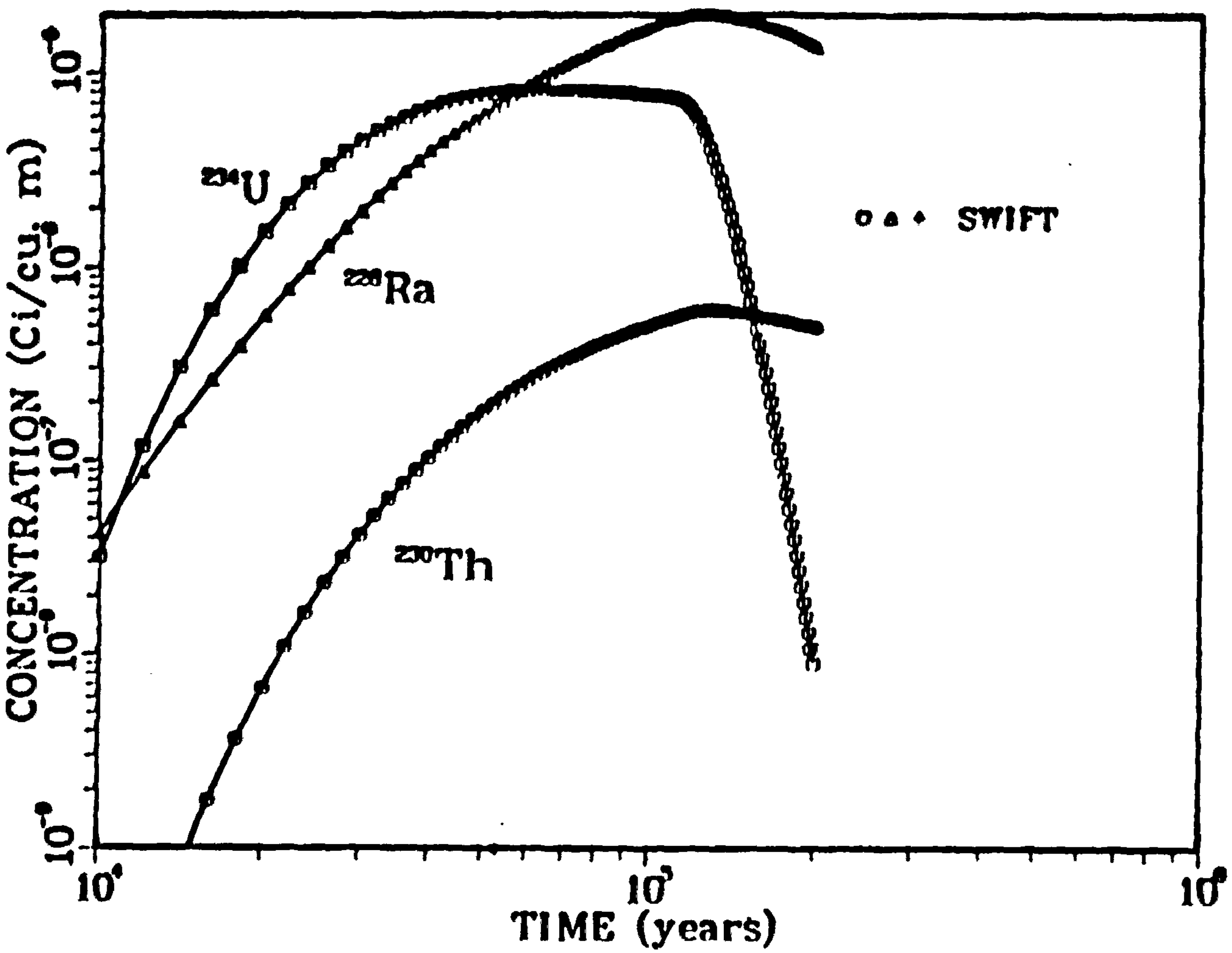

Figure 2-14 Radionuclide Discharge Concentration as a Function of Time - Chain 1, Run 2. (Ward et al., 1984a)

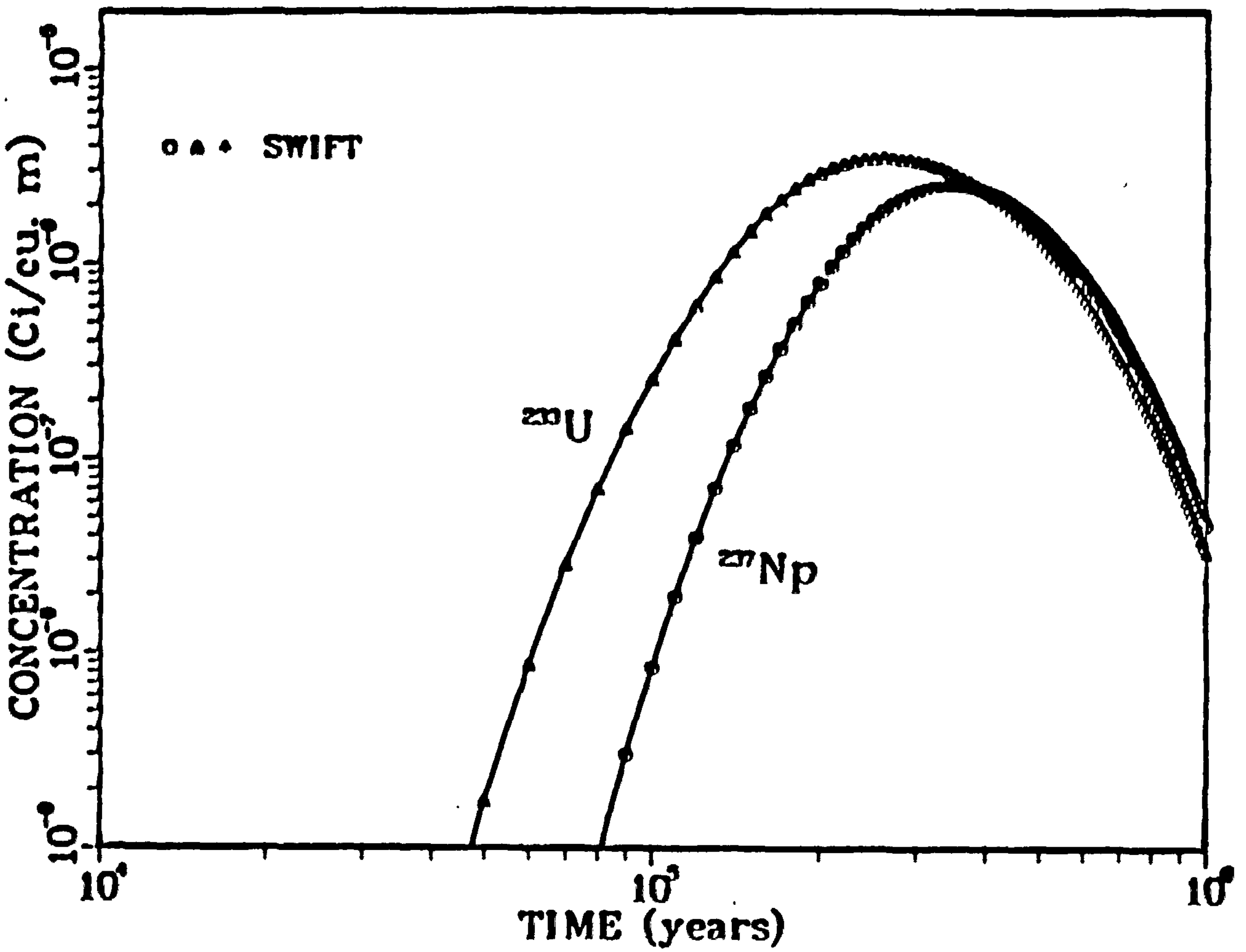

Figure 2-15 Radionuclide Discharge Concentration as a Function of Time - Chain 2, Run 1. [Ward et al., 1984a]

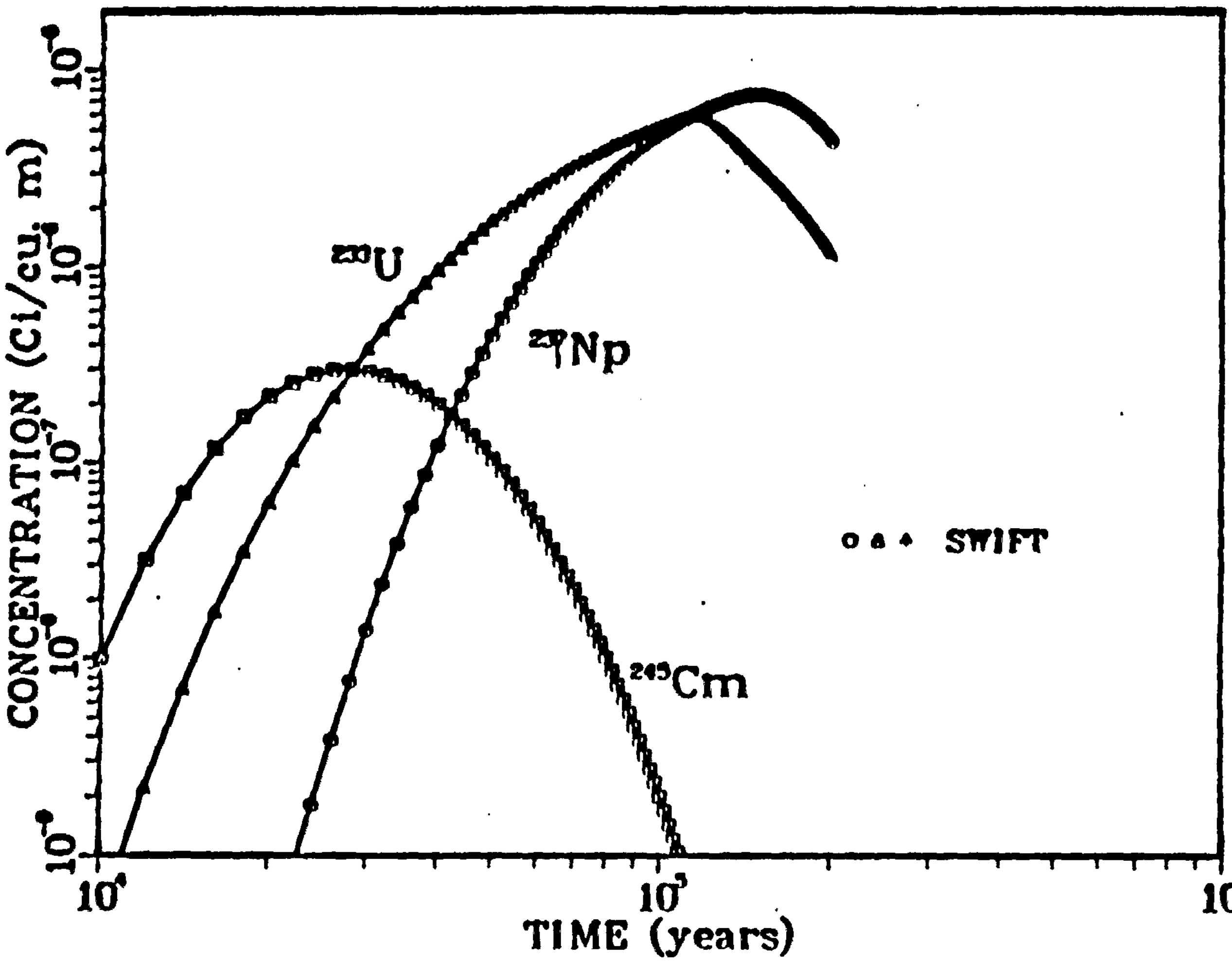

Figure 2-16 Radionuclide Discharge Concentration as a Function of Time - Chain 2, Run 2. [Ward et al., 1984a]

is a local grid consisting of prismatic blocks internal to the global blocks. Each local grid is 1.2 m long and contains 12 nodes, of which the distance between the first pair of nodes is 0.01 m. Subsequent node-to-node distances for the local grid are generated automatically by SWIFT II.

A steady-state flow rate is maintained by injection of 1.157×10^{-11} m^3/s water at the radionuclide source end of the grid and extraction of an equal amount of water at the other end of the grid. This maintains the flow velocity of water of 0.01 m/d within the fracture. The concentration of the radionuclide at the source is maintained at 1.0. A zero concentration flux is applied at the opposite end of the grid. Initially, there is no concentration of radionuclides in either the fracture or porous matrix.

The simulation is based on the following hydrologic and contaminant transport data:

Fracture width	$1. \times 10^{-4}$ m
Matrix porosity	0.01
Matrix tortuosity	0.1
Fracture dispersivity	0.5 m
Molecular diffusion in water	1.6×10^{-9} m^2/s
Radionuclide half-life	12.35 yr
Matrix retardation	1.0
Fracture velocity	0.01 m/d
Fracture porosity	1.0

Reeves et al. (1986c) present the comparison of the SWIFT II results with the analytical solution. Figures 2-17 and 2-18 graphically depict the comparisons. Figure 2-17 presents the comparison of the SWIFT II and analytical solutions for points along the fracture at times of 100, 1000, and 10,000 days. For a time of 100 days, there is very good agreement between the solutions for distances less than approximately 0.5 m. At distances greater than approximately 0.7 m, the SWIFT II solution predicts slightly higher concentrations than the analytical solution. For times of 1000 and 10,000 days, the

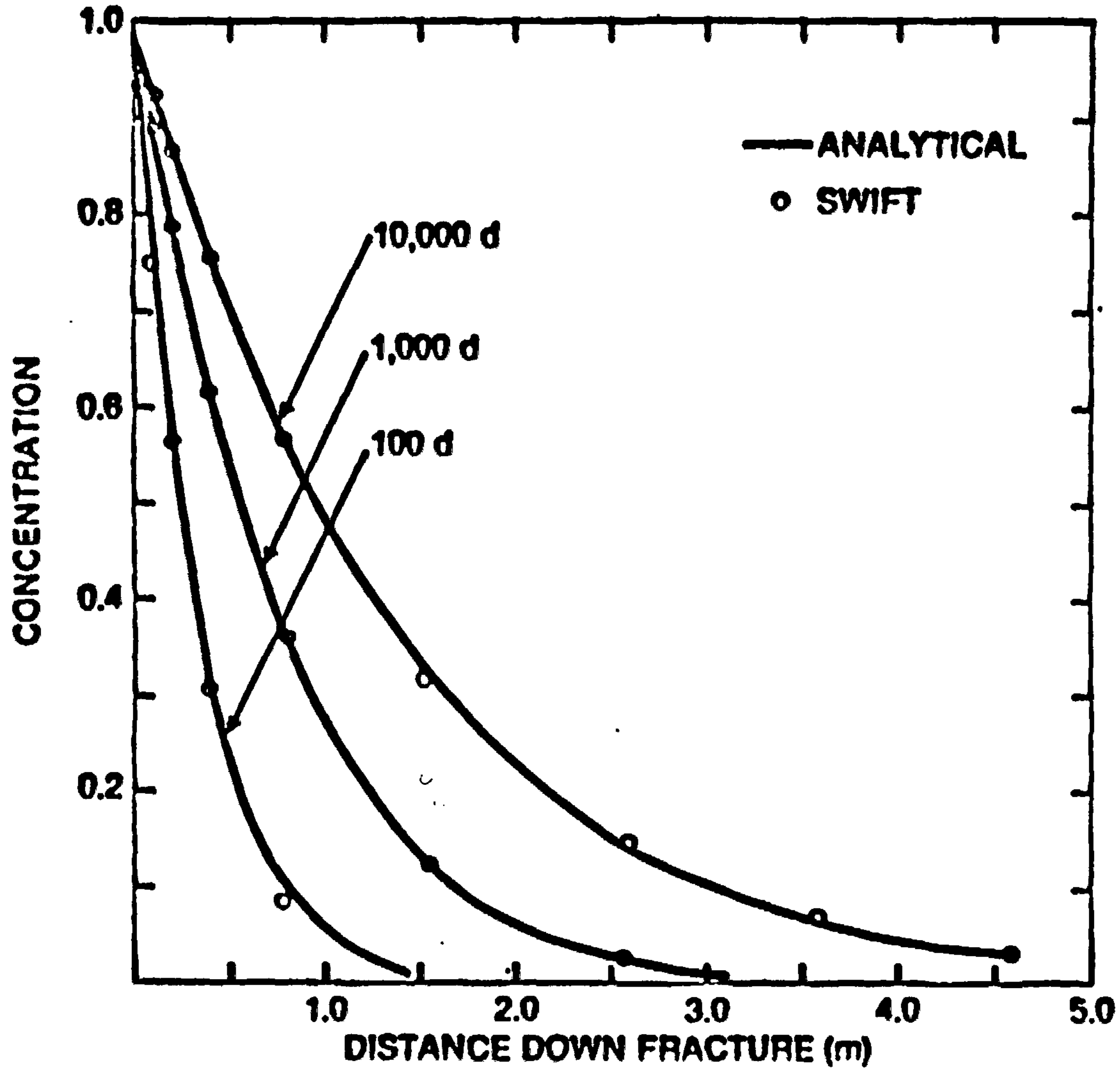

Figure 2-17 Radionuclide Concentrations Within the Fracture for a Prismatic Characterization of the Rock Matrix. [Reeves et al., 1986c]

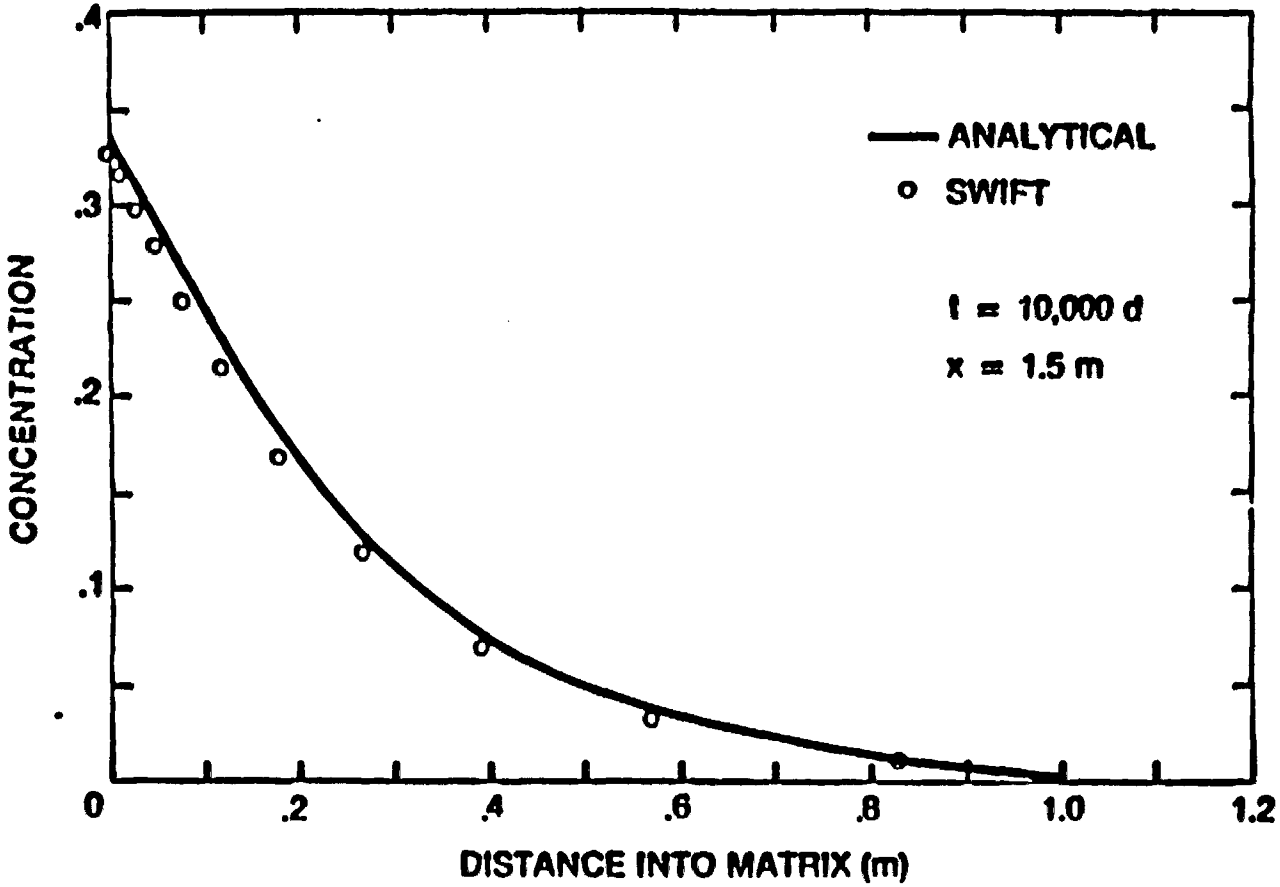

Figure 2-18 Radionuclide Concentrations Within the Rock Matrix for a Prismatic Characterization of the Rock Matrix. [Reeves et al., 1986c]

SWIFT II and analytical solutions compare extremely well for the length of each curve. Overall, there is excellent agreement between the SWIFT II and analytical solutions for radionuclide concentrations within the fracture.

Figure 2-18 presents a comparison of the SWIFT II and analytical solutions for radionuclides within the porous matrix at a distance of 1.5 m down the fracture and a time of 10,000 days. The SWIFT II solution slightly overpredicts the concentrations from the analytical solution for distances from the fracture of less than 0.6 m. At a distance of approximately 0.82 m into the porous matrix , the SWIFT II and analytical solutions agree. The trend of the SWIFT II solution appears to follow that of the analytical solution. The agreement between the SWIFT II and analytical solutions within the porous matrix is good.

2.2.4 Transport of a Decaying Radionuclide in a Fractured Porous Medium (spherical representation of matrix)

In this problem the SWIFT II code is used to simulate the transport of a radionuclide in a fractured porous medium. The problem is described in Reeves et al. (1986c). A radionuclide is injected into a fractured, porous medium that is initially free of the radionuclide. The radionuclide is transported by dispersion and convection in the fractures and by diffusion in the porous matrix. The porous matrix is represented by spheres. This problem is designed to test the following aspects of the SWIFT II code: steady-state pressure solution, transient radionuclide solution, radionuclide transport by convection and dispersion, retardation, diffusion in a porous matrix, spherical representation of the porous matrix, and SI units.

A description of the modeling setup is presented in Reeves et al. (1986c). The grid consists of 21 grid blocks. The first grid block is large and is used as a well-mixed reservoir to provide a source of radionuclides to the subsequent grid blocks. The next twenty grid blocks are each 1.0 m deep, 2.4 m high, and of variable lengths. The lengths of these twenty grid blocks are: 5.0×10^{-4} m, 1.0×10^{-3} m, 2.0×10^{-3} m, 4.0×10^{-3} m, 8.0×10^{-3} m, 1.6×10^{-2} m, 3.2×10^{-2} m, 6.4×10^{-2}m, 0.128 m, 0.256 m, 0.512 m, and nine blocks at 1.024 m. Local grid blocks used to represent the porous matrix are attached to all the global grid blocks except the first one, which represents the large well-mixed reservoir. The local grids are placed internally to the global grid blocks. The block sizes are generated automatically by the SWIFT II code, starting with grid block size of 0.01 m and continuing until all 12 grid blocks total 1.2 m in length, the sphere radius.

A steady-state flow is maintained in the system by placing a well at each end of the grid. The well at the radionuclide source end of the grid is used to inject 1.157×10^{-11} m^3/s of water into the system, while the same amount of water is withdrawn from the well at the other end of the grid. This flow rate, coupled with the 2.4 m height of the grid block and a fracture porosity of 4.167×10^{-5}, produces a ground-water velocity of 0.01 m/d in the fracture.

Initially, there is no radionuclide in any grid block except the first one, the well mixed reservoir. This first grid block essentially acts as a constant-source boundary condition. As the radionuclide within it decays and leaves, the radionuclide is replaced so that the concentration of the reservoir always remains constant at 1.000. A zero flux boundary condition is applied at the other end of the system.

Other hydraulic and transport parameters include a retardation of one in both the fracture and the matrix, a fracture porosity of 4.167×10^{-5}, a matrix porosity of 0.01, a fracture dispersivity of 0.50, and a matrix diffusivity (i.e. molecular diffusion times matrix porosity times matrix tortuosity) of 5.787×10^{-13} m/s. Molecular diffusion within the fracture, and convection and dispersion within the porous matrix are neglected.

The results of this simulation are presented in Reeves et al. (1986c) and are shown in Figures 2-19 and 2-20. Figure 2-19 presents a comparison of transport in the fracture between the SWIFT II results and both the numerical simulation from the FTRANS code and the analytical solution of Rasmuson (1984). Overall, the SWIFT II solution agrees with both the FTRANS code and analytical solutions very well. The SWIFT II code seems to track the analytical solution better than the FTRANS code for distances greater than approximately 1.0 meter and a time of 441 days. Both numerical codes compare very well with the analytical solution for later times, with the SWIFT II code providing a slightly better comparison.

Figure 2-20 presents a comparison of transport in the matrix at one meter into the fracture between the SWIFT II and the FTRANS codes. The SWIFT II solution overpredicts the FTRANS solution at a time of 441 days. The largest difference occurs at the fracture-matrix interface and the difference decreases with distance into the matrix. Because the SWIFT II solution overpredicts the FTRANS solution at one meter into the fracture, it should be expected that the SWIFT II solution overpredicts the FTRANS solution in the matrix at one meter into the fracture also. At one meter into the fracture, the comparison between the SWIFT II solution and the analytical solution is very good and it should be expected that the SWIFT II solution would agree with the analytical solution for the

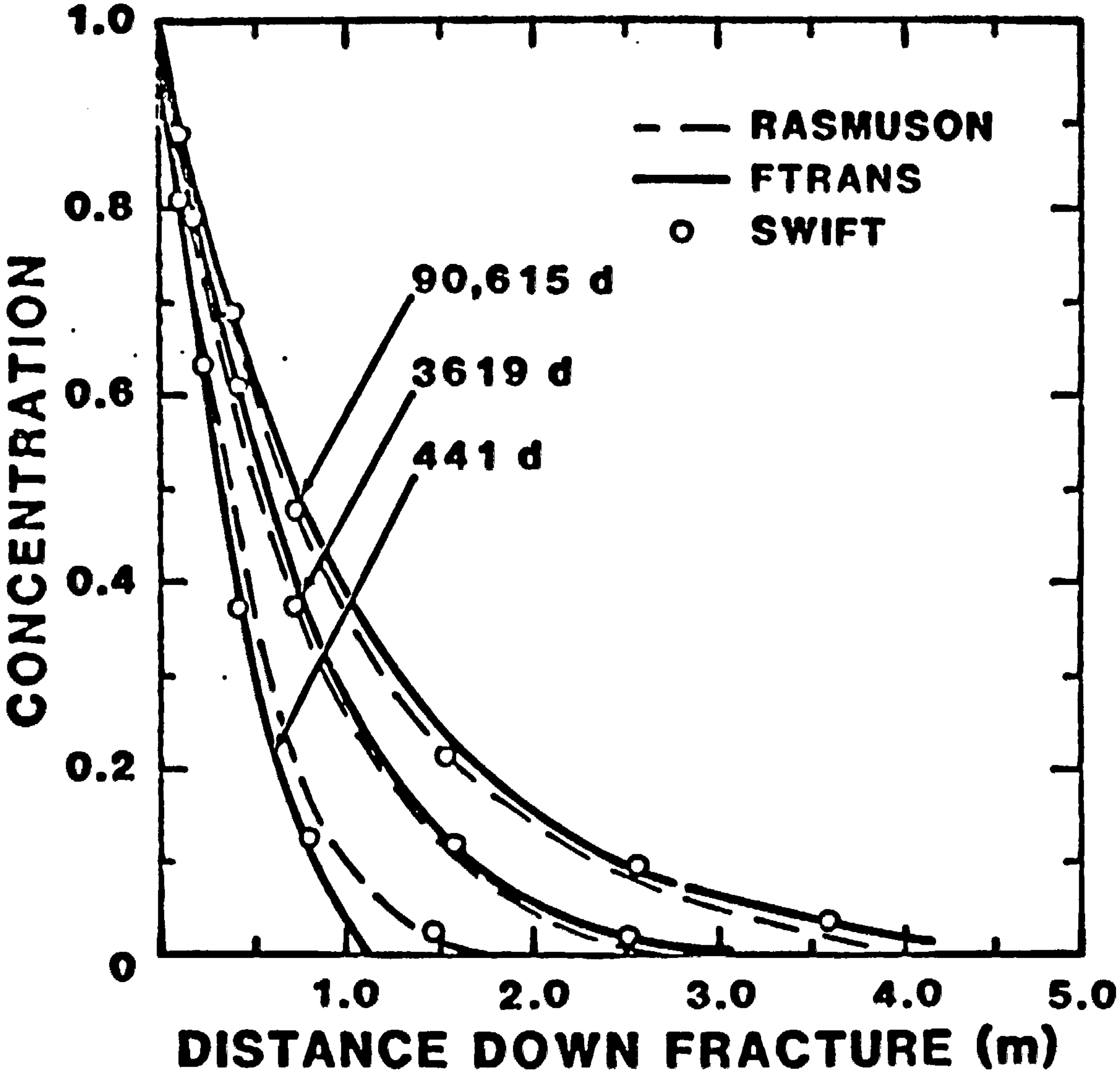

Figure 2-19 Radionuclide Concentrations Within the Fracture for a Spherical Characterization of the Rock Matrix. [Reeves et al., 1986c]

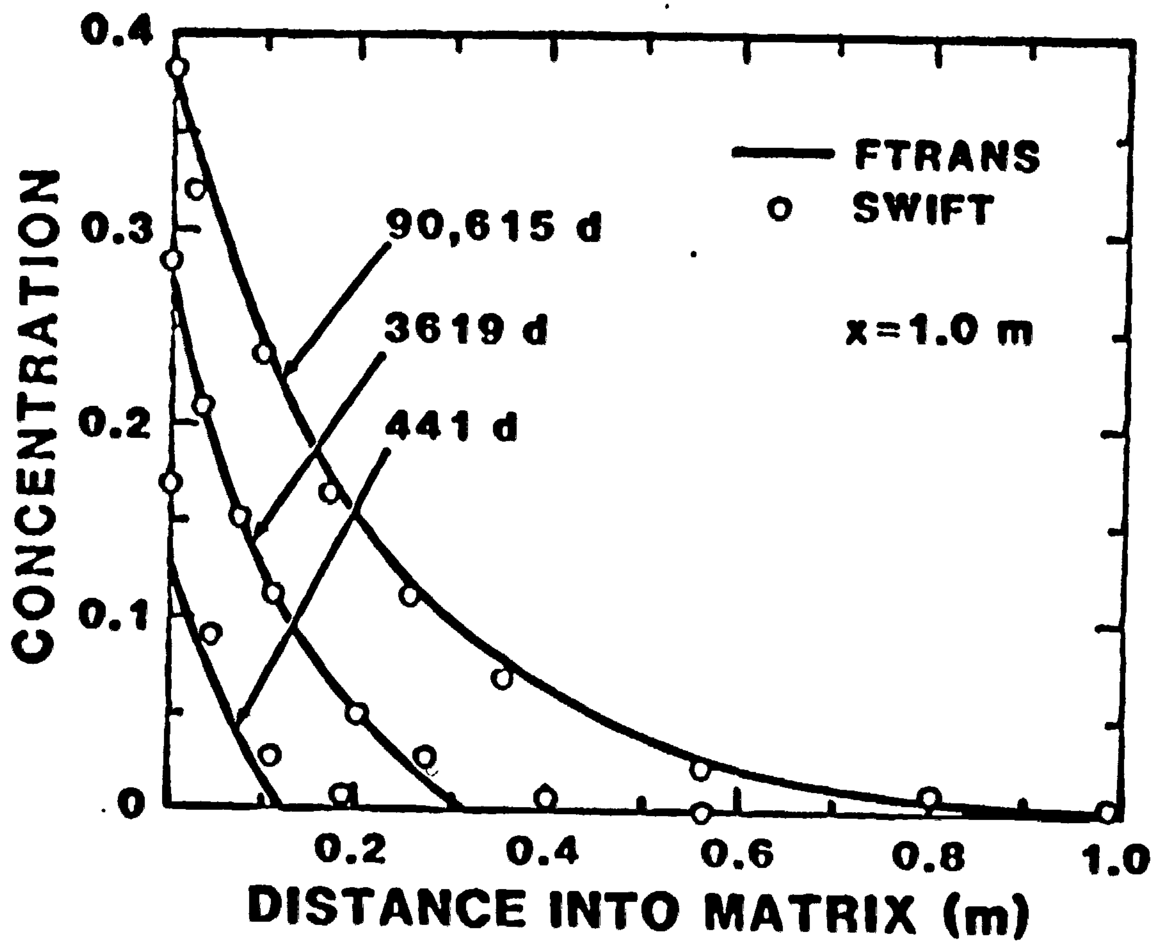

Figure 2-20 Radionuclide Concentrations Within the Rock Matrix for a Spherical Characterization of the Rock Matrix. [Reeves et al., 1986c]

porous matrix. For the larger times, the SWIFT II solution agrees very well with the analytical solution for small distances. At larger distances the SWIFT II solution slightly overpredicts the FTRANS solution.

Overall, the SWIFT II agrees very well with the analytical solution. However, the SWIFT II solution shows some small discrepancies when it is compared with the FTRANS solution. Because this is a verification exercise, more weight should be given to the excellent SWIFT II comparison with the analytical solution.

2.3 VERIFICATION OF HEAT TRANSPORT

2.3.1 One-Dimensional Convective-Dispersive Heat Transport

For this problem, the SWIFT II code is used to model a one-dimensional, convective-dispersive heat transport equation (Coats and Smith, 1964). Ward et al. (1984a) briefly describe the problem. In this problem a hot liquid is injected into an infinitely long, one-dimensional, homogeneous, confined aquifer. There is no heat loss through the aquifer confining layers and buoyancy of water is neglected. The problem is designed to test the following aspects of the SWIFT II code: thermal convection, thermal dispersion, thermal conduction, thermal retardation, aquifer influence functions, heat injection by wells, and SI and English engineering units.

Two types of boundary conditions are modeled at the point of injection (Ward et al., 1984a). The first condition, a type one or Dirichlet condition, assumes that the water temperature at the point of injection is kept at a constant value, i.e. $T(x=0,t) = T_I$, where T is temperature, T_I is the temperature at the boundary, x is distance, and t is time. The second boundary condition, known as a type three boundary condition, is based on conservation of energy principles. It states that heat injected at the boundary enters the aquifer due to convection and dispersion. Mathematically, this is written as $VT_I = VT - D \frac{\partial T}{\partial X}$, where V is ground-water velocity and D is a combination of fluid dispersion and fluid/rock conduction.

Ward et al. (1984a) provide details of the modeling of this problem. To model the semi-infinite system, a 609.6 m length of aquifer was used. The aquifer was long enough so that the boundary condition opposite the injection boundary would not affect the results. The one-dimensional grid consisted of 20 grid blocks, each with a width of 30.48 m and a height of 0.3048 m, which is the aquifer thickness. The grid and time steps were chosen so that numerical overshoot was minimized. Both centered-in-space and centered-in-time differencing were used.

Two problems were run, one with the type one boundary condition at each end of the grid and the other with the type three condition at each end of the grid. The type three boundary condition at the injection end of the grid is handled as a well injecting a hot liquid, while at the other end, a well withdraws the aquifer fluid. The hydrologic and thermal properties are:

Thermal conductivity of the medium	2.16 W/(m-°C)
Heat capacity of the rock	2.01×10^6 J/(m^3-°C)
Porosity	0.1
Density of rock	1602 kg/m^3
Dispersivity	14.4 m
Darcy velocity	3.53×10^{-7} m/s
Specific heat of fluid	4185 J/(kg°C
Density of fluid	1000 kg/m^3
Initial temperature	37.78 °C
Injection temperature	93.33 °C

Results of the modeling are presented in Ward et al. (1984a) and on Figure 2-21. The figure presents results for both boundary condition types. The results are plotted as

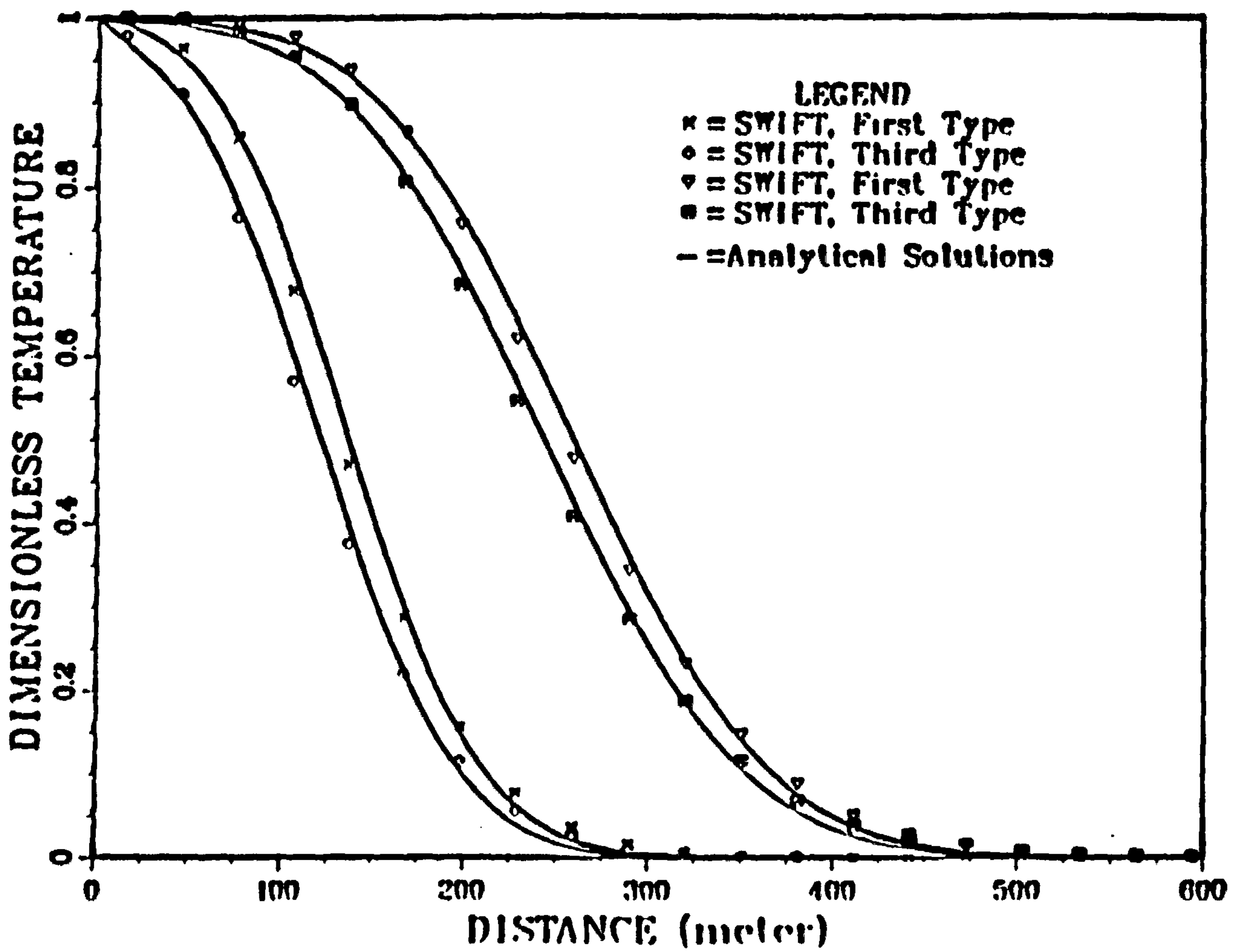

Figure 2-21 Dimensionless Temperature Profiles at Two Values of Time. [Ward et al., 1984a]

dimensionless temperature, $(T - T_o)/(T_I - T_o)$, versus distance. For both types of boundary conditions, the SWIFT II results compare very well with the analytical solution. There does not appear to be either any numerical dispersion or overshoot. This reflects the proper grid block and time sizes when performing the numerical calculations.

2.3.2 Linear Heat Transport During Injection

In this problem SWIFT II is used to model the injection of cold water into a hot water aquifer (Avodonin, 1964). The problem is described in Ross et al. (1982). A one-dimensional, infinitely long, homogeneous, aquifer containing hot water is injected at one end with cold water. Heat transport within the aquifer occurs by thermal convection and thermal conduction. Buoyancy of the fluid is neglected. Heat is allowed to escape from the aquifer to the over/underburden confining the aquifer. In the over/underburden, heat transport occurs by thermal conduction in the vertical direction only. This problem is designed to test the following capabilities of the SWIFT II code: thermal convection, thermal conduction, thermal retardation, thermal conduction in confining layers, heat loss to confining layers, and SI and English engineering units.

Ward et al. (1984a) present details of the modeling of this problem. The grid was designed to minimize numerical overshoot. Time steps were calculated internally by SWIFT II to minimize numerical overshoot. Centered-in-space and centered-in-time schemes were adopted for solving the equations. The grid consisted of 250 grid blocks, each 0.2 m wide, 1 m thick and 100 m high, the height of the aquifer. The overburden and underburden each consisted of 7 grid blocks which were capable of heat conduction only. Grid spacing for the over/underburden blocks were 0.25 m, 0.50 m, 0.75 m, 1.0 m, 2.0 m, 4.0 m, and 10.0 m. The temperature was set to 160°C at the injection end of the grid. A type three boundary condition at a temperature of 170°C was applied at the other end of the grid. The initial temperature was 170°C. A steady state flow with a volumetric flow rate of .010881 m^3/S was set up prior to injection of the cold fluid. The following hydrologic and thermal properties were used in the modeling:

Injection rate	10 kg/s
Injection temperature	160 °C
Initial temperature	170 °C
Thermal conductivity over/underburden	20 W/(m-°C)
Specific heat, over/underburden	1000 J/(kg-°C)
Density, over/underburden	2500 kg/m^3
Thermal conductivity, aquifer	20 W/(m-°C)
Specific heat, aquifer	1000 J/(kg-°C)
Density, aquifer	2500 kg/m^3
Specific heat, water	4185 J/(kg-°C)
Density, water	919 kg/m^3
Aquifer thickness	100 m
Aquifer porosity	0.2

Ward et al. (1984a) present results of the modeling of this problem. A plot of temperature versus time for a distance of 37.5 m downstream from the injection point is presented on Figure 2-22. Between one day and two and one-half days, the SWIFT II results are slightly higher than the analytical solution results. After approximately three and one-quarter days, the SWIFT II solution appears to oscillate slightly. At other times the SWIFT II results seem to compare very favorably with the analytical solution results. Overall, the SWIFT II and analytical solutions agree very well.

A plot of temperature versus distance for a time of 130,000 seconds after the onset of injection is presented on Figure 2-23. Between the injection point, and sixteen meters downstream from the injection point, the SWIFT II results track the analytical solution results extremely well. At distances greater than sixteen meters downstream, the SWIFT II results seem to overpredict the analytical results very slightly. Overall, though, the SWIFT II results compare very favorably with the analytical solution results.

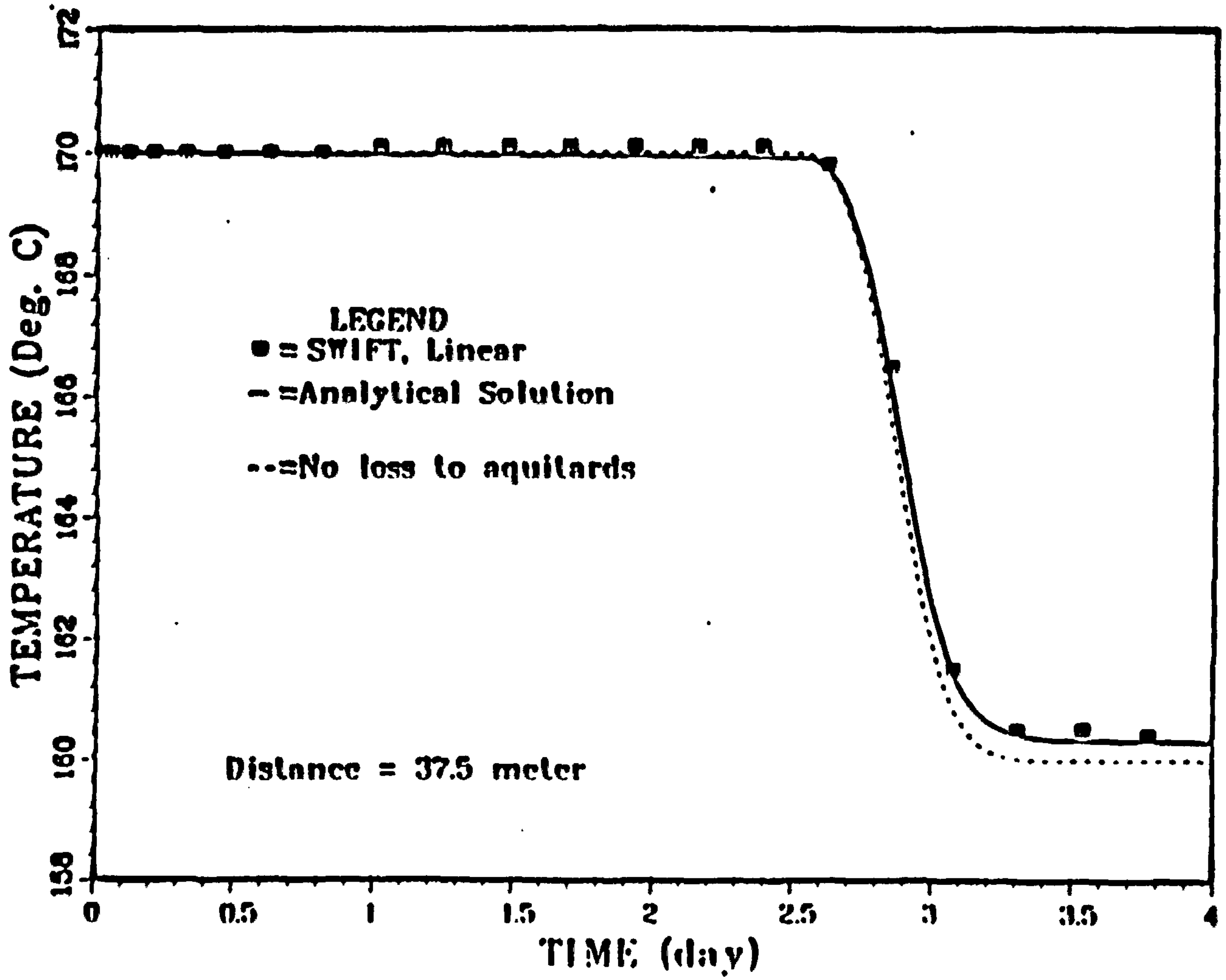

Figure 2-22 Temperature as a Function of Time at a Fixed Distance for a Linear Aquifer System. [Ward et al., 1984a]

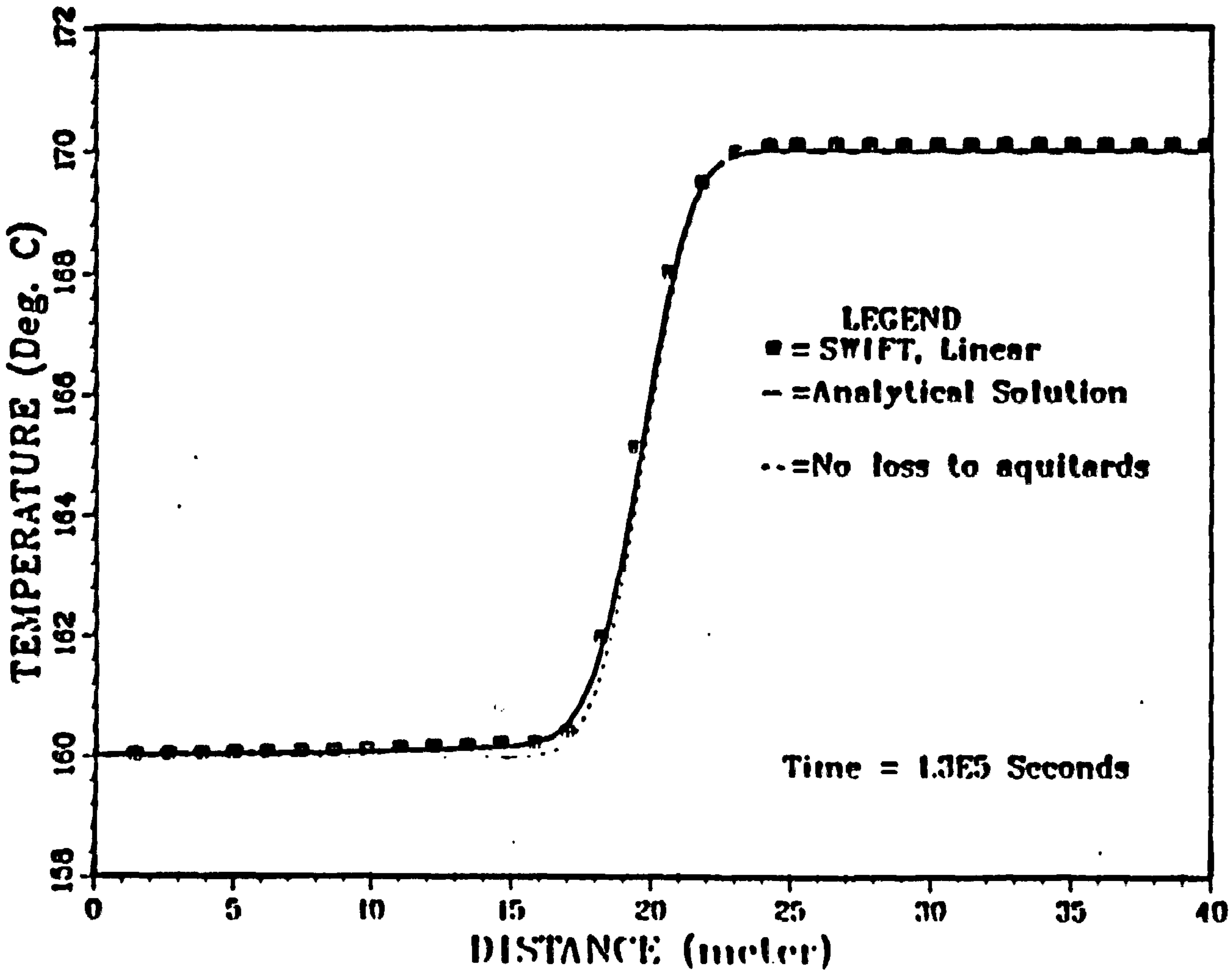

Figure 2-23 Temperature as a Function of Distance at a Fixed Time for a Linear Aquifer System. [Ward et al., 1984a]

2.3.3 Radial Heat Transport During Injection

For this problem SWIFT II is used to model injection of cold water into a hot radial aquifer (Avodonin, 1964). The problem is described in Ross et al. (1982) and, except for this problem being formulated in radial coordinates, is the same as the previous heat transport problem. This problem tests the use of radial coordinate systems in the SWIFT II code, in addition to the aspects listed in the heat transfer problem described in the previous section.

Ward et al. (1984a) present the details of the modeling of this problem. The radial grid consisted of 30 grid blocks. The distance from the center of the injection well to the center of the first grid block was 0.7655922 m. Distances from the center of the injection well to the center of subsequent grid blocks were approximately 1.28 times the distance to the center of the previous grid block. The radial grid spacing was chosen from a trial and error procedure. The radius of the well was 0.090223 m and the distance to the outer boundary was 1000 m. The grid in the over/underburden consisted of seven grid blocks each and was used for heat conduction only. The gridding was 0.5 m, 2 m, 8 m, 32 m, 120 m, 480 m, and 1000 m. These one-dimensional grids were attached to each grid block of the radial grid. A backward-in-time, centered-in-space differencing was chosen to discretize the equations. A type-three boundary condition was applied at the well by injection of cold water. The steady-state flow was maintained by placing an extraction well at the outer boundary and making its pumping rate equal to the injection rate. Hydrologic and thermal properties of the aquifer are the same as for the linear heat transport during injection problem.

Ward et al. (1984a) present comparisons of the SWIFT II modeling results with the analytical solution. The comparisons are reproduced in Figures 2-24 and 2-25. On both figures the SWIFT II results accurately reproduce the analytical solution.

2.3.4 Radial Heat Transport with Loss to Confining Beds

In this problem, the SWIFT II code is used to model the injection of cold water into an infinitely large, hot water aquifer (Avodonin, 1964). The cold water is pumped into the cylindrical aquifer through an infinitesimally small well. This problem is the same as described in Section 2.3.3. However, it is modeled somewhat differently here to take advantage of the local grid capability of SWIFT II. This problem tests the following capabilities of the SWIFT II code: thermal convection, thermal conduction, and thermal retardation in both local and global coordinate systems, SI units, and radial coordinate systems.

The modeling of the radial heat injection problem is described in detail in Reeves et al. (1986c) and is similar to the modeling described in Section 2.3.3 in many respects. The radial grid is the same for both problems. However, the modeling of this problem requires the use of local grid blocks rather than over/underburden grid blocks to transport the cooler temperature away from the aquifer. The local grid consists of thirty sets of fifteen local grid nodes, one set for each grid block of the radial grid. The length of each set of local grids is 300 m, with the distance between this first two nodes in each set being 10 m. Distances between subsequent pairs of nodes are determined by multiplying the distance of the preceding pair of nodes by approximately 1.11.

The boundary conditions necessary to maintain the flow rate are handled differently in this problem, too. In the problem described in Section 2.3.3, the flow rate is maintained

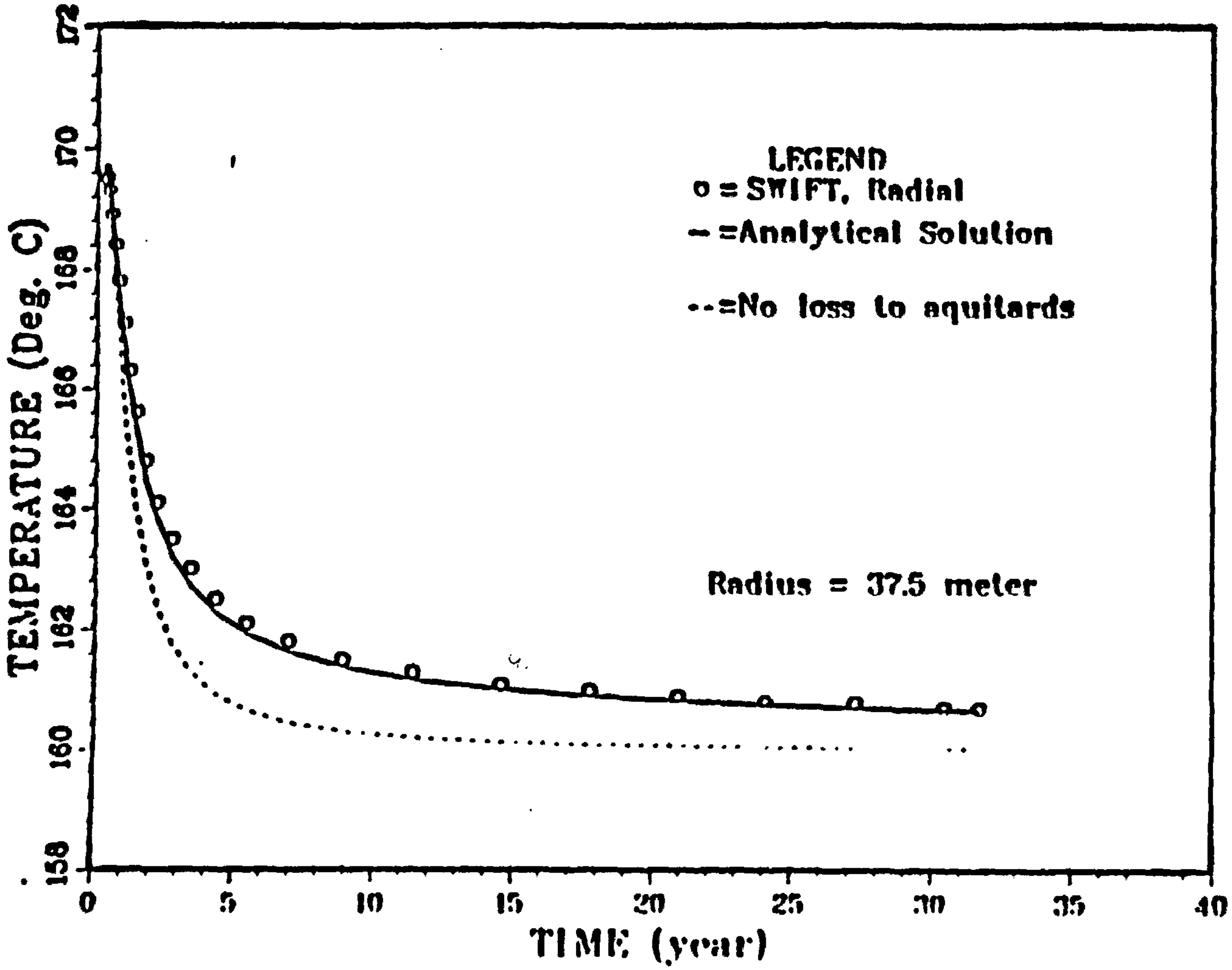

Figure 2-24 Temperature as a Function of Time in a Radial Aquifer System. [Ward et al., 1984a]

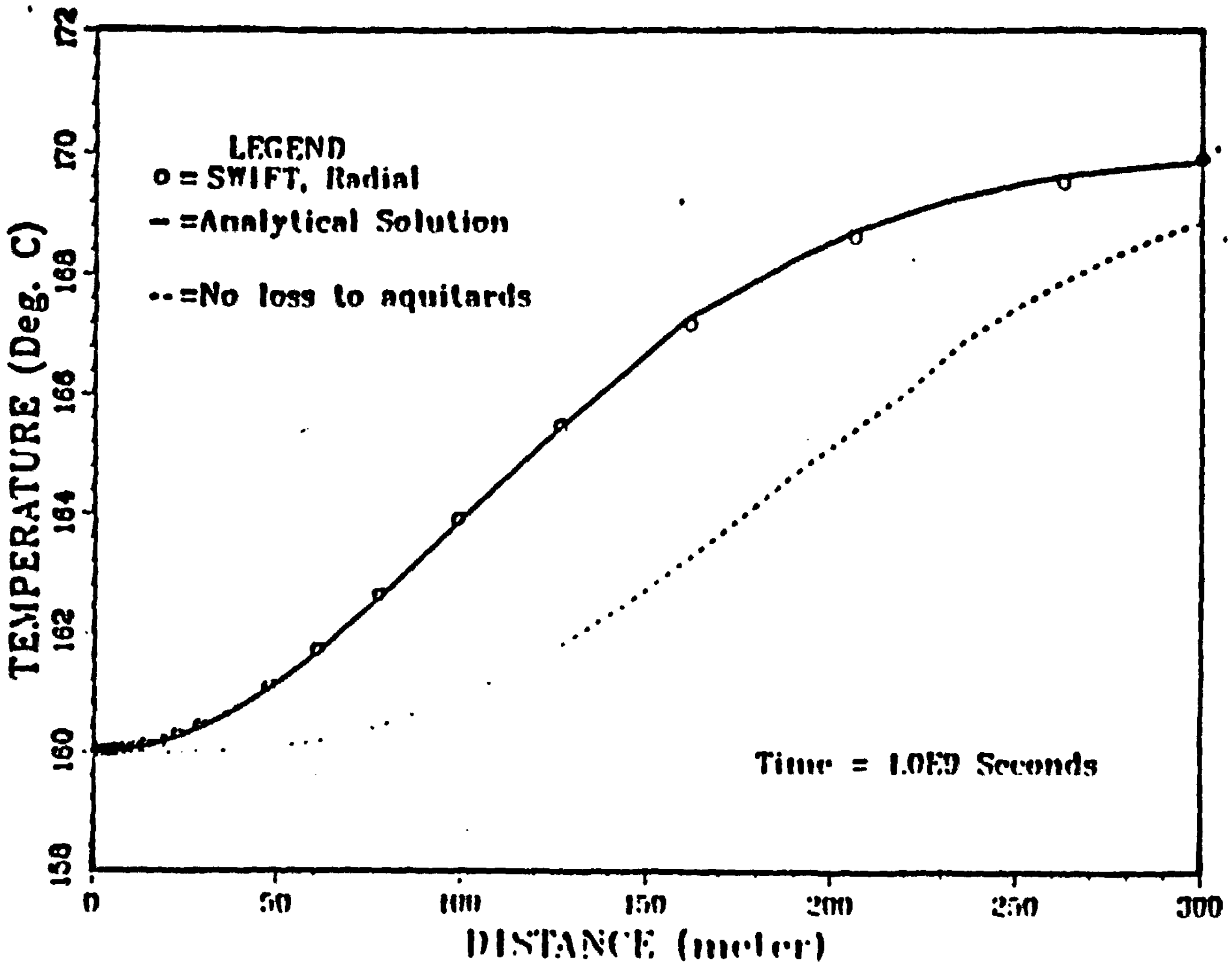

Figure 2-25 Temperature as a Function of Distance in a Radial Aquifer System. [Ward et al., 1984a]

by application of an injection rate at the well and a pumping rate at the exterior boundary. However, in this problem a constant pressure is applied at the exterior boundaries instead of a pumping rate to maintain the same flow as in Section 2.3.3. The hydrologic and thermal properties of the aquifer and aquitard are the same for both heat injection problems except for rock heat capacity. For this simulation rock heat capacity is $2.07875 \times 10^6 J/m^3$-°C, while for the other it is $2.5 \times 10^6 J/m^3$-°C.

Reeves et al. (1986c) compares the SWIFT II solution with the analytical solution, which is presented on Figure 2-26, for a distance of 37.5 m from the injection well. For both early and late times, the SWIFT II and analytical solutions compare extremely well. Between three and fifteen years, the SWIFT II solution predicts slightly higher temperatures than the analytical solution. Overall, the SWIFT II and analytical solutions agree very well.

Because of the difference in the heat capacity for this simulation and the one presented in Section 2.3.3, the temperature profiles with respect to distance between the two are slightly different. At points near the injection well and the exterior boundary, temperatures are almost equal. At interior grid points, the SWIFT II solution presented here predicts a maximum temperature difference of 0.2 °C higher than the SWIFT II solution presented in Section 2.3.3. This indicates that as much as a twenty percent difference in heat capacities has only small impacts on the temperature profile.

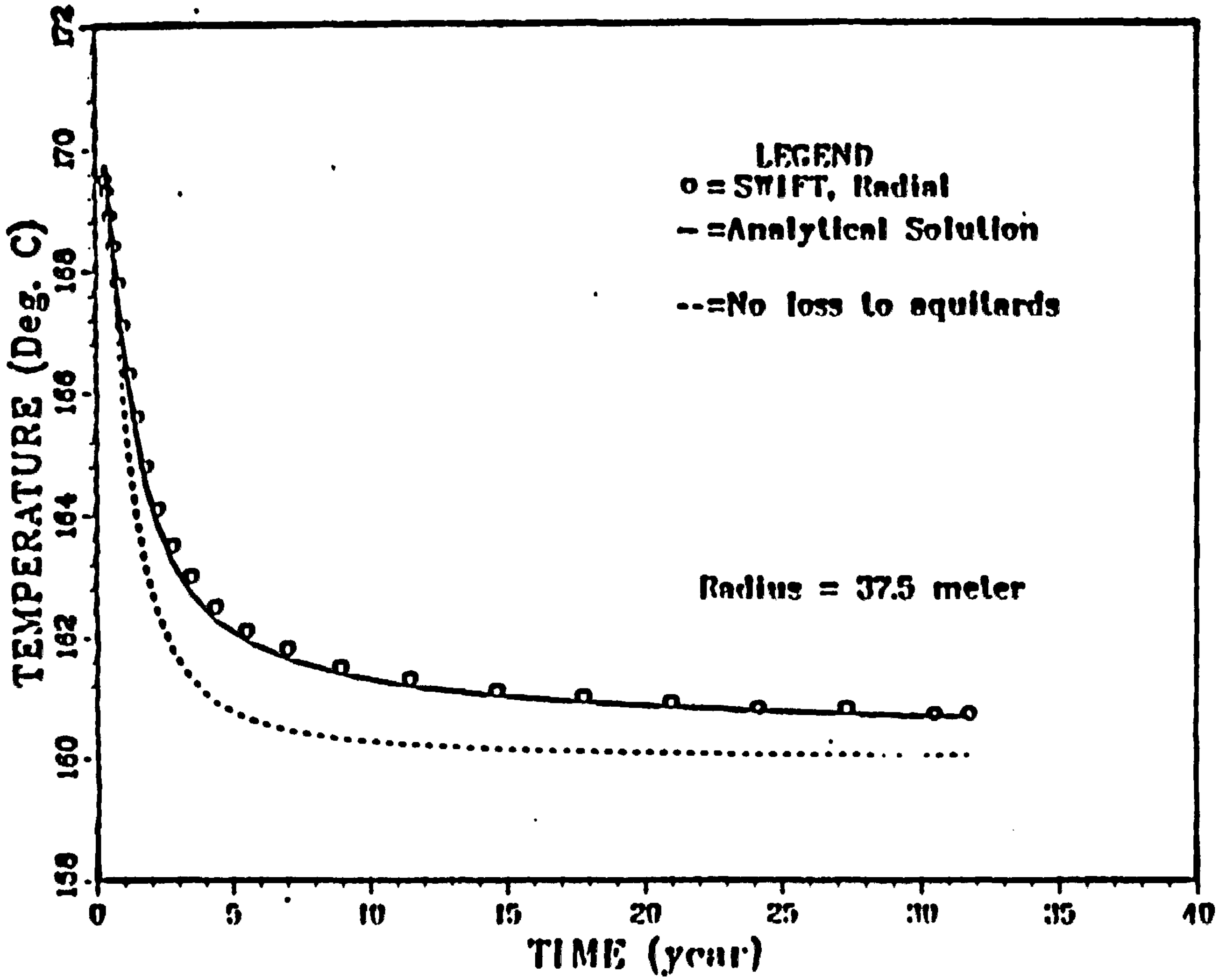

Figure 2-26 Temperature Breakthrough Within the Aquifer at 37.5 m from the Injection Well. [Reeves et al., 1986c]

3. EXISTING VALIDATION TESTS

3.1 VALIDATION OF FLOW

3.1.1 Analysis of Well Test-Data for a Dolomite Formation

In this test the SWIFT II code was used to compare a numerical solution with field data from a slug test performed at the WIPP site in New Mexico. The modeling and comparison are described in Reeves et al. (1986c). The conceptual model of the flow system treats the aquifer as a porous matrix with a zone of stress relief fractures around the wellbore. This problem tests the following aspects of the SWIFT II code: a pressure solution, a local grid, a pressure controlled well, radial coordinates, and English engineering units.

A description of the problem and its simulation are provided in Reeves et al. (1986c). The results of the simulation are compared with slug test data from a well in New Mexico. In the conceptual model of the flow system, the aquifer is initially assumed level, horizontal and infinitely large. The aquifer is assumed to be homogeneous, isotropic and porous with no fractures except for a small fractured region around the wellbore. In the fractured region around the wellbore, about a radius of one foot, the aquifer is assumed to consist of a porous matrix with stress relief fractures. A fully penetrating well at the center of the aquifer is injected with a slug of water, which is allowed to flow into the aquifer. Both pressure changes and flow rates are measured in the well as a result of water flowing from the well into the aquifer.

A cylindrical grid consisting of 50 grid blocks was used to model the system. The first grid block had a radius of one foot and the distance from the middle of the well to the outer radius of the modeled area was 2000 m. Grid block widths were expanded in a geometric fashion. The wellbore had a radius of 0.276 feet.

A one-dimensional local grid block was attached to the first global grid block to simulate the fracture zone around the wellbore. No other global grid block had a local grid block attached to it.

The aquifer was initially static. A time-dependent pressure was applied at the well. The pressure started at 200 psi at the start of the simulation and declined to 158 psi at the end of the simulation, three days later. A Carter-Tracy boundary condition was applied to the external boundary of the grid. This condition provides for a flux of water into the modeled region to help simulate an infinitely large aquifer.

Hydraulic parameters were assigned as follows:

Aquifer thickness	25.0 ft
Primary porosity rock hydraulic conductivity	2.0×10^{-4} ft/day
Primary porosity rock specific storage	3.03×10^{-7}/ft
Secondary porosity rock hydraulic conductivity	200.0 ft/day
Secondary porosity rock specific storage	1.86×10^{-6}/ft

The primary porosity hydraulic parameters were taken from Pahwa and Baxley (1980) and the secondary (fracture) hydraulic parameters were estimated from calibration of the model.

The results of the model runs are presented and discussed in Reeves et al. (1986c). Figure 3-1 presents a comparison of measured wellbore flow rate and calculated flow rate. Except at a few times, the agreement between the measured and calculated flow rates are very good. The biggest difference occurs at the end of the simulation, where the measured flow rate appears to drop dramatically compared to the calculated flow rate. Other points where there is disagreement between measured and calculated flow rates are probably attributable to measurement error or noise.

This problem does not appear to be a good validation problem for two reasons. First, this problem has been solved using a different conceptual model (Finley and Reeves, 1982). In the Finley and Reeves model, the conceptual model consisted of a system of fractures within a porous matrix over the entire simulated domain. The fact that we have two conceptual models indicates that the flow system cannot be adequately described for a validation problem. As a result, we end up with a system that can have many parameters to be estimated. Given enough parameters, just about anything can be modeled.

The second weakness of this validation problem is that the hydraulic parameters for the fracture zone were obtained from a model calibration procedure. Values of the hydraulic conductivity and specific storage were chosen from a trial and error procedure until a good fit with the observed data were made. As a result, this problem is more a curve-fitting problem than a validation problem.

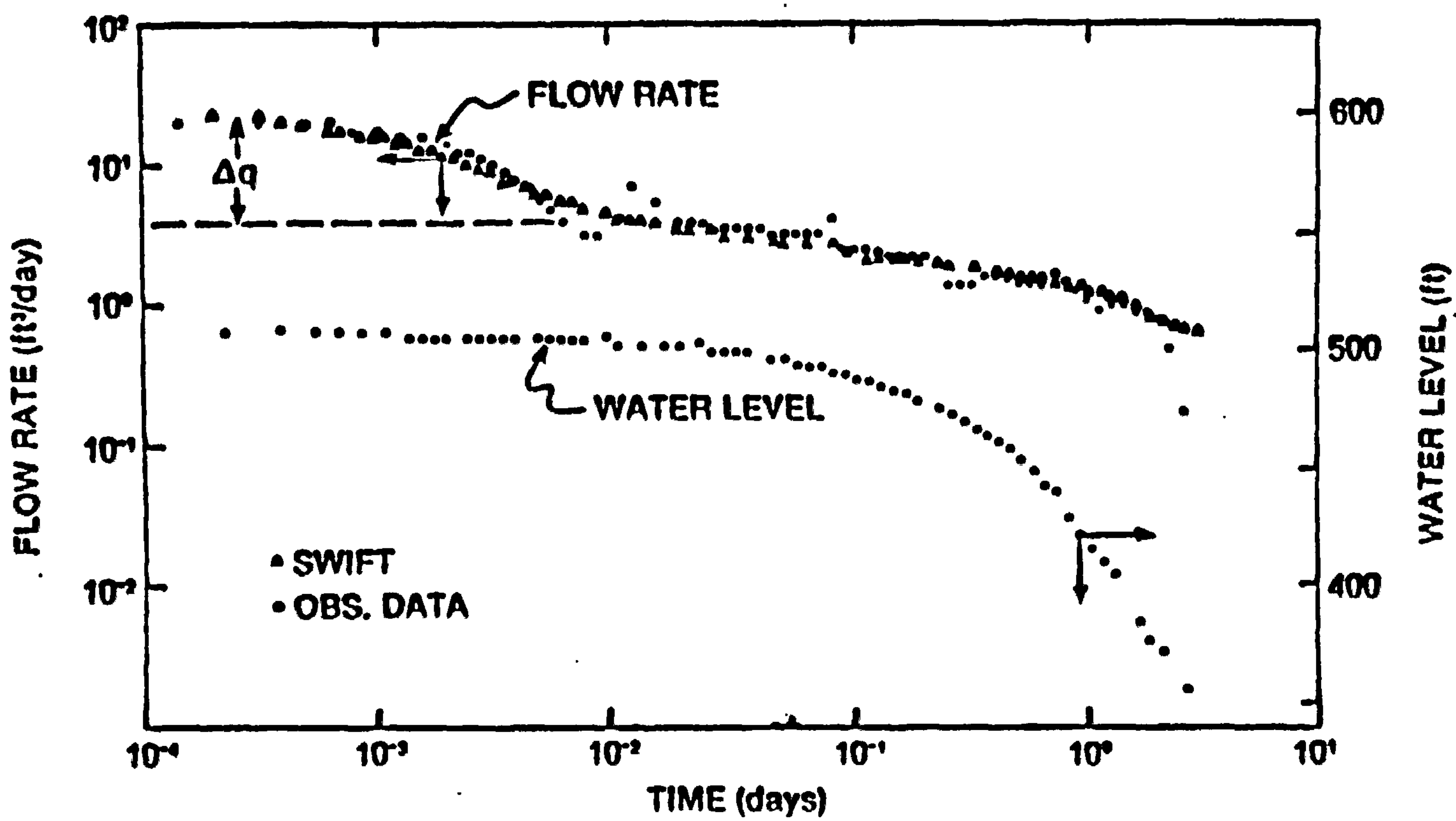

Figure 3-1   Flow Rate During H2A Slug Test.   [Reeves et al., 1986c]

3.1.2 Hydraulic Testing for Thermal-Energy Storage in an Aquifer

In this problem SWIFT II is used to calibrate and simulate two aquifer tests. These tests were originally presented in Parr et al. (1983) and Buscheck et al. (1983). The SWIFT II modeling was described in Ward et al. (1984a). The purpose of these tests was to estimate the hydraulic parameters of an aquifer prior to some thermal energy storage experiments. The first experiment, known as the anisotropy test, was designed to determine the ratio of horizontal to vertical hydraulic conductivity and the storage coefficient of the aquifer. The second, known as the standard pumping test, was designed to compare the numerical solution with aquifer test data from a fully penetrating well. The tests are designed to test the SWIFT II code in the following ways: the pressure solution, anisotropic aquifer characteristics, pumping and observation wells, and English engineering units.

<u>Anisotropy Test</u>

The modeling of the anisotropy test is described in Ward et al. (1984a). A description of the hydrology and geology of the test site, and the test operation and analysis are described in Parr et al. (1983). Another modeling study of the same test is described in Buscheck et al. (1983). Some of the results from these two studies were used in the SWIFT II modeling of the anisotropy test.

Ward et al. (1984a) modeled this problem because of thermal buoyancy effects. Buoyancy causes water to rise vertically from the bottom of an aquifer to the top. Because of this vertical movement of water, it is necessary to know the vertical hydraulic conductivity and, hence, the anisotropy ratio of the aquifers. Such numbers are useful when performing thermal modeling of heat injection experiments.

The 70-ft thick aquifer consists of three zones. The bottom zone is 22.0 ft thick and has a horizontal hydraulic conductivity of 128 ft/day. The middle zone is 16.5 ft thick and has a horizontal hydraulic conductivity of 322 ft/day. The top zone is 31.5 ft thick and has a horizontal hydraulic conductivity of 128 ft/day. The storage coefficient was 6×10^{-4} and the test well was pumped at 28890 ft^3/day.

The hydraulic conductivities are based on a study by Buscheck et al. (1983). They performed an analysis of a thermal injection test and found that a single zone aquifer did not produce a good comparison between observed and predicted temperatures. They then performed a parametric study and found that a three-zone aquifer with the above hydrologic parameters produced a better fit to measured temperatures than the single zone aquifer. The transmissivity of the three zone aquifer was the same as for the single layer aquifer.

Ward et al. (1984a) used a thirteen layer cylindrical grid to model the aquifer test. The bottom zone of the aquifer consisted of five grid layers, the middle zone consisted of two grid layers, and the top zone consisted of six layers. From top to bottom the thicknesses of the grid layers were 3.0 ft, three layers at 5.0 ft, 4.0 ft, 8.0 ft, 8.5 ft, 6.5 ft, 7.0 ft, three layers at 5.0 ft, and 3.0 ft The hydraulic conductivity of each grid layer was assigned a value representative of the aquifer zone that the grid layer was located in.

The gridding in the radial direction consisted of twenty-two grid blocks. The problem assumed an infinitesimally small well bore. The distance from the center of the well bore to the center of the first grid block was 0.6 ft. Subsequent distances between the center of the well bore and the remaining grid block centers were variable, but the distance between adjoining grid block centers generally increased with increasing distance from the well bore. The outer radius of the simulated region was 4000 ft from the well bore center.

A constant flux boundary condition, representing a pumping rate of 28890 ft^3/day, was applied to the boundary grid block representing the well bore. A Carter-Tracy boundary was applied to the outer boundary of the modeled region. The fluid level in the aquifer was initially assumed static.

The results of the modeling are presented in Ward et al. (1984a) Because the purpose of this modeling effort was to estimate the anisotropy ratio and storage coefficient of the aquifer, several computer runs were made with differing values of the anisotropy ratio and the storage coefficient. After several runs, Ward et al. found that a ratio of horizontal hydraulic conductivity to vertical hydraulic conductivity of five and a storage coefficient of 6.0×10^{-4} fit the observed data very well.

A comparison of the computed results with the observed measurements is presented in Figure 3-2 for three observation wells. The agreement between the calculated and observed data is very good for the first 0.035 days (approximately 45 minutes). After that, the calculated and observed data begin to diverge. This deviation may be caused by impermeable boundaries or a low transmissivity zone in the aquifer, which were not accounted for in the modeling.

While the results between computed and observed results are very good, this modeling effort has several fundamental flaws as a validation problem. First, the conceptual model is based on the modeling results of Buscheck et al. (1983). Because the original conceptual model of Buscheck et al. could not reproduce the measured results, the conceptual model was changed to match the measured data. Therefore, the conceptual model is based on calculations and not on the geology and hydrology of the system.

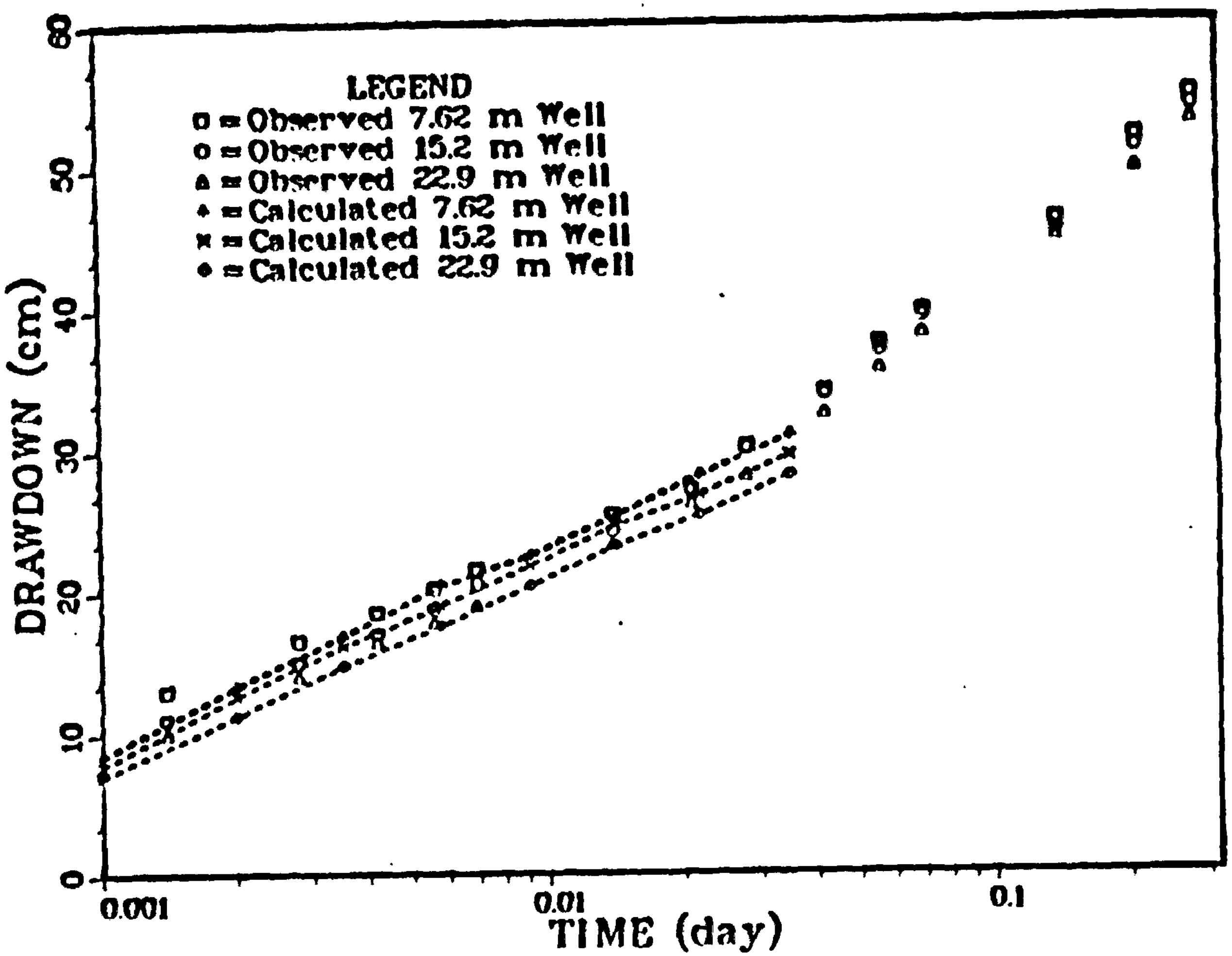

Figure 3-2 Aquifer Drawdown as a Function of Time at Three Observation Wells for the Anisotropy Test. [Ward et al., 1984a]

Second, the parameters for the hydraulic conductivity of the various layers in the new conceptual model were based on a trial and error procedure (Buscheck et al. 1983). This again, is a calibration procedure and not a validation exercise.

Third, the modeling effort is a model calibration exercise rather than a validation exercise. The calculated results are forced to fit the observed data by varying the anistropy ratio and the storage coefficient. No calculations were ever performed to compare future predicted drawdowns with observed ones.

Standard Pumping Test

In this problem the SWIFT II code is used to make predictions on an aquifer with several impermeable boundaries. The modeling effort is described in Ward et al. (1984a). The hydraulic parameters used in this modeling exercise are based on the work of Parr et al. (1983), mentioned in the anisotropy test section. In contrast to results from the Buscheck et al. (1983) report, Parr et al. treated the aquifer as sharing only one layer. They estimated an aquifer transmissivity of 12160 ft^2/day and a storage coefficient of 6.9×10^{-4}. However, when Ward et al. modeled this problem they used a storage coefficient of 6.0×10^{-4}. They also estimated slightly different location of the nearest impermeable boundary than estimated by Parr et al.

The modeling of the problem is described in Ward et al. (1984a). They modeled the system as a strip aquifer, ie, one with parallel impermeable boundaries. One boundary was placed 599 ft away from the pumping well and parallel to the y-axis and the other 2594 ft from the pumping well and parallel to the y-axis. Because this problem is symmetric about the x-axis, only the plane on the positive side of the x-axis was modeled.

The grid consisted of highly variable grid block sizes in the x-direction. Grid block sizes ranged from 2.0 ft at pumping and observation wells to 174.0 ft and 500.0 ft near the impermeable boundaries. In the y-direction, grid block sizes increased as distance from the symmetry boundary increased. The sizes ranged from 1.0 ft at the symmetry boundary to 19683 ft at the boundary, representing an infinitely large distance from the symmetry boundary.

Two types of boundary conditions were applied to boundaries of the modeled region. The line of symmetry and the boundaries parallel to the y-axis were treated as zero flux boundaries. As such, boundaries did not require any input data because the SWIFT II code implicitly assumes that all boundaries are impermeable unless stated otherwise. The boundary located a very large distance away from the line of symmetry was treated as a constant head boundary. A static initial condition was also applied to the system.

The results of the modeling are presented by Ward et al. (1984a). Figures 3-3 and 3-4 present the results of the modeling after 1.4 days and 4.0 days, respectively. On both figures the calculated SWIFT II results diverge from the observed results after approximately 0.01 days. This divergence increases with increasing time.

The cause of this divergence could be twofold. First, in their modeling Ward et al. (1984a) lowered the value of the storage coefficient to 6.0×10^{-4} from the 6.9×10^{-4} value calculated by Parr et al. (1983). This would result in an increased calculated drawdown. Second, the location of the two impermeable boundaries may be inexact. The location of impermeable boundaries as calculated from aquifer test data is dependent on the storage coefficient. If the storage coefficient is wrong or changed, the calculated distance to the impermeable boundaries will change also. Further, the data

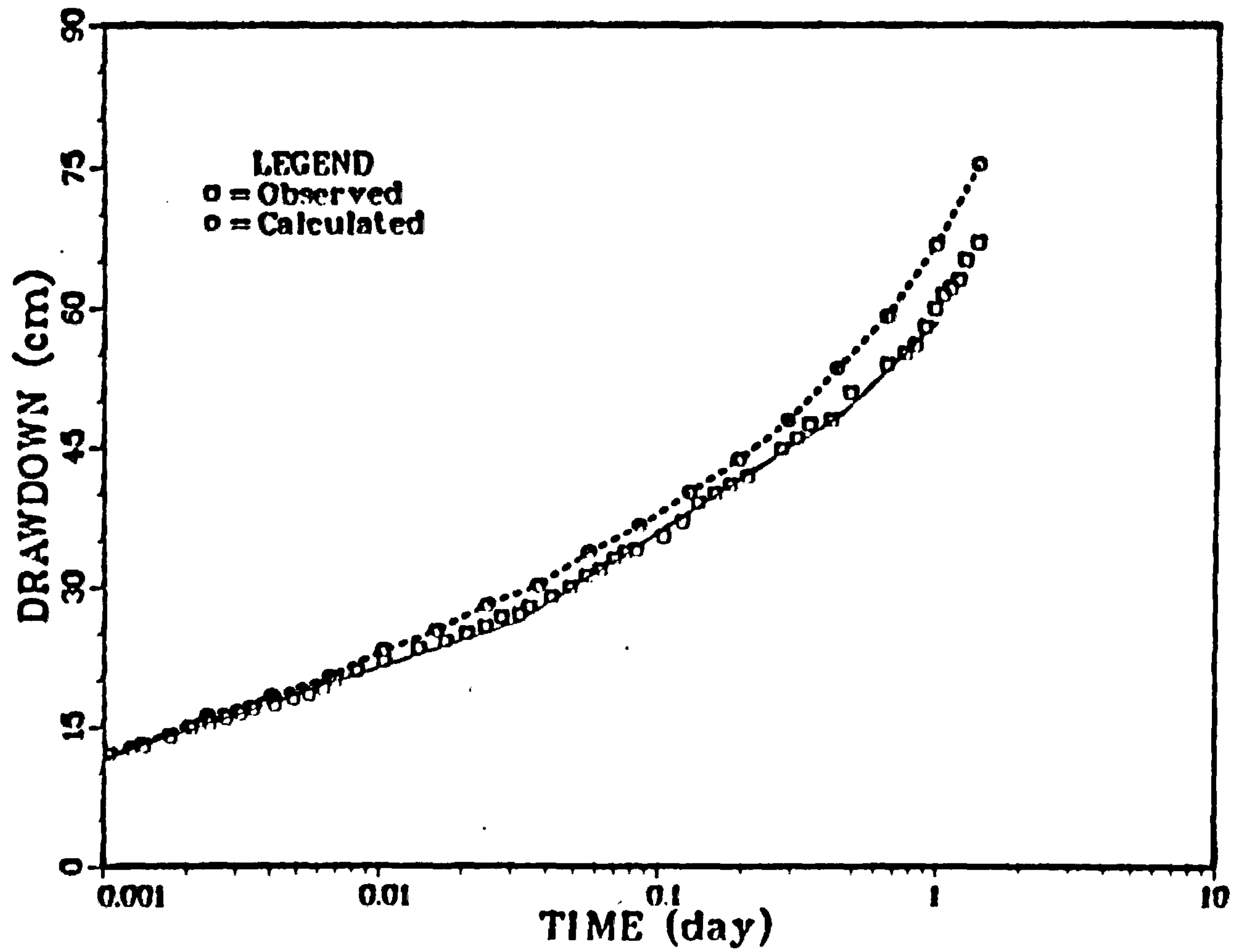

Figure 3-3 Aquifer Drawdown as a Function of Time for the Standard Pumping Test. [Ward et al., 1984a]

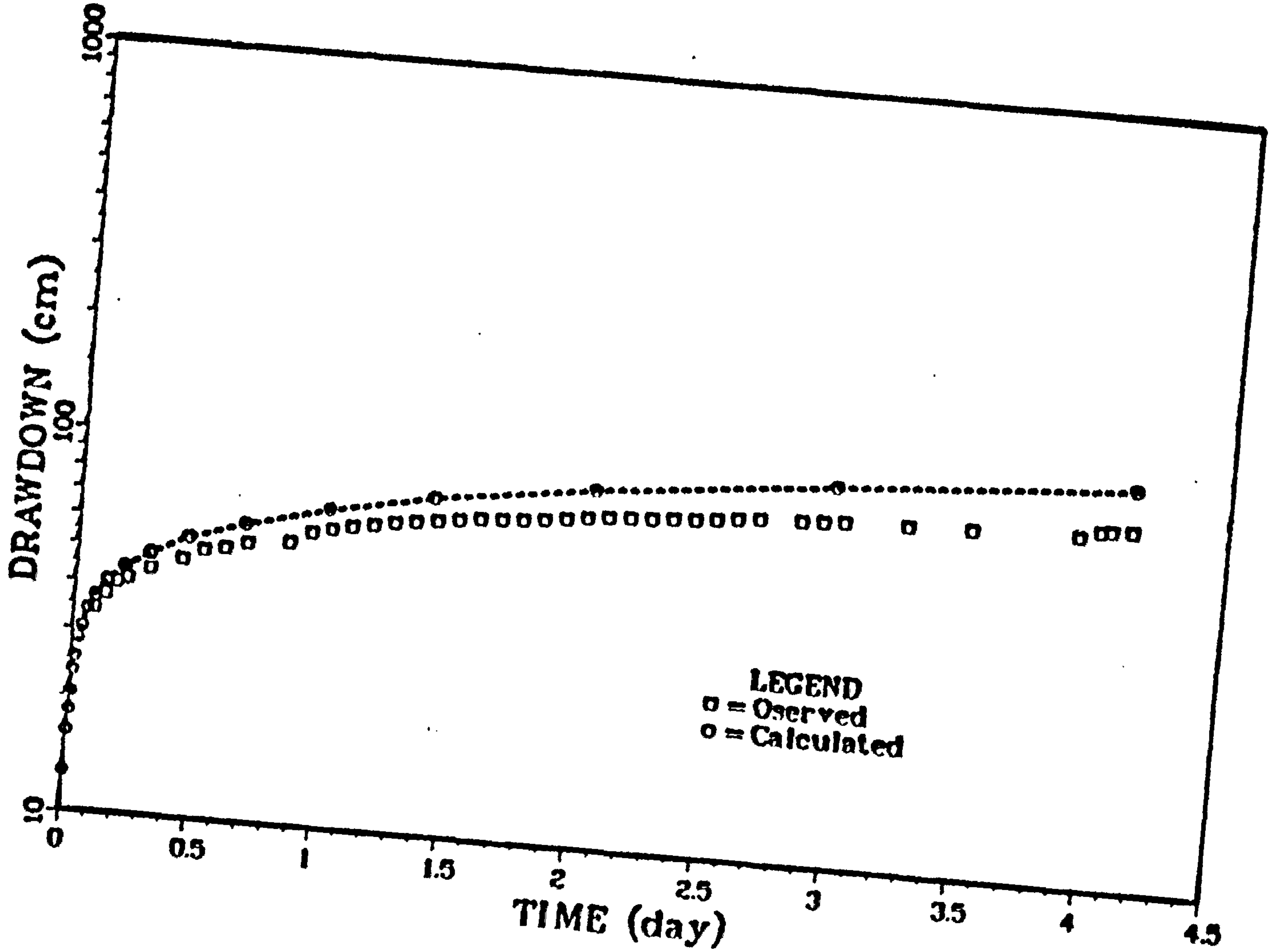

Figure 3-4 Aquifer Drawdown at a Fully Penetrating Observation Well as a Function of Time for the Standard Pumping Test. [Ward et al., 1984a]

from an aquifer test with a single observation well is insufficient to determine the orientation of the impermeable boundaries. So, although the aquifer test data may show two impermeable boundaries, it is impossible to tell if the boundaries are parallel to or perpendicular to each other.

This problem is not a good validation problem. The SWIFT II code is calibrated based on a model implemented in both the SWIFT II code and the Theis (1935) equation, which is used to analyze the aquifer test data. In essence, the SWIFT II run's purpose is to reproduce the calibrated aquifer test results.

This may have been a good validation test had Ward et al. (1984a) made predictions based on the calibrated model and compared the results to measured data. They made predictions but did not have any observations to which to compare their predictions. Therefore, this problem does not provide a validation test of the models implemented in the SWIFT II code.

3.2 VALIDATION OF MASS TRANSPORT

Contaminant Migration from a Landfill

In this problem, the SWIFT II code is used to simulate the ground-water transport of chloride ions away from a landfill site. This contaminant migration problem has been studied by Cleary (1978), Kimmel and Braids (1975, 1980) and has been modeled by Gureghian et al. (1981). The SWIFT II modeling of the problem has been performed by Ward et al. (1984a). This modeling has been performed in order to determine the rates and times that chloride had leached (i.e. landfill staging) into a ground water system in Long Island, New York. This problem is designed to test the SWIFT II code in the following ways: contaminant convection and hydrodynamic dispersion, steady-state velocity, time- and space-dependent contaminent source terms, and aquifer influence functions.

A description of the SWIFT II modeling of the landfill problem is provided by Ward et al. (1984a). In the conceptual model of this system, a landfill leaches chloride ions into a ground-water flow system. The location of the chloride source term, the strength or amount of chloride leaving the landfill and the time of leaching varies over the thirty year existence of the landfill. These landfill parameters are determined from the SWIFT II modeling. The aquifer is assumed to have a one-dimensional flow field with a constant velocity. The aquifer is further assumed to have both homogeneous and isotropic hydraulic parameters. With respect to contaminant transport, the chloride ion is assumed to be well mixed in the vertical direction. Therefore, it is only necessary to model the contaminant transport in a two-dimensional horizontal plane. The aquifer dispersivity is considered to be anisotropic.

Ward et al. (1984a) present a description of the data input for this modeling effort. A Cartesian grid consisting of 53 grid blocks in the x-direction and 24 grid blocks in the y-direction are used to model the problem. Gridding in the x-direction (direction of flow) away from the landfill consists of thirty 200 ft long grid blocks, twenty 300 ft long grid blocks, and three 600 ft long grid blocks. Gridding in the y-direction (perpendicular to the flow) consists of four 300 ft long grid blocks, eighteen 200 ft long grid blocks, and two 300 ft long grid blocks. Thus, an area of 13,800 ft by 5,400 ft is modeled.

Two types of boundary conditions were applied to the grid system to maintain a constant flow velocity in the x-direction. At the landfill site (x=0) a constant pressure of 11.95 psi was maintained. At the end of the grid down gradient from the landfill a constant pressure of 0.00 psi was maintained. This pressure gradient coupled with a hydraulic conductivity of 165 ft/day maintained a steady-state one-dimensional Darcy velocity of 0.33 ft/day in the x-direction. The boundaries parallel to the x-axis were treated as impermeable.

Two types of boundary conditions were applied to the grid system to calculate chloride concentration. The two boundaries parallel to the x-axis and the boundary down gradient from the landfill were treated as impermeable. The boundary condition at the landfill was a time-dependent Dirichlet condition. The concentrations input into the model were determined from a trial and error procedure. Basically, a set of concentrations was input into the model, the model was run simulating a 29 year period from the start of the landfill operation and a comparison between the calculated and observed chloride concentrations was made. If the results did not compare favorably, some of the concentrations were changed and a new comparison was made. If the results compared, the model was considered calibrated.

Because this is both a steady-state flow and transient state contaminant transport simulation, several hydraulic and mass transport parameters had to be included in the input data. As mentioned in a preceding paragraph, a homogeneous, isotropic hydraulic conductivity of 165 ft/day was used to solve the flow simulation. A longitudinal and transverse dispersivity of 100.0 ft and 15.0 ft, respectively, and a porosity of 0.30 were used for the transport simulation. The sources for this data are not presented in Ward et al. (1984a). However, they do state that the dispersivities are inferred from the output data. This implies that they were determined from some type of calibration procedure.

Results of the landfill simulation are presented in Ward et al. (1984a). Figure 3-5 presents a comparison of observed and calculated chloride concentrations 29 years after the start

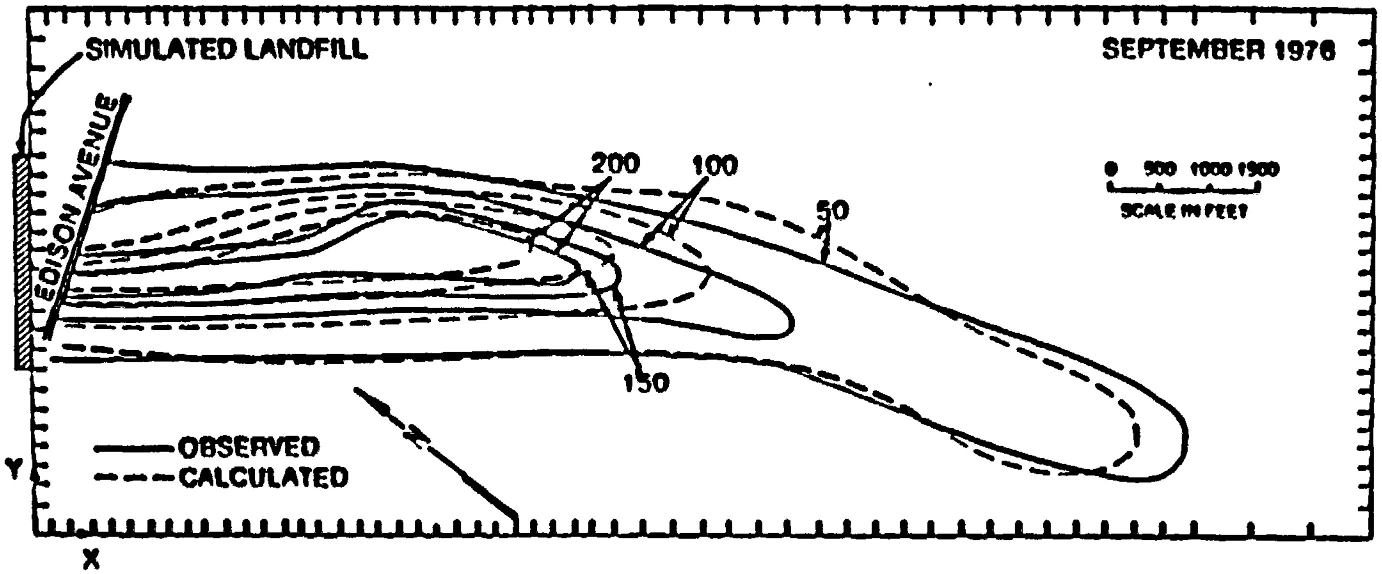

Figure 3-5 Observed (September, 1976) and Simulated Chloride Concentrations (observed data from Cleary [1978]). Tic marks denote the numerical gridding. [Ward et al., 1984a]

of landfill operation. Considering the rather simplistic approach taken to simulate the problem (homogeneous aquifer flow and mass transport parameters, isotropic hydraulic conductivity, uniform velocity), the results are very good. The downward curve of the 50 and 100 isopleths and the upward hump of 150 and 200 isopleths are probably a result of the staging of the landfill. Staging means that only a small part of the landfill is in use at any one time and that the part in use moves with time. The history of the landfill indicates that usage started at the bottom or just above the y-axis and moved upward and to the top of the grid and possibly back down. Thus the downward bend of the 50 and 100 isopleths is probably a result of the early time operation of the landfill. The humps in the 150 and 200 isopleths are probably a result of the intermediate time or very late time operation.

This simulation does not represent a good validation test problem for the SWIFT II code. The landfill source term and, probably, the longitudinal and transverse dispersivities were determined from a trial and error procedure. No future predictions were made and compared to later measured data. Therefore, the landfill problem should be considered a calibration rather than a validation problem.

3.3 VALIDATION OF HEAT TRANSPORT

Thermal Energy Storage in an Aquifer

In this problem, the SWIFT II code is used to model an aquifer thermal energy storage (ATES) experiment performed by Molz et al. (1983). Some of the data developed for this experiment has been described in Section 3.1.2 of this report and in the references quoted there. The SWIFT II modeling of the experiment is described in Ward et al. (1984a). The experiment has been modeled previously by Buscheck et al. (1983). In this experiment, hot water is injected into a cool aquifer for approximately one month, stored in the aquifer for approximately one month, and then pumped out for approximately one month. The modeling is designed to test aspects of the SWIFT II code in the following ways: coupled pressure and temperature solutions, anisotropic aquifer characteristics, injection and observation wells, aquifer influence functions, heat loss to aquitards, and SI units.

A description of the flow system and the modeling are described in Ward et al. (1984a). In this system the aquifer is assumed to be infinitely large for the temperature calculations. The aquifer is assumed to consist of three zones as described in Section 3.1.2 and Buscheck et al. (1983). The aquifer has aquitards both overlying and underlying the aquifer. The aquitards are capable of transmitting heat by conduction and convection, but are fairly resistant to flow. Lying above the upper aquitard and below the lower aquitard are an overburden and underburden, respectively. The overburden and underburden are capable of transmitting heat only.

An axisymetric cylinder grid is used to represent the modeled portion of the aquifer. The grid consists of 21 grid blocks in the vertical direction and 19 in the radial direction. Attached to each grid block in both the upper and lower layer of grid blocks is a one-dimensional grid representing the overburden and underburden. Four layers of grid blocks of heights 7.32 m, 3.65 m, 1.52 m, and 2.06 m represent the gridding of the lower aquitard. Three grid blocks, each of height 2.20 m, represent the gridding in the lower zone of the aquifer. Three grid blocks of height 1.667 m are used to represent the grid in the aquifer's middle zone. Six 1.6 m high grid blocks represent the gridding in the aquifer's upper zone. Finally, five grid block heights of 1.22 m, 1.22 m, 1.68 m, 1.49 m, and 1.52 m represent the gridding in the upper aquitard. The one dimensional gridding in the overburden and underburden is 1.0 m, 2.0 m, 3.0 m, 4.0 m, 6.0 m, 10.0 m, and 20.0 m.

The distance from the center of the injection/pumping well to the outer boundary is 80 m. The distance from the center of the well to the center of the first grid block is 0.6 m. Subsequent distances from the center of the well to the center of a grid block are estimated by multiplying the distance from the well center to the preceding grid block center by a factor of approximately 1.31. This factor varies between 1.22 and 1.41.

The hydraulic and thermal properties of the aquifer and aquitards are presented in Table 3-1. Included on this table are references that provide sources for much of the data. Analysis for determining the aquifer hydraulic parameters as presented in Section 3.1.2. The hydraulic conductivities of each of the three zones of the aquifer are presented in Table 3-2. In addition, the overburden and underburden had the following thermal properties: thermal conductivity of 1.872 W/m-°C and a heat capacity of $1.81 \times 10^6 J/m^3$-°C.

Several boundary conditions were applied to the system to help control the water flow and heat transport. Along the injection well, a boundary condition representing zero flux of water was applied where the well bore abutted both aquitards. Along the well bore abutting the aquifer, a flux boundary condition representing pumping or injecting of water was applied. The injection and pumpage of water was variable but injection averaged 9.27×10^{-3} m^3/s over the 31.7 day injection period and pumpage averaged 1.14×10^{-2} m/s over the 25.7 day pumpage period. Impermeable flow boundaries were specied at the top of the upper aquitard and at the bottom of the lower aquitard. A Carter-Tracy boundary condition was applied at the outer edge of the simulated region to represent an approximately infinitely large aquifer.

Table 3-1 Hydraulic and Heat-Transport Parameters Adopted for Aquifer Thermal Energy Storage Problem

Parameter	Source[1]	Symbol	Value
Aquifer thickness	Parr	b	21.2 m
Hydraulic conductivity, aquifer[2]	Parr	K	6.17×10^{-4} m/s
Storativity, aquifer		S	6×10^{-4}
Porosity, aquifer	Buscheck	ϕ	0.25
Heat capacity, aquifer	Molz	c_p	1.81×10^{6} J/(m$^3\cdot$°C)
Thermal conductivity, aquifer	Molz	K_m	2.29 W/(m$\cdot$°C)
Thickness, upper aquitard	Parr	b'	5.6 m
Porosity, aquitard	Buscheck	ϕ'	0.35
Heat capacity, aquitard	Buscheck	c'_{pR}	1.81×10^{6} J/(m$^3\cdot$°C)
Thermal conductivity, aquitard	Molz	K'_m	2.56 W/(m$\cdot$°C)
Hydraulic diffusivity, upper aquitard	Parr	D'	8.22×10^{-6} m^2/s
Hydraulic diffusivity, lower aquitard	Parr	D''	1.27×10^{-5} m^2/s
Rock density	Buscheck	ρ_R	2600 kg/m^3
Thermal expansion of water	Clark	c_T	5.3×10^{-4} (°C)$^{-1}$
Injection duration	Molz	Δt_1	2.74×10^{6} s
Storage duration	Molz	Δt_2	2.70×10^{6} s
Production duration	Molz	Δt_3	2.20×10^{6} s
Initial temperature	Parr	T_o	20°C
Aquifer permeability ratio[3]		R	1:6

1 The references are Parr [1983], Buscheck [1983], Molz [1983] and Clark [1966]. No reference indicates an assumption by the authors.

2 Composite value of horizontal conductivity. Refer to Table 3-2 for hydraulic conductivities of individual layers.

3 Composite value. The ratio is 1:5 for individual layers.

Table 3-2 Values of Hydraulic Conductivity for the Three-Zone Aquifer (from Buscheck et al [1983]).

	Thickness (m)	Hydraulic Conductivity (m/s)
Upper Layer	9.6	4.51×10^{-4}
Middle Layer	5	11.4×10^{-4}
Lower Layer	6.6	4.51×10^{-4}
Composite Value	21.2	6.17×10^{-4}

A zero heat flux boundary condition was applied along the well bore intersecting both aquitards, at the outer edge of the simulated region, and at the top of the overburden and the bottom of the underburden. Along the well bore abutting the aquifer, a type 3 heat boundary condition was applied. The injection temperature used in the simulation averaged 60.4°C.

Initial conditions applied to the system included a static velocity and a 20°C temperature. In addition, water density and viscosity were temperature dependent, providing a fully coupled water flow and heat transport problem.

Ward et al. (1984a) present and describe the results of modeling the problem. Some of the results of the experiment are shown on Figures 3-6 and 3-7, and results of the modeling on Figures 3-8 and 3-9.

Figures 3-6 and 3-7 generally show a fingering of the temperature contours in the middle zone of the aquifer. The fingering is not too noticeable in the west area of Figure 3-6. Some buoyancy effects are noticeable in the east on Figure 3-6 and in the north on Figure 3-7 at the end of injection. At the end of the storage period some thermal conduction and buoyancy effects are noticeable, as well as the fingering of the temperature contours. During the storage period, thermal conduction moves the temperature contours out, down and up and buoyancy moves them up.

Simulated ground-water temperatures are shown in Figure 3-8. At the end of the injection period, the fingering of the temperature contours in the middle zone of the aquifer is very evident. At the end of the storage period, thermal buoyancy effects are very evident, but conduction is not. The buoyancy effects probably mask the conduction effects. There is, at least, some qualitative agreement between the observed and measured temperatures.

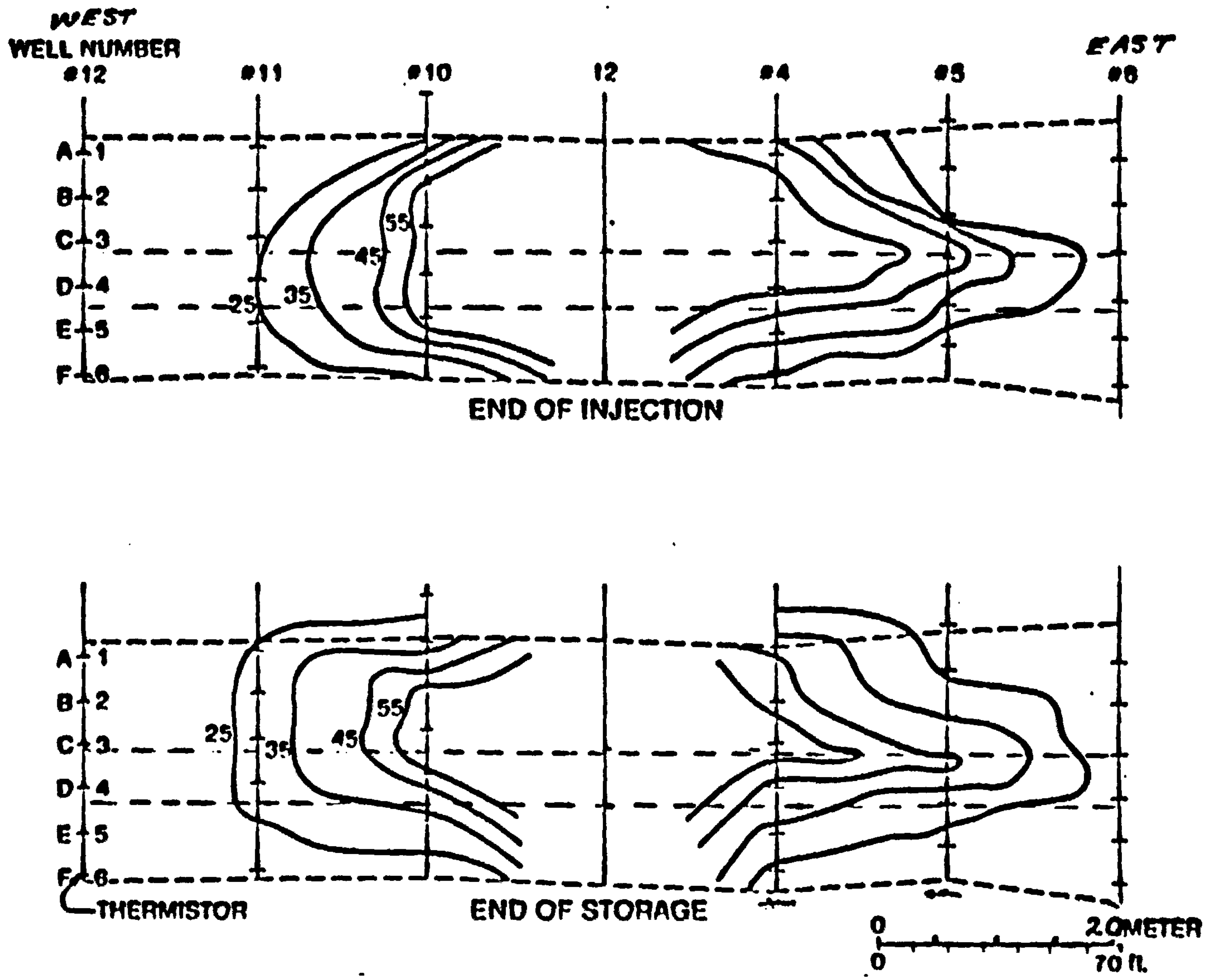

Figure 3-6 East-West Ground-water Temperature Distributions at Selected Times. The vertical sections run between Wells 12 and 6. [Ward et al., 1984a]

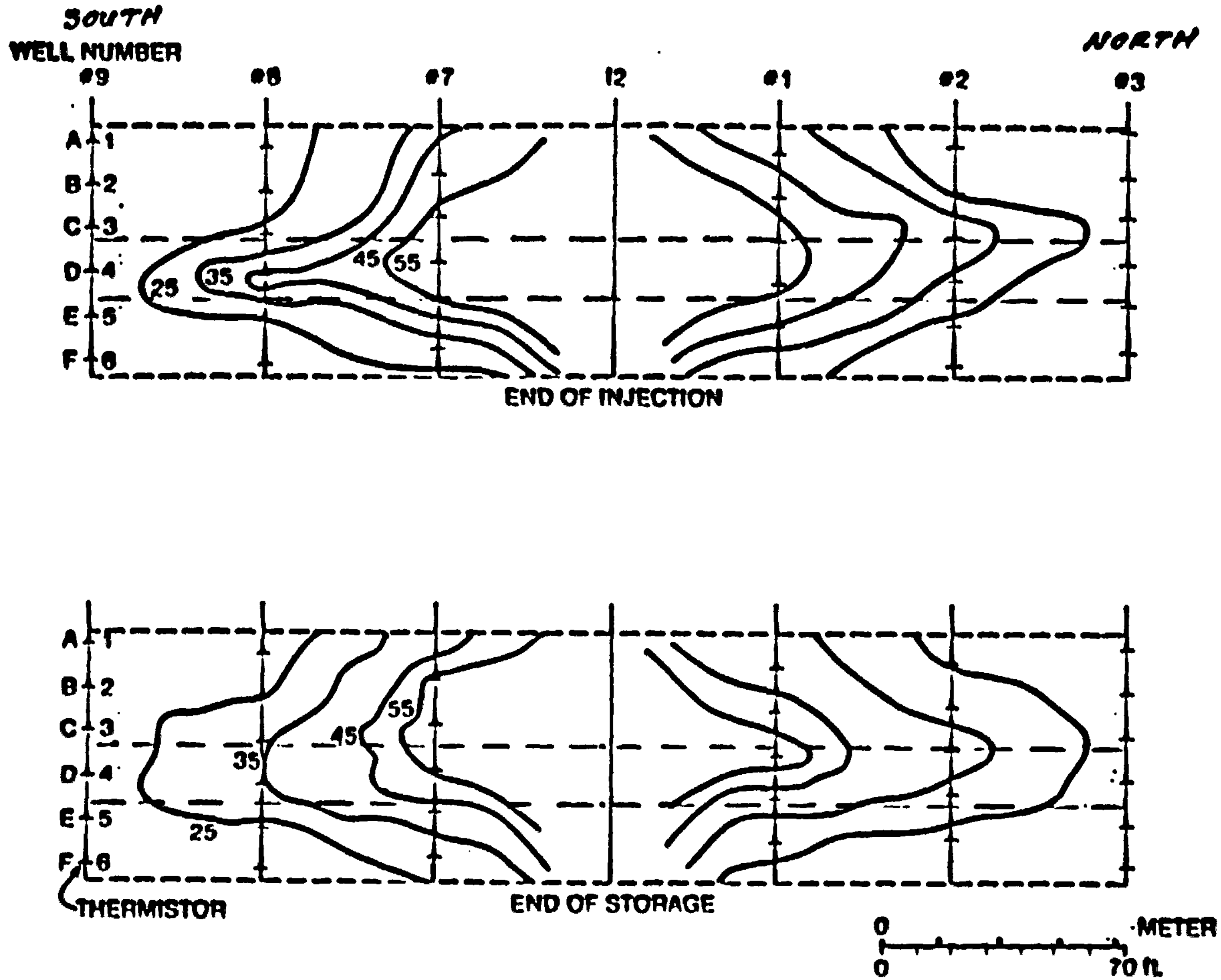

Figure 3-7 North-South Ground-water Temperature Distributions at Selected Times. The vertical sections run between Wells 9 and 3. [Ward et al., 1984a]

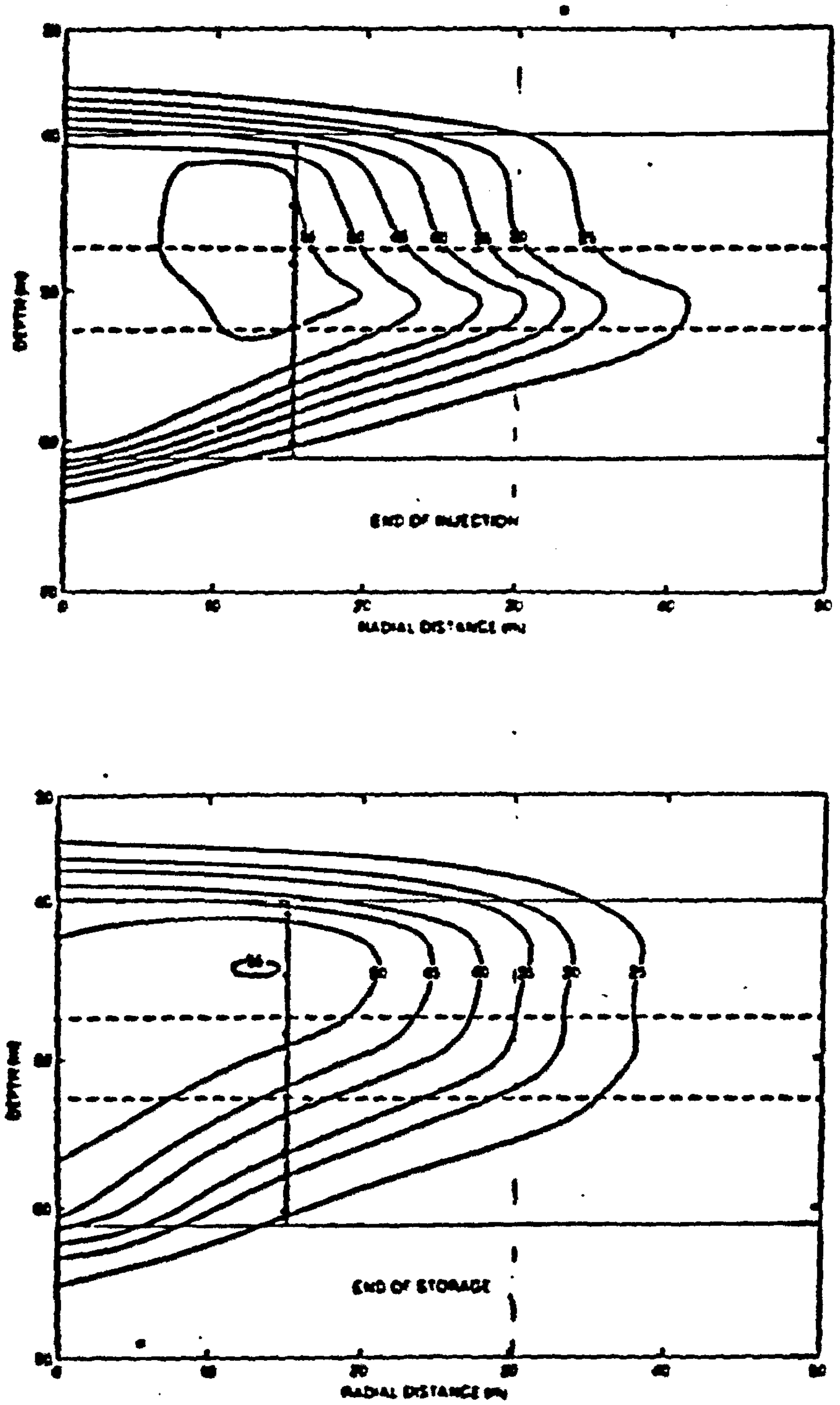

Figure 3-8 Simulated Ground-Water Temperature Distributions at Selected Times. [Ward et al., 1984a]

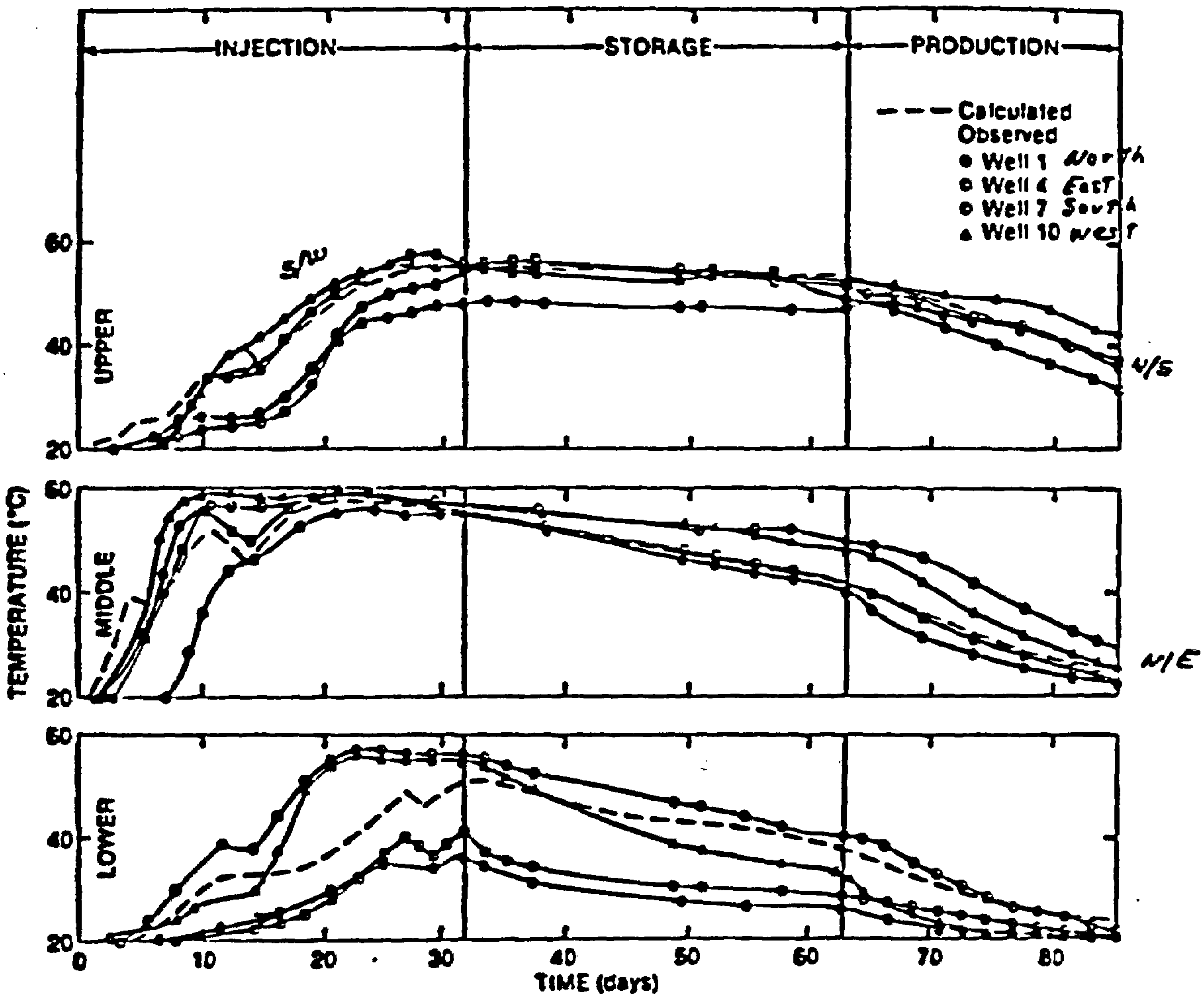

Figure 3-9 Observed and Simulated Temperature as a Function of Time at a Radial Distance of 15 m in the Upper (Probe B), Middle (Probe D) and Lower (Probe E) Zones of the Aquifer. [Ward et al., 1984a]

Figure 3-9 compares the simulated temperatures with those measured 15 m north, east, west and south of the injection well. In the upper aquifer zone there is fairly good agreement between the measured and calculated results in the south and west for the injection and storage periods. For the storage and production periods, there is good agreement in the north and south but not in west and east. For the middle zone of the aquifer there is good agreement in the east for the injection period but not in the other directions. For the storage and production periods there is good agreement in the north and east but not in the south and west. There is poor agreement in the lower layer of the aquifer for all times. The results on Figure 3-9 reflect the use of an axisymetric grid in trying to model a system that is heterogeneous in the radial direction.

Figures 3-10 through 3-12 present comparisons between observed temperatures in all four directions with calculated temperatures for the ends of pumping, storage, and production, respectively. It appears that at most distances the calculated temperatures represent an average of the temperatures in the four directions. The agreement between observed and calculated temperatures appears very good during the storage and production periods. During these periods, the effects of the aquifer heterogeneities are not apparent.

Figure 3-13 presents a comparison of the measured and calculated production temperatures after about day 72, both the calculated and measured temperature plot as coincident lines on the figure. Before that time, observed temperatures are slightly less than calculated ones.

Although there is a reasonably good comparison between measured and observed temperatures, this experiment does not provide a good validation test for the models implemented in the SWIFT II code. First, a comparison between the observed

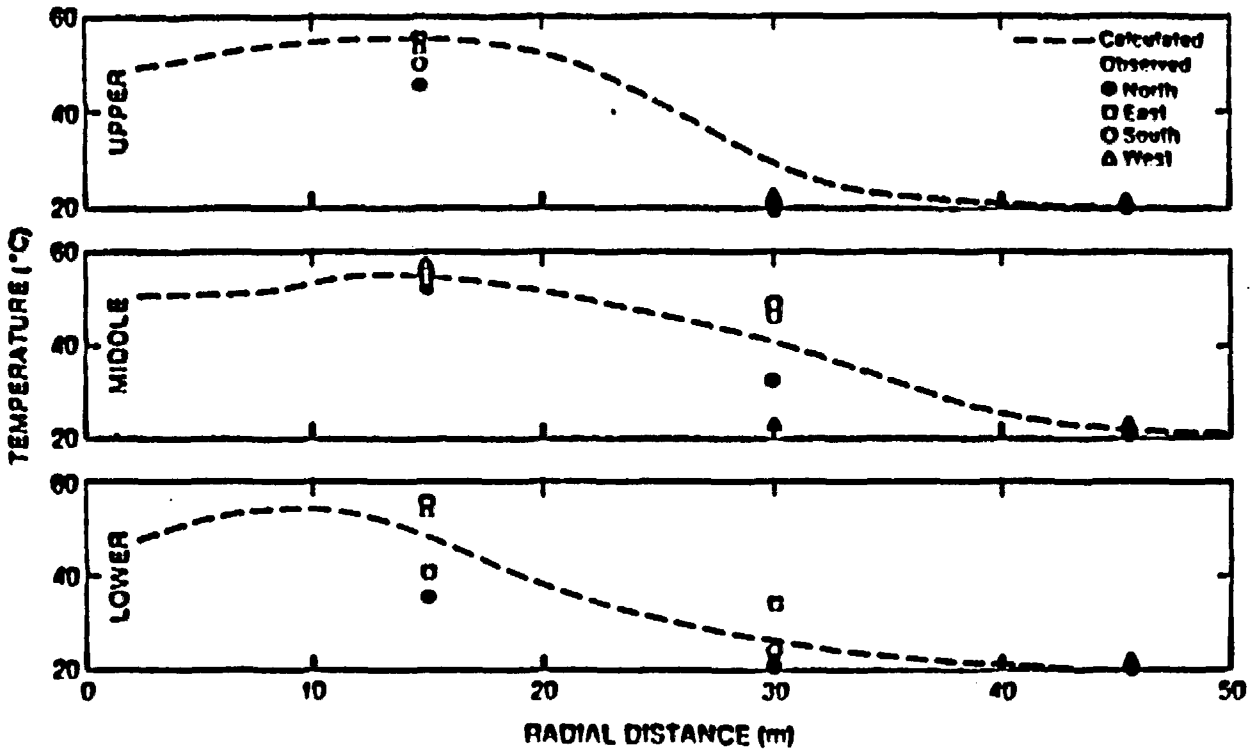

Figure 3-10 Observed and Simulated Temperature as a Function of Distance at the End of the Injection Period in the Upper, Middle and Lower Layers of the Aquifer. [Ward et al., 1984a]

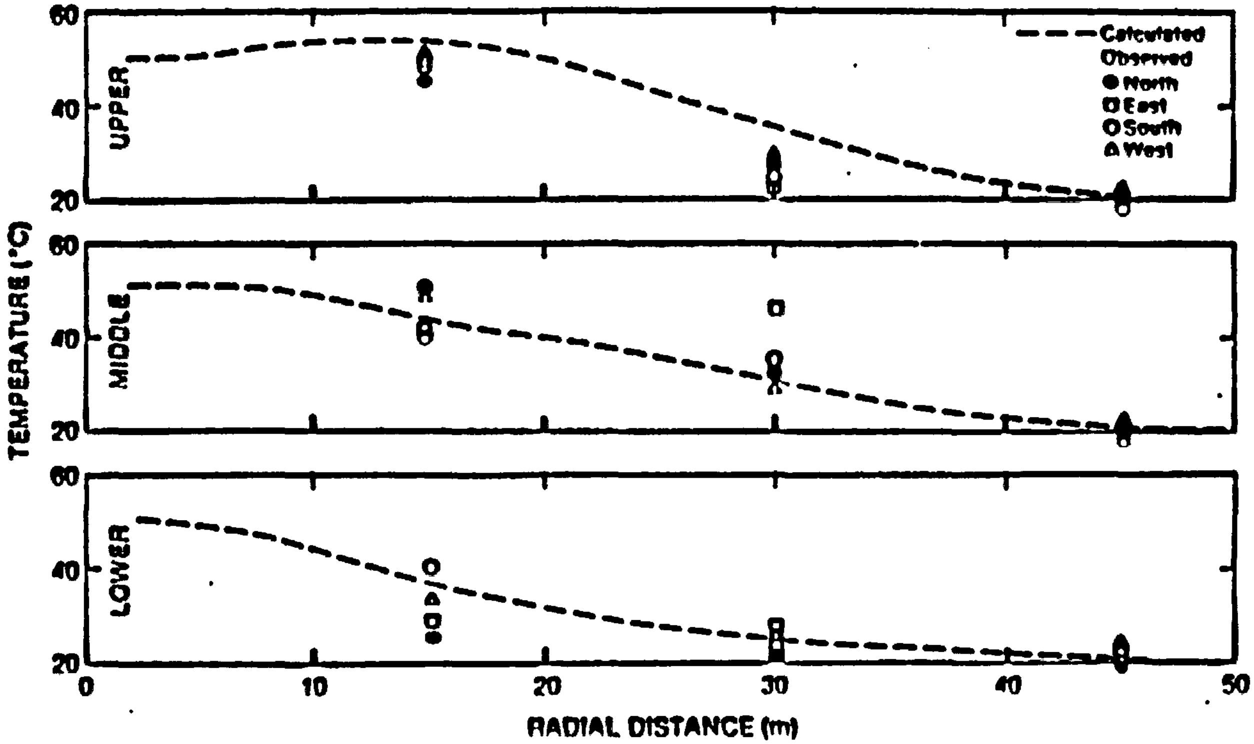

Figure 3-11 Observed and Simulated Temperature as a Function of Distance at the End of the Storage Period in the Upper, Middle and Lower Layers of the Aquifer. [Ward et al., 1984a]

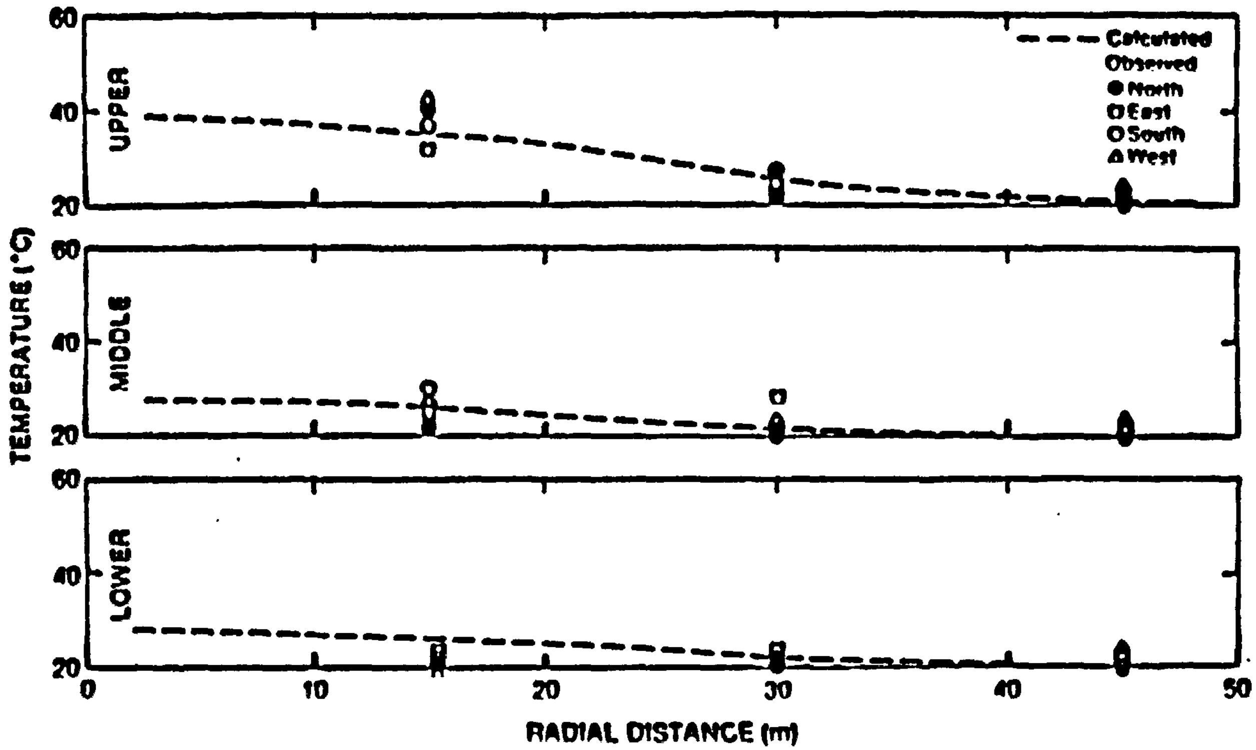

Figure 3-12 Observed and Simulated Temperature as a Function of Distance at the End of the Production Period in the Upper, Middle and Lower Layers of the Aquifer. [Ward et al., 1984a]

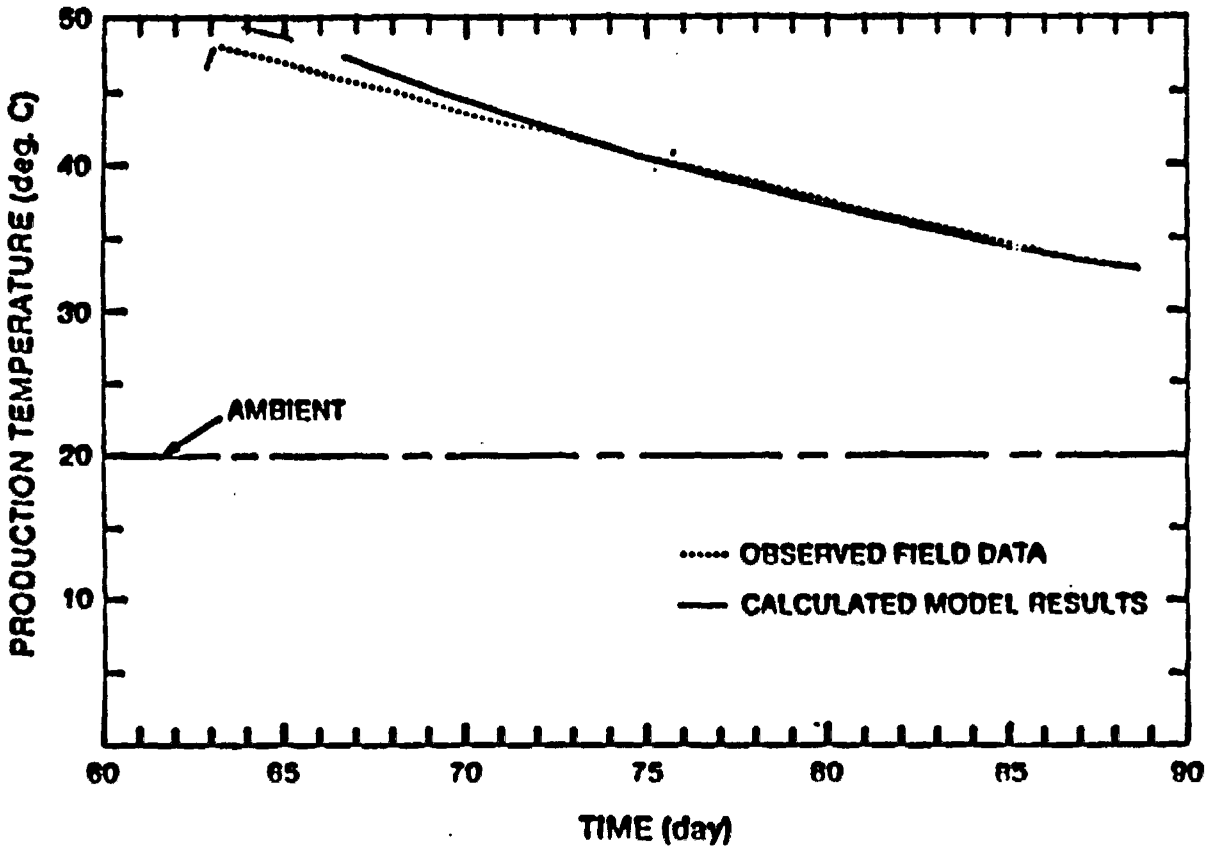

Figure 3-13 Observed and Simulated Production Temperature as a Function of Time (after Molz et al. [1983]). [Ward et al., 1984a]

temperatures of Figures 3-6 and 3-7 and the calculated temperatures of Figure 3-8 provide enough discrepancy to wonder if the aquifer had been adequately characterized or if an axisymetric geometry is adequate to model the experiment. Second, the conceptual model and many of the hydraulic and thermal properties of the system are based on a prior modeling effort of Buscheck et al. (1983). They obtained a calibrated conceptual model based on repeated "trial and error" runs. Therefore, the results presented by Ward et al. (1984a) should be considered as a calibration rather than a validation.

4. SUMMARY AND RECOMMENDATIONS

In the previous two chapters, several verification and validation problems have been reviewed. It was generally found that many of the flow and transport features of the SWIFT II computer program have been verified. On the other hand, all the validation problems are actually calibration problems. For instance, the SWIFT II computer program was used to find the hydraulic and transport parameters necessary to match field results to SWIFT II results.

4.1 VERIFICATION RECOMMENDATIONS

Many capabilities of the SWIFT II code have been tested. Pressure solutions, mass transport solutions, and heat transport solutions using both global and local coordinate systems have been successfully compared to analytical solutions for both single and double porosity media. Many types of boundary conditions, aquifer influence functions, and aquifer submodels have been tested. Of the three new capabilities included in the SWIFT II computer program, i.e. fractured porous media, conductive confining beds, and phreatic aquifers, all have been successfully tested against analytical solutions. It appears that many features of the SWIFT II computer program have been successfully verified.

Some capabilities of the SWIFT II computer program have not been tested, including both the global and local equations of the brine solution, parts of the repository submodel, and the well bore submodel. It is recommended that these areas be tested.

The global equation for the brine equation can be tested in a straightforward manner that neglects density effects. Based on this assumption, the global brine equations can be solved analytically. SWIFT II has the capability to solve variable density problems, where the density changes are due to dissolution of brine. What needs to be specified in the problem input data is that the fluid density does not change as the fluid becomes more saturated with brine. This essentially reduces the brine equation to a convective-diffusive mass transport equation with both a continuous source term and radioactive decay and decouples the brine equation from the flow equation. The problem should specify a zero brine condition initially and at the $x=0$ boundary, and a constant velocity field. The grid should be infinitely long and one-dimensional.

The local brine equation in conjunction with the global brine equation can be tested in much the same manner as the global equation. However, the analytical solution still needs to be solved and is much more complicated than for the global equation above.

The solubility limits portion of the repository submodel needs further testing. The solubility limits have been tested in several mass transport problems (see Sections 2.2.1 and 2.2.2). Unfortunately, the solubility limits are always set much higher than the maximum concentrations of the solute, so that the solubility limits are never given a chance to be tested. It is recommended that the mass transport problem of Section 2.2.1 be run with solubility set to much less than the maximum concentration of a solute. This is equivalent to running a convective-diffusive equation with a constant source strength boundary condition.

In addition, the heat loading capability of the repository submodel has not been tested. It is recommended that a one-dimensional heat transport problem with a constant heat source boundary condition be set up and run using the heat capability of the repository submodel. Possibly the problem described in Section 2.3.1 could be modified to be used as the repository submodel.

It is doubtful that the well bore submodel can be adequately tested. The equations describing the submodel are nonlinear and an analytical solution cannot be generated for them. It is recommended at this time to not test the well bore submodel.

4.2 VALIDATION RECOMMENDATIONS

It has been found in Chapter 3 that all problems run with the SWIFT II computer program that could be called validation problems are actually calibration problems or reruns of someone else's calibrated data set. The source for many of these problems (Ward et al., 1984b) mentions that the purpose for these problems is field comparison and calibration and not validation. The other source (Reeves et al., 1986c) presents problems for instructional purposes only. These calibration problems are essentially trial and error procedures to determine hydraulic, mass transport, and thermal transport properties for given field experiments. There is no proof that these parameters are unique or that the physics of the models are correct. All that is known is that a set of parameters has been found that causes the numerical models implemented in the SWIFT II computer code to match the field data.

At this time is is recommended that the SWIFT II computer program not be used for validation of mathematical models. First, the SWIFT II computer code is a field oriented program whose purpose is to solve field problems. Therefore, any mathematical models implemented in it should have been validated previously.

Second, the equations implemented in the SWIFT II computer program may contain several physical models. For instance, the flow equation has an aquifer compressibiity model, a fluid compressibility model, a variable viscosity model, and Darcy's law included in it. As a result, it may be difficult to validate a model in the flow equation separate from the rest. It is probably a good idea to validate a physical model separately from others. However, this may be difficult to do in all cases.

Third, SWIFT II is a difficult and cumbersome code to use, even for simple problems. Therefore, its use to model simple problems should be discouraged.

Instead it is recommended that a literature search be made to determine if the models implemented in the SWIFT II code have been previously validated. Such a study would include an effort to evaluate porous and fracture flow and transport models to determine if they have been validated. Such a study could easily be extended to models implemented in codes other than SWIFT II.

Instead, it is recommended that the models implemented in the SWIFT II computer code be validated with simpler analytical or numerical models, if possible. For instance, the flow equation could be validated with Theis (1935) equation, decaying radionuclide mass transport with Coats and Smith (1964), heat transport with Avdonin (1964) and mass transport in dual porosity media with Rasmuson (1984). Many other analytical solutions with different boundary conditions or assumptions for these transport processes are available in the literature.

The reason for the above recommendation is that many of the physically based models in the SWIFT II computer code are also available in analytical solutions or easier-to-use computer codes. The physics being validated is the same whether it is implemented in analytical or numerical models. Therefore if the physics is shown to be correct with an analytical solution, it is not necessary to test it with a numerical one. Ease of use and simplicity are the main reasons for this recommendation. Models unique to SWIFT II, such as transport by convection in the porous matrix of a dual porosity media are the only models that should be validated with the SWIFT II computer code.

4.3 PROBLEMS WITH VALIDATION

A few words are in order concerning the difficulty in validating models. The meaning of model and validation need to be adequately defined. The Nuclear Regulatory Commission defines model as "a representation of a process, component, or system" (Goller, 1985). This obviously can mean either analog or mathematical models, but only mathematical models are of consequence here. The ground-water flow equation could probably be described as a system model. This model is derived from several other models, which could probably be described as models of system components. For instance the ground-water flow equation consists of a mass conservation model, a water compressibility model, an aquifer compressibility model, and a flow resistance model (Darcy's law). The problem arises in determining which model, whether system or component, needs validation. Certainly, all of them could be validated, but it may be inadequate to validate the system model only or the component models only. However, validating the system and component models or various combinations of component models may require many comparisons of models with experiments, an expensive and time consuming operation.

The NRC defines validation as "the process of obtaining agreement between the empirical observation of a phenomena or set of phenomena and the theoretical description (as embodied in mathematical model, for example) of the same phenomenon or phenomena" (Goller, 1985). Agreement can be obtained by calibration, but this does not necessarily imply that the model physically represents the data. It only implies that the model can be made to fit the data. An extreme case can be made with the one-dimensional convective-diffusive equation for contaminant transport and a similar model for heat transport. The models are physically different but mathematically equivalent, and both can be made to fit one-dimensional mass transport data. Another case may be made with a three parameter model and two data points. Such a system is underdetermined and an infinite number of parameter sets can fit the data. In this case, no set of parameters is unique. Finally, a very noisey data set can result in several sets of parameters fitting the data. For this case, no data is unique.

Another potential problem with validation is comparing model results with existing experimental results. Since the data exist and are available for comparison, the modeler can modify space and time steps and parameters so that code results match experimental results. This is really a form of calibration instead of validation and indicates that published experimental data may be inadequate for model validation.

Another problem with model validation is the issue of either laboratory or field data. Laboratory experiments are generally well controlled, producing generally smooth results. On the other hand, field experiments cannot be well controlled because of soil layering, fractured rock, sand lenses, and other geologic discontinuities. These factors, in general, produce noisey results and are sometimes difficult to implement in a model. As a consequence, a model may not exactly reproduce the field experiment, and model results may compare poorly against field results.

Finally, if the model is validated against laboratory experiments, the experiments should be dynamically similar to the field problems the model would be used for. This means that the laboratory dimensionless parameters, such as Peclet numbers, should be the same as those for potential field problems. This insures a consistency between laboratory and field experiments.

4.4 SUMMARY

Many problems have been reviewed for verification and validation purposes. It has been found that many capabilities have been successfully verified. However, a few of the submodels need further testing. These include the local and global brine equations, and parts of the repository submodels. Recommendations for testing these have been provided in Section 4.1.

The problems reviewed for validation purposes have been found to be inadequate for that purpose. The problems reviewed are more like "trial and error" calibration procedures rather than validation problems. It is recommended that the SWIFT II computer code not be used for validating mathematical or physical models.

5. REFERENCES

Avdonin, N. A., 1964, Some Formulas for Calculating the Temperature Field of a Stratum Subject of Thermal Injection, Neft'iGaz, vol. 7, no. 3, pp. 37-41.

Bear, J., 1972 Dynamics of Fluids in Porous Media, American Elsevier Publishing Co., New York.

Buscheck, T. A., C. Doughty, and C. F. Tsang, 1983, Prediction and Analysis of a Field Experiment on a Multilayered Aquifer Thermal Energy Storage System and Strong Buoyancy Flow, Water Resources Research, vol. 19, no. 5, pp. 1307-1315.

Clark, S. P., Jr., 1966, Handbook of Physical Constants

Coats, K. H., and B. D. Smith, 1964, Dead-End Pore Volume and Dispersion in Porous Media, Society of Petroleum Engineers Journal, vol 4., no. 1, p. 73.

Finley, N. C. and M. Reeves, 1982, SWIFT Self-Teaching Curriculum, NUREG/CR-1968 and SAND81-0410, U. S. Nuclear Regulatory Commission, Washington, D.C.

Gureghian, A. B., D. S. Ward, and R. W. Cleary, 1981, A Finite Element Model for the Migration of Leachate from a Sanitary Landfill in Long Island, New York-Part II: Application, Water Resources Bulletin, vol 17, no. 1, pp 62-66.

Hantush, M. S., 1960, Modification of the Theory of Leaky Aquifers, Journal of Geophysical Research, vol. 65, no. 11, pp. 3713-3725.

INTRACOIN, 1984, Final Report Level 1, Code Verification, International Nuclide Transport Code Intercomparison Study, SKI84:3, Swedish Nuclear Power Inspectorate.

Jacob, C. R., and S. W. Lohman, 1952, Non-steady Flow to a Well of Constant Drawdown in an Extensive Aquifer, American Geophysical Union Transactions, vol. 33, no. 4, pp 559-569.

Kimmel, G. E., and O. E. Braids, 1975, Preliminary Findings of a Leachate Study on Two Landfills in Suffolk County, New York, J. Res. U. S. Geological Survey, vol. 3, no. 2, pp 273-280.

Kimmel, G. E. and O. E. Braids, 1980, Leachate Plumes in Ground Water from Babylon and Islip Landfills, Long Island, New York, U. S. Geological Survey, Prof. paper p-1085, 38 pp.

Molz, F. J., J. G. Melville, A. D. Parr, D. A. King, and M. T. Hopf, 1983, Aquifer Thermal Energy Storage: A Well Doublet Experiment at Increased Temperatures, Water Resources Research, vol. 19, no. 1, pp 149-160.

Papadopulos, I. S., 1965, Nonsteady Flow to a Well in an Infinite Anisotropic Aquifer, Symposium International Association of Scientific Hydrology, Dubrovinik.

Parr, A. D., F. J. Molz, and J. G. Melville, 1983, Field Determination of Aquifer Thermal Energy Storage Parameters, Ground Water, vol. 21, no. 1, pp. 22-35.

Rasmuson, A., 1984, Migration of Radionuclides in Fissured Rock: Analytical Solutions for the Case of Constant Source Strength, Water Resources Research, vol. 20, no. 10, pp. 1435-1441.

Reeves, M., D. S. Ward, N. D. Johns, and R. M. Cranwell, 1986a, Data Input Guide for SWIFT II, The Sandia Waste-Isolation Flow and Transport Model for Fractured Media, Release 4.84, NUREG/CR-3162 and SAND83-0242, Sandia National Laboratories, Albuquerque, NM.

Reeves, M., D. S. Ward, N. D. Johns, and R. M. Cranwell, 1986b, Theory and Implementation for SWIFT II, the Sandia Waste-Isolation Flow and Transport Model for Fractured Media, Release 4.84, NUREG/CR-3328 and SAND83-1159, Sandia National Laboratories, Albuquerque, NM.

Reeves, M., D. S. Ward, P. A. Davis, and E. J. Bonano, 1986c, SWIFT II Self-Teaching Curriculum, NUREG/CR-3925, U. S. Nuclear Regulatory Commission, Washington, D.C.

Ross, B., J. W. Mercer, S. D. Thomas, and B. H. Lester, 1982, Benchmark Problems for Repository Siting Models, NUREG/CR-3097, U. S. Nuclear Regulatory Commission, Washington, D.C.

Tang, D. H., E. O. Frind, and E. A. Sudicky, 1981, Contaminant Transport in Fractured Porous Media: Analytical Solution for a Single Fracture, Water Resources Research, vol. 17, no. 3, pp. 555-564, June.

Theis, C. V., 1935, The Relation Between the Lowering of the Piezometric Surface and the Rate and Duration of Discharge of a Well Using Ground Water Storage, American Geophysical Union Transactions, pp. 519-524.

Ward, D. S., M. Reeves, and L. E. Duda, 1984a, Verification and Field Comparison of the Sandia Waste-Isolation Flow and Transport Model (SWIFT), NUREG/CR-3316, U. S. Nuclear Regulatory Commission, Washington, D.C.

Ward, D. S., M. Reeves, P. H. Huyakorn, B. Lester, B. Ross, and D. Vogt, 1984b, Benchmarking of Flow and Transport Codes for Licensing Assistance, NUREG (to be published). U. S. Nuclear Regulatory Commission, Washington, D.C.

Wilkinson, G. F. and G. E. Runkle, 1986, Quality Assurance (QA) Plan for Computer Software Supporting the U. S. Nuclear Regulatory Commission's High-Level Waste Management Program, NUREG/CR-4369 and SAND85-1774, Sandia National Laboratories, Albuquerque, NM.